Electrospun nanofibers for medical face mask with protection capabilities against viruses: State of the art and perspective for industrial scale-up

A. Cimini [a],[b],[*], E. Imperi [b], A. Picano [b], M. Rossi [a],[c]

[a] Department of Basic and Applied Sciences for Engineering, University of Rome Sapienza, Rome 00161, Italy
[b] LABOR s.r.l., Industrial Research Laboratory, Via Giacomo Peroni, 386, Rome, Italy
[c] Research Center for Nanotechnology for Engineering of Sapienza (CNIS), University of Rome Sapienza, Rome 00185, Italy

ABSTRACT

Face masks have proven to be a useful protection from airborne viruses and bacteria, especially in the recent years pandemic outbreak when they effectively lowered the risk of infection from Coronavirus disease (COVID-19) or Omicron variants, being recognized as one of the main protective measures adopted by the World Health Organization (WHO). The need for improving the filtering efficiency performance to prevent penetration of fine particulate matter (PM), which can be potential bacteria or virus carriers, has led the research into developing new methods and techniques for face mask fabrication. In this perspective, Electrospinning has shown to be the most efficient technique to get either synthetic or natural polymers-based fibers with size down to the nanoscale providing remarkable performance in terms of both particle filtration and breathability. The aim of this Review is to give further insight into the implementation of electrospun nanofibers for the realization of the next generation of face masks, with functionalized membranes via addiction of active material to the polymer solutions that can give optimal features about antibacterial, antiviral, self-sterilization, and electrical energy storage capabilities. Furthermore, the recent advances regarding the use of renewable materials and green solvent strategies to improve the sustainability of electrospun membranes and to fabricate eco-friendly filters are here discussed, especially in view of the large-scale nanofiber production where traditional membrane manufacturing may result in a high environmental and health risk.

1. Introduction

In recent years, the common commercial microfibers have been replaced with nanofibers in manufacturing personal protective equipment (PPE), such as face mask/respirators, which are specifically designed to protect the wearer from inhaling harmful airborne particles, including infectious agents, such as coronavirus, SARS, and bacteria spores. The 2019 coronavirus (SARS-CoV-2) pandemic has forced a widespread use of face coverings as a mandatory step for reducing spreading and infection by the virus, in fact the face masks turned out to be an essential barrier for preventing the transmission of infected aerosols among its user and the surrounding people [1–3]. Especially at the start of the pandemic outbreak face masks played a fundamental role, since information about the transmission mechanism of the virus was not yet clear and only isolation/ quarantine appeared to be the most significant strategy for infection control [4].

The size of the Corona virus has been observed to range from 60 to 140 nm [5]. The transmission of the virus can occur for close-distance contacts in the form of aerosols or droplets [6], because of its ability to coalesce with solid or liquid pollution particles present in the atmosphere, which makes it extremely infectious [7,8]. Therefore, the aerosol carrier of the virus (diameter $< 5 -10$ μm) can be transmitted from an infected person to a healthy one by means of respiratory droplets either for breath, coughs, or sneezes [9,10]. The short-range airborne route results to be the primary way to spread either pathogens or respiratory infection [11,12] such that wearing face masks is the most effective solution to prevent the transmission of this disease [13].

Despite the vaccination campaign against COVID continues to progress [14], the importance of wearing a face mask or a respirator in outdoor/indoor places is recommended as an effective measure for the infection control [15–17]. This led the research community to find more appropriate technologies and advanced materials to design novel high-efficiency mask, with extreme attention to particle filtration, cleaning treatments, adequate breathability, fluid penetration resistance, light weight, and user comfort, along with large-scale production and low costs. In this scenario, electrospun fibers showed their uniqueness and potential as active membranes, due to their reduced pore size as well as their extremely high surface-to-volume ratio [18]. The high performance in filtration is owed to the reduced pore size, which goes from sub-micron to several micrometers, involving a more effective capture mechanism for the small airborne particles below 300 nm, as well as to the high ratio of surface area/volume, which

significantly increases the possibility of pollutant deposition on the surface of the fiber, thus reducing the air pressure drop and increasing the air breathability of the mask [19]. Although the melt blown (MB) is a low-cost process commonly used to produce nonwoven filter media [20–23], the electrospinning (ES) technique has proved to produce nanofibers with better filtration performance in removing submicron particles/contaminants. Compared to the MB microfibers, whose fibers size are generally difficult to control and the diameters range from 1 to 10 μm, the electrospun fibers diameter can be ten or a hundred times smaller, thus providing a higher surface area as well as a lower inter-fiber pore size [24–26]. Several Reviews reported about the potentiality in using electrospun membranes for new generation face mask/respirators production [27–30]. An increasing number of papers was found by using the keyword "Electrospinning filter face mask "in the Scopus database (Fig. 1).

Besides the high filtering efficiency benefits, the functionalization of electrospun nanofibers through the addition of several compounds, such as metallic and not metallic nanomaterials, vesicles, and cellulose nanocrystals, allows designing advanced nanofibers with outstanding properties, including antibacterial, antiviral, and self-sterilization. Such customizability makes the electrospun nanofibers the ideal material for tackling the current issues from bacterial contamination on PPE surfaces to the reusability of both disposable single use facemask and respirator's filters. Also, modified ES set-ups combined with modern textile techniques turned out to be an innovative way to manufacture nanofiber bio-textiles with suitable mechanical and bioactive properties which effectively support cell tissue regeneration in clinical use [30,31]. Electrospun nanofibers composed by natural and biodegradable polymers can be easily degraded in environment or absorbed by the body, thus preventing the negative long-term degradation effects due to high consume of plastic, ensuring a safer approach to the realization of scaffold and drug delivery system for biomedical application [32–35]. Although a great number of research in the electrospinning field has been carried out at laboratory scale, alternative techniques have been developed so far to expand the production of electrospun nanofibers on large industrial scale [36]. To date, many companies and start-ups operating in small and large textile manufacturing have been utilizing ES technology to fabricate face masks and protective controls with better performances on personal protection from particulate matter (PM) and airborne hazard. The leading ES research is focusing on the optimization of more sustainable filters to minimize the impact of disposable face masks on

the environment, but the large volume of hazardous solvent still used in traditional membrane manufacturing involves a serious environmental issue. With this regard, particular attention has been given to more environmental-friendly ES processes to drastically reduce or completely give up toxic organic solvents, which are strictly used to solubilize polymer in conventional spinning solution.

This Review aims to give a general overview about the recent developments in ES techniques and its further application to produce electrospun nanofiber-based face mask. Firstly, a brief introduction about the fundamental principles behind the filtering mechanism, classification, and the standards for testing the face mask is provided. Then, is presented a description on conventional and alternative ES technologies, evaluating the possible developments for industrial scale-up. After that, are reviewed in detail the innovative scalable strategies present in literature for the processing of electrospun based face masks, highlighting the effects induced by the surface morphology, fibers geometry, and materials properties on the particle filtration, breathability, antibacterial, and antiviral performance. A brief introduction about the recent progress in the manufacturing of bio-textiles by using electrospun nanofiber yarns is also given in this Review. Finally, we discuss about the industrial implementation of ES for nanofiber manufacturing, giving to the reader further insight into the well-defined nanofiber market.

2. Face mask's structure and filtration mechanism

2.1. Surgical mask and respirator standards

Face masks have the important role to protect the wearer from the biological contaminants that can be present in the form of droplet or aerosols in the atmosphere, since respiratory infection may be transmitted due to either talking or coughing droplets from an infected person. The method of infection has been observed to depend on the droplet size [4,37]. Large droplets with diameter ranging between 2.5 and 10 μm can deposit due to gravity either in the nasal, oropharyngeal, laryngeal, or tracheal regions of the respiratory system, whereas the smaller ones ranging between 0.25 and 1 μm can evaporate midair involving airborne transmission eventually depositing in the respiratory tract. In addition, intense coughs and sneezes have been observed to propel larger droplets over 20 feet that can remain airborne for hours [38]. Therefore, face masks are expected to prevent the penetration of contaminant present in the surroundings such as particulate and dust, which can be potential bacteria or virus carriers. Among the various classifications, both the surgical masks and the face piece respirators have been taken in consideration as effective devises in preventing viral infection by airborne contamination.

A surgical or medical mask is used as medical device for health care workers (HCWs) to avoid that patient in hospitals become infected from possible expiratory droplets. These devices are generally used for surgical operations, since they are fluid resistant providing a useful physical barrier from larger droplets and body fluids, despite their loosely fit on the wearer face. The common surgical masks are made of three nonwoven layers, all of which are generally composed of polypropylene (PP) thermoplastic polymer [18,27,39–41] (Fig. 2 a). The cover and shell layer are fabricated with spunbond fabric to provide high tensile strength and good breathability in the mask, respectively. These layers show fibers diameter ranging between 15 and 40 μm, and do not provide any contribute to the overall filtration system. On the other hand, the inner layer is fabricated by means of MB process, which allow to obtain submicron fibers with diameter size ranging between 0.5 and 10 μm. This latter layer sandwiched between spunbond fabrics performs as the filtering system. As their relatively large diameter is insufficient to efficiently filter small airborne particles, electrostatic treatment is performed on the filter to improve the filtration efficiency. However, the static electricity quickly depletes due to long use of the mask with a consequent reduction of the filtration properties, so that they can be used for one time only. The grade of protection from bacteria is obtained
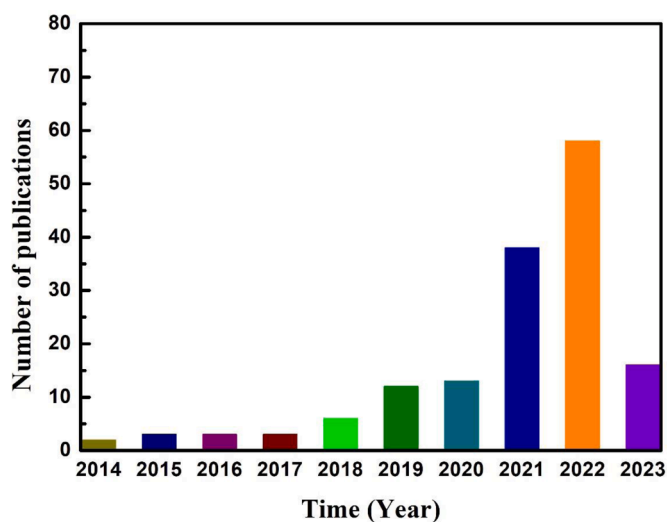
Fig. 1. Number of annual publications on Electrospun filters for face mask applications. The data have been collected in a search carried out on the "Scopus" database on 2023–04–06 by using the keyword "Electrospinning filter face mask".
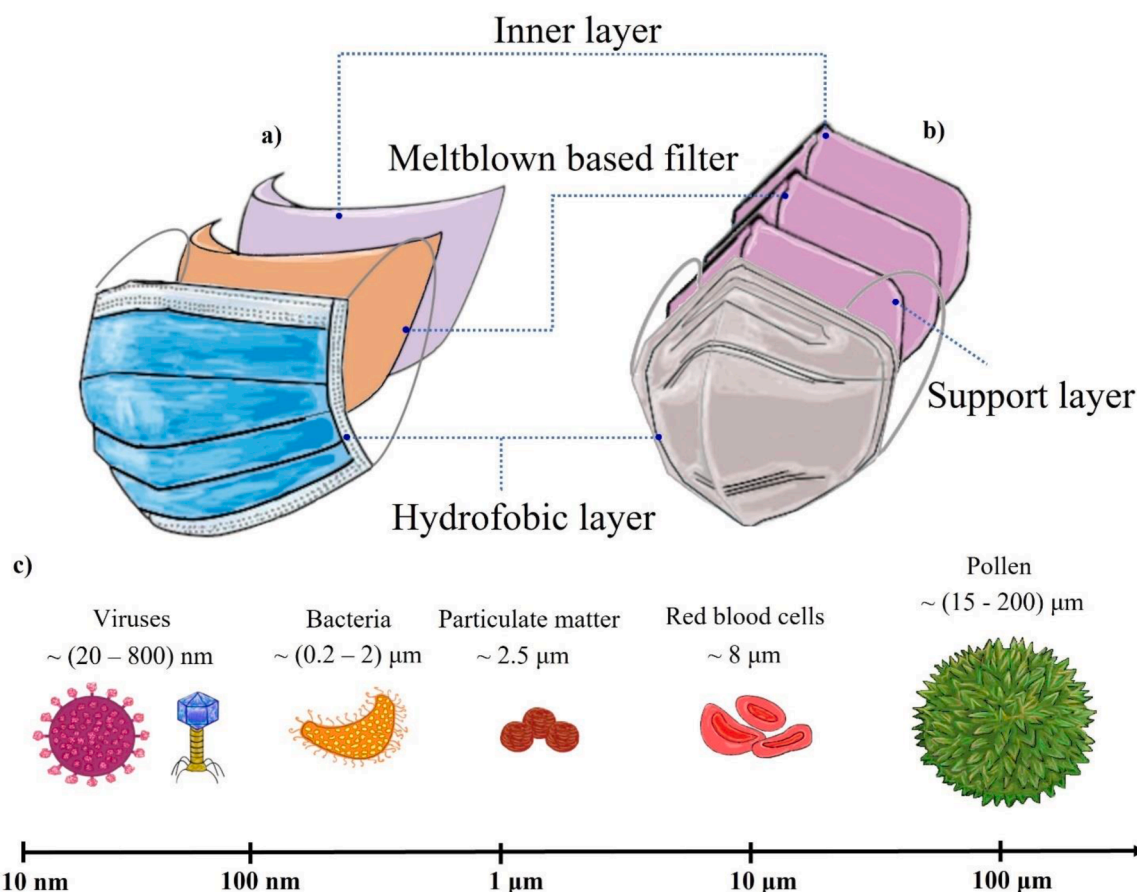
Fig. 2. Structure of a surgical mask (a) and filtering half mask (b). (c) Schematic image of different pathogens and air pollutants for a size comparison.

by means of Bacterial filtration efficiency test (BFE). This test allows to obtain a measurement of the device's resistance to the penetration of *Staphylococcus aureus (S. aureus)* aerosols, which is shot with a flow rate equal to 28.3 L/min through the mask by using particle size of 3.0 µm [41]. As the degree of efficiency is reported in percent, higher percent values correspond to better filtration performances from the face mask. According to the European standard (EN 14,683:2019), a surgical mask is classified either as type I, if it presents at least a value of 95% BFE, or as type II, if it provides better filtration performances (BFE ≥ 98%) (see Table 1). Furthermore, a third class, namely IIR, includes a splash resistance test to penetration of synthetic blood. About the ASTM F2100–19 standard used in United States, the classification of the surgical masks is almost the same as the EN 14,683:2019, with the exception of a more relevant test required, concerning particle filtration efficiency (PFE) of the submicron particles, with mean diameter of 0.1 µm [42,43].

Like surgical masks, a facepiece respirator is composed of polymer-based multiple layers (Fig. 2 b). The outer layers are composed of non-woven fabric with grams per square meters (gsm) ranging between 20 and 50 to create a barrier against moisture. Besides, a higher dense layer of around 250 gsm is employed to provide more stiffness and thickness to the face mask, whereas a more internal layer made via MB process acts as filter. Compared to the surgical masks, the facepiece respirators are tighter and more adherent to the face, in order to avoid inhalation of both droplets (particle size > 0.5 µm) and smaller particles, such as dust, and aerosols (particles size < 0.5 µm), and to provide a real protection from both potential viruses and bacteria [18] (Fig. 2 c). With regards to the EN 149:2001, these respirators are classified as filtering half masks (i.e., Filtering Face Pieces (FFP)) and are divided in three different types, namely FFP1, FFP2, and FFP3, depending on the filtration efficiency values, for both PFE and BFE, equal to 80%, 94%, and

Table 1

European and USA standards required for surgical mask and facepiece respirators.

Surgical mask	USA ASTM F2100–19 Standard			EN 14,683:2019 Standard		
	Level 1	Level 2	Level 3	Type I	Type II	Type IIR
BFE (%)	≥95	≥98		≥95	≥98	
PFE (%)	≥95	≥98		Not required		
Fluid resistance	>80 mmHg	>120 mmHg	>160 mmHg	Not required		>120 mmHg
Differential pressure drop	< 5.0 mmH₂O/cm²	< 6.0 mmH₂O/cm²		< 40 Pa/cm²	< 40 Pa/cm²	< 60 Pa/cm²
Facepiece respirator	NIOSH 42 CFR Part 84–2019 standard			EN 149:2001+A1 2009		
	N95	N99	N100	FFP1	FFP2	FFP3
BFE (%)	≥95	≥99	≥99.97	≥80	≥94	≥99
PFE (%)	≥95	≥99	≥99.97	≥80	≥94	≥99
Inhalation differential pressure	343 Pa at 85 l/min			210 Pa at 95 l/min	240 Pa at 95 l/min	300 Pa at 95 l/min
Exhalation differential pressure	245 Pa at 85 l/min			300 Pa at 160 l/min		

EN (European Norm); ASTM (American Society for Testing and Materials); NIOSH (The National Institute for Occupational Safety and Health); CFR (Code of Federal Regulations); BFE (Bacterial Filtration Efficacy); PFE (Particle Filtration Efficiency).

99%, respectively [44–46] (Table 1). In addition to the filtration performance, the National Institute for Occupational Safety and Health (NIOSH), in the USA, also adopts a classification by letter, namely N-, R-,

and P-, to indicate the lack of resistance in oil, somewhat oil resistant, and strongly resistant, respectively. According to this standard, three distinct filtration efficiencies degrees are adopted for the respirators, such as 95%, 99%, and 99.97%, and for each series of letters three facial pieces are classified, for instance N95, R95, and P95 for 95% filtration performance, etc. [4,18].

In high-risk situations both the Centers for Disease Control and Prevention (CDC) and the World Health Organization (WHO) currently recommend to health workers the use of protective sources of respirators with performances of 95% or higher, such as FFP2 and N95 [47,48]. The rigorous standards adopted in Europe and USA have made that these respirators provide higher protection than loose surgical masks, so to prevent users to be infected from either large droplets, originated in air for short periods during cough, sneeze, and talking, or from fine airborne particles which remained in air for long time and have been transported for longer distances. However, there are some clinical researches that have brought to conflicting results. For instance, some studies have evidenced a better effectiveness of N95 respirators in reducing viral infections compared to surgical masks [49,50], while other works reported no significant difference between N95 respirators and medical masks in terms of viral preventing from respiratory infections, including that of influenza [51,52]. Even though concrete evidence about the efficacy in protecting health workers against viral SARS-COV-2 of respirators compared to surgical mask is not totally reliable yet, the utilization of respirators for high-risk setting pandemic is strongly recommended [41,53,54].

2.2. Filtration mechanism of face masks

The filtration effectiveness of a face mask is an estimate of the ability of the inner layer in trapping undesired airborne particles, which could introduce harmful microorganisms or viruses through inhalation of air. The capture mechanism of fibrous media strictly depends on the particle size and can be divided in the following way (Fig. 3 a): direct interception, diffusion, electrostatic deposition, gravitational forces and inertial deposition [18,27,39,55,56]. The interception mechanism generally involves the capture of particles with diameter size lower than 1 μm. When the particle carried by air streamlines is moving in the proximity of the fiber surface, so that their radius is less than the fiber-particle distance, it is affected by Van der Waals attraction forces thus remaining stuck on the mat. Diffusion is another effective method

to capture smaller particles, usually those with diameter far below 1 μm. The random collision with other particles from Brownian motion near the fiber brings the aerosol particle to deviate from their original streamline thus impacting with high probability to the fiber surface. Besides, charged fibers can effectively trap submicron particles of opposite charge via electrostatic attraction.

The effect of the electrostatic charges is that of improving the overall particles filtration efficiency without affecting the morphology of the fiber and either the interception or the diffusion mechanical capture. Corona discharge and triboelectrification methods are commonly used to apply electrical charge on electrically active polymer materials [58, 59]. Finally, larger particles ranging from 1 to 10 μm are expected to be easily captured from gravity and inertia mechanisms. Indeed, bigger particles moving along the stream can be deposited on the fiber surface due to the gravity. On the other hand, the inertial deposition results to be a more effective method to capture either aerosols or dust particles larger in size than 1 μm. Particles moving at high velocity near a fiber can come out from the main streamlines and impact on the fiber surface due to the inertia, hence the higher is the particles velocity the better is the capture efficiency. The mechanical efficiency of the commercial face masks in the submicron particle range is mainly due to the interception and diffusion mechanisms, whereas the contribution of inertial impact and gravity are practically negligible. The lowest filtration particle measured is defined as the most penetrating particle size (MPPS) and corresponds to the least efficiency value ensured by the standards adopted (Table 1). The MPPS differs from one filter system to another and is found in the point of intersection between the diffusion and interception curves, which generally falls in the range between 0.1 and 0.3 μm [26,56] (Fig. 3 b). To improve the overall mechanical efficiency against fine particles for the most commonly produced face masks, industries typically rely on the electrostatic charge effect. The performance obtained for charged fibers in face mask are better than those observed in uncharged one [60]. While the mechanical filtration of large droplets in face masks come mainly from the micro-pore size of the fibers, which in a MB-based filter is about ~20 μm, the filtration of aerosols is due to the electrostatic attraction of smaller particles at the fibers surface. The polymer materials forming these mask devices are generally electrostatic microfiber media, such as PP, that can be electrostatically charged by means of corona discharge. To charge them a high voltage is applied between the two electrodes and the electret filter, thus allowing the ionization of the air to induce a positive or negative
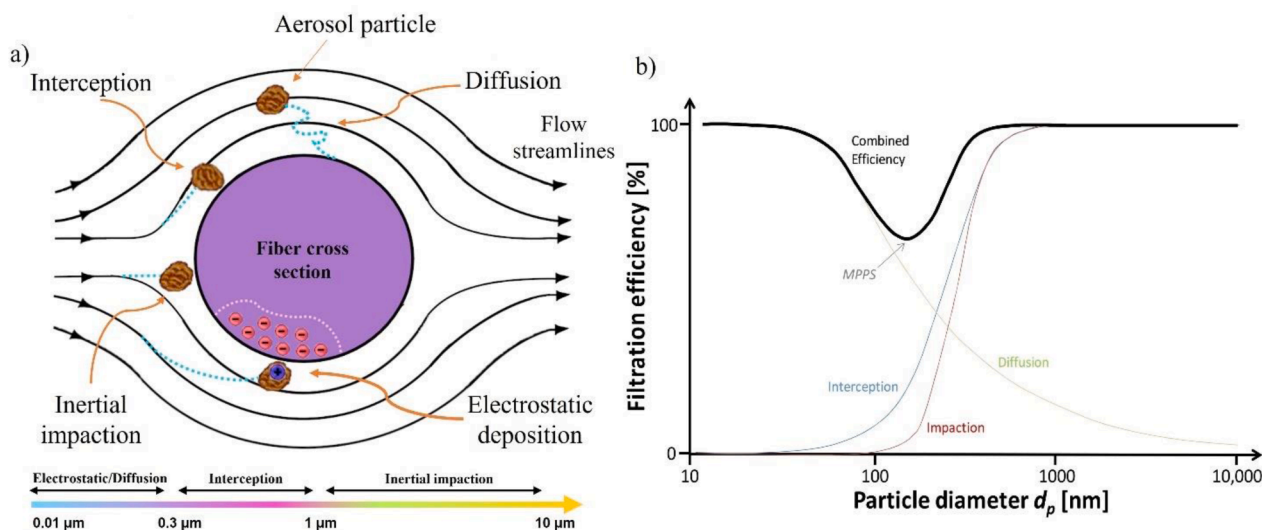

Fig. 3. (a) A schematic image of the principal capture mechanisms for fibers. Below, a simplified diagram which displays the particles size range where Electrostatic, Diffusion, Interception, and Inertial impact mechanism are more efficient; an example of electrostatic deposition is represented in the schematic picture from the electrostatic attraction occurring between a negative charge fiber (minus sign) and a charged aerosol particle (blue sign). (b) Graphic representation of the main filtering efficiency curves for a single fiber as function of the particle size; adapted with permission from [57].

charge on the fiber surface [58,60]. Even though this treatment involves a better performance in respirators/ face mask, the effect of either air humidity or liquid contact on charge decay no longer ensure a proper coverage against small particles. It has been stated that longer exposition to air humidity leads to a reduction of the charge on the fibers, thus resulting in a decrease in the filtration performance [56]. Moreover, ethanol and autoclave sterilization treatment remove electrical charges from the polymer filter media thus affecting the performance of the face mask not guaranteeing a proper protection if reused [61]. If on the one hand respirators are expected to provide a greater filtration performance compared to surgical masks due to the effective seal on the face, lower air leakage, and multi-layer structure, on the other hand the lowering of the electret fiber charge can bring to a significant decrease in the overall collection efficiency and make both the class types useless to face coronavirus disease.

2.3. Breathability test

In addition to filtration efficiency, the overall layers constituting either a surgical mask or a facepiece respirator must be both comfortable and breathable for the users. Indeed, the fabric fibers used to make a mask have to provide an effective barrier against airborne particles, but they also must ensure the person to breath properly [39,58,62–64]. The pressure drop is the most commonly used parameter to quantify a mask breathability, being an index of the air flow resistance of the filter for a specific material surface, which makes it a suitable indicator to assess the filter performance. Pressure drop is obtained at specific flow rates by measuring the difference in pressure between the two outer layers of a face mask [63]. Lower values of pressure drop involve better breathability for the face device, thus making breathing more comfortable for the wearers. The difference in pressure between the upstream and downstream measured on the two outer layers side is proportional to the volumetric air per unit area, also known as face velocity, that crosses through the face mask. The presence of multiple layers as well as the occurrence of inhomogeneity in the air flux in the fabric fiber can affect in many ways the pressure difference measurement for a given tested area. Therefore, a comparison between pressure drop measurements obtained in different experiments with different values of tested face velocity is not advised [63]. The measure of the pressure drop is usually reported in units of Pascal for surface area (Pa/cm^2) and varies depending on the standard adopted by the different countries. About surgical masks for instance, the flow rate values, which is generally expressed in liters per minutes (Lpm), used for the test performed both in USA and Europe, according to ASTM F2299 or F2101 and EN 14, 683:2019 standards respectively, is fixed to 8 L/min over a tested mask surface of 4.9 cm^2, but the maximum pressure drop specified for these tests varies from $40/40/60$ Pa/cm^2, for type I, II, and IIR in Europe, to $50/60/60$ Pa/cm^2 for barrier levels equal to 1, 2, and 3 in USA [63,64]. The high number of layers that structure a face piece respirator provide a better resistance to flow stream compared to surgical masks but results also in a large pressure drop which makes breathing more difficult for the user (Table 1). Because of the shortage as well as the intense workload and patient flow during the pandemic outbreak, face masks were allowed to be worn for an extended period longer than that recommended. Nevertheless, a prolonged use can involve a serious of discomfort due to an increase of the facial temperature, both during exhalation and inhalation [65]. Recent studies investigated the possible factors involved in the discomfort increase and in the protection drop due to long-term usage of common face mask by testing particle filtration, breathability, and humidity. Experimentally it has been observed that high breathing resistance and low moisture permeability make a respirator more discomfortable than a surgical mask, especially after many hours of use [66]. Additionally, an increase in temperature and humidity due to moist air expired and inspired in repeated breathing cycles have been observed to promote the growth of bacteria on the face mask, thus putting the most vulnerable people at risk of infection [66,

67]. Also, evident drop in humid air filtration efficiency after prolonged wearing of common face mask, with also further proliferation of fungi and bacteria colonies, have been recently reported [68]. A research stated that the use of surgical masks of high quality, like the Type IIR, can be extended to 8 h, and then beyond the recommended time of 4 h, but only under restricting conditions and for that specific brand and standard [69]. These studies highlights that a prolonged use of commercial face mask over the usual recommendation can then involve a considerable discomfort for the combined effect of high humidity and temperature rise on the face but can also expose the user to other potential health risks.

3. Introduction to electrospinning

3.1. Electrospinning as alternative method for the fabrication of face mask filters

The layers forming a commercial face mask are mainly produced by means of Melt-blowing (MB) and Spunbond (SB) methods. Both the techniques are based on the extrusion process of melted polymers in a continuous fluid jet through a spin- hole, which size generally range between 250 and 1000 μm [58]. However, the two methods involve a different process during the collection of the nonwoven fibers. While in the SB process the fluid moving across a quench chamber is cooled by flow air, thus leading to a stretch of the fibers diameter in the range 10–35 μm, in the MB process the polymer fluid is further heated by high-speed hot air thus involving the formation of finer fibers with diameter size ranging between 1 and 10 μm. Since the hot filament spontaneously bond in MB process, no further processing is provided on the nonwoven fiber. Conversely, to improve the bonding in air cooled non-woven fibers, additional treatments, such as thermal, mechanical, or chemical, are carried out in SB method [58]. Because of the smaller diameter size and poor mechanical strength, the MB fibers are usually sandwiched between the SB fabric ones providing filtration performance in commercial face mask. Despite PP is the most popular polymer employed in filters formation, many other viscous thermoplastic polymers, such as polyethylene, polystyrene, polyesters, or polyamides, can be melt blowing [21].

The electrospinning is another flexible technique to fabricate polymer nonwoven fibers and has been attracting great attention from the scientific research community and from industries due to its application in air filter systems [70]. The physical phenomena of the ES dates to the 16th century when William Gilbert for the first time observed the formation of a cone shaped droplet as a consequence of the exposure to the electrostatic field [71]. The behavior of the formation of aerosols of charged liquid have been investigated also by Rayleigh, who obtained an estimate of the maximum charge that a liquid droplet can carry before the liquid jets are ejected from the surface [72]. In addition, Zeleny has conceived a mathematical model to explain the physics of this process [73]. The first patented ES set-up was that of Cooley in1900 [74], which involved the use of many electrodes bringing fiber deposition on a continuously rotating drum similar to that conventionally employed nowadays, but only between the 1930s and the1940s Formhals implemented an alternative set-up, which paved the way to the modern electrospinning techniques [75–77]. The basic set-up for conventional ES consists of four major components, which include a syringe for containing the electrospun solution, a spinneret which usually consist of a metallic needle with a blunt tip, a high-voltage power supply which can be either direct current (DC) or alternating current (AC), and a conductive grounded collector [78]. During the ES process the syringe pump is used to push a polymer solution at a constant and controllable rate. To obtain the ES solution, the polymer compound is being dissolved by means of a proper organic solvent. When high voltage is supplied between the needle tip and the ground collector, opposite charges will separate within the liquid, due to the electrostatic repulsion among them, thus involving an increase of density charge on the surface of the

droplets.

The surface tension will promote the formation of a spherical shape to minimize the electrostatic pressure induced by the external electrical field, which will tend to deform the shape of the droplets. From the syringe a charged jet will flow out initially in a straight line towards the grounded collector following the direction of the applied electric field (Fig. 4 a). As this latter reaches a critical voltage, the surface tension will be exceeded by the electrostatic pressure and an instability of the liquid solution occurs with further deformation of the droplets from spherical to cone shape (i.e., Taylor cone formation) [79] . While the jet extends towards the grounded collector, it undergoes a whipping motion due to the bending instability. While the external perturbation field accelerates the charged jet to move forward the collector, the effect due to the electrostatic repulsion among the opposite charges on the surface of the jet will generate upward and outward forces thus forcing the jet to bend during the motion. Meanwhile, the trajectory is subjected to form a series of loops, resulting in the formation of a coil with several turns. As the distance from the tip increases, the diameter of the charged jet tends to decrease and to continuously stretch. With further elongation the jet solidifies, as a consequence either of the solvent evaporation or the cooling of the melt, forming thin fibers. Finally, the collection of the jet as solid and stable fibers involves the dissipation of the charges through the ground collector. Modifications of the basic set up have been adopted over the years to enhance the fabrication of more complex nanofibers. An example of advancement in standard needle-based ES methods is given by the introduction of a coaxial spinneret, which allows the fluids from different polymer solutions to be ejected in a coaxial jet thus forming a core−sheath electrospun nanofiber with controlled size [80] (Fig. 4 e). Another example is the triaxial ES method, in which triaxial needles are used to fabricate nanofibers that are structured in three layers [81] (Fig. 4 c). Similar to coaxial, the side-by-side ES technique allows to produce a hierarchical Janus fibers composed of two different sides starting from different polymer solutions [82] (Fig. 4 b).

As well as for MB membranes, the overall electrospun membranes generally provide low mechanical properties and therefore auxiliary outer layers are provided for face mask applications to make them more resistant. Although several processing parameters, such as air velocity, melt flow index, processing temperature, and orifice size can be tuned to obtain smaller MB based fibers [21,26], the MB fibers developed so far on laboratory scale as filter media for face mask application are characterized by fiber diameter of about the submicron size [23,86–88]. Unlike the MB process, the fibers obtained with ES method can reach diameter size down to 100 nm and a broad range of polymer materials have been successfully electrospun into nanofibers so far [26,89]. A decrease of the fiber diameter to the nanoscale has been observed to contribute in increasing the capture of fine aerosols particles (< 0.5 µm) [62,90,91]. Since the diameter of electrospun nanofiber can be comparable with the free path of air molecules at ambient condition, a slip flow regime occurs around the single nanofiber [26,70,92]. In this regime the fiber's drag force friction is substantially reduced, therefore a low momentum exchange between the fine particles and the fiber surface occurs, resulting in a low pressure drop [93]. Besides, the air streamlines behave in a straight-line fashion getting closer to the nanofiber thus resulting in a higher filtration efficiency due to interception mechanisms [70]. On the other hand, many drawbacks in conventional ES are due to the use of volatile organic solvents, which represents almost the 80% of the solution used for polymer solubility. Some of them are toxic and a small part of them may remain in the nanofiber fabric, without evaporating completely during the process [26]. Instead, many different MB set-up are solvent-free and can also achieve high production rates, thus providing low cost and eco-friendly manufacturing of nonwoven fabric compared to ES [21]. Although ES is a relatively new and promising method for the manufacturing of nanofiber-based filter in application for face masks, new technologies and strategies should be developed to reduce the high cost of hazardous solvent and promote a safer production of nanofiber on large scale.

3.2. Electrospinning design for high production

Because of the long fiber deposition time occurring in conventional
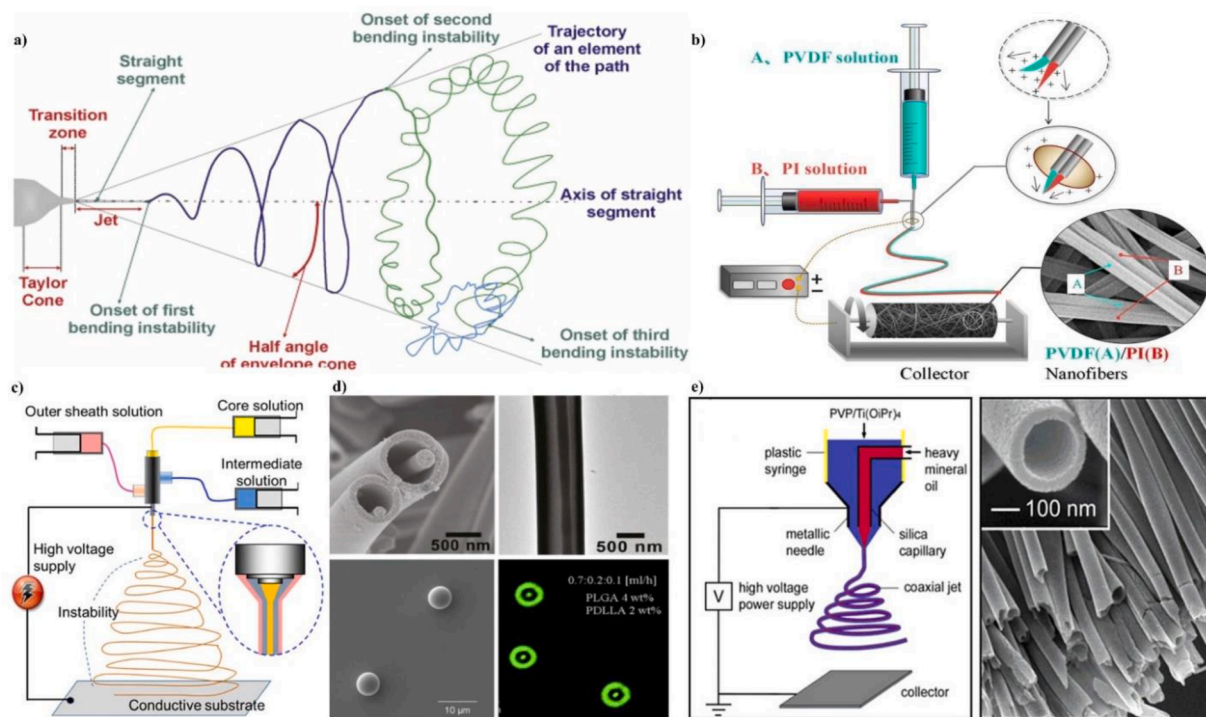

Fig. 4. ES process: (a) Formation of Taylor cone and further stretch of polymer jet under bending instability, adapted with permission from [83]. (b) Side-by-side ES set-up, adapted with permission from [84]. (c) Triaxial ES setup and (d) fiber structure: SEM image of fiber; TEM image of fiber; laser confocal image of fiber. (e) Coaxial ES and SEM image of aligned TiO$_2$; adapted with permission from [85].

ES using a single needle (capacity of ∼ 0.01- 0.1 g/h), several techniques such as multi-needles, needleless, free solvent or melt, and centrifugal ES have been developed to improve the production rate of nanofiber membranes [94,95]. The idea behind the multi-needle is based on conventional ES, but with the utilization of a nozzles array that allow the outflow of several polymer solution simultaneously (Fig. 5 a).

Although better production rates have been observed by increasing the number of nozzles in several ES spinnerets, drawbacks due to either the needle clogging or electric field interference between the close needles arranged on the array may affect the nanofiber productivity [99]. Unlike the multi-needle method, the needleless ES overcomes the shortcoming of clogging, because of the absence of needles use [83] (Fig. 5 b). The spinneret in this case generally consists of a rotating cylinder with large surface area that is partially immersed into the spinning polymeric solution. As a result of the rotation, a continuous production of thin polymer layer occurs on the spinneret surface with the further formation of steady conical spikes. The application of high voltage to the spinning solution intensifies the perturbations, thus leading to the formation of Taylor cones, from which polymer jets are further stretched out to finally results in fibers. In comparison with multi-needle method the needleless ES can produce the highest quality fibers and can have higher rates of production by exploiting different spinneret shapes in the set-up, such as cylinder, ball, disk, coil, and beaded chain [100,101]. Centrifugal ES has proven to be also a promising method to produce ultrathin fiber with large volume and high efficiency compared to other techniques [97,102]. This technique combines centrifugal and electrical forces to manufacture fiber from micrometers to nanofibers scale (Fig. 5 c). Because of both rotating spinneret and applied electric field, the stretching effect on the polymer jet expelled from the nozzle rim is higher than that observed in conventional ES. The combination of centrifugal, viscous, electrical, and gravity forces leads to a greater elongation of the polymer jet with lower bending instability, thus resulting in a better orientation in the formation of fibers [97]. As it can be observed in Table 2, several synthetic polymer membranes, including Polyacrylonitrile (PAN), Polyvinylpyrrolidone (PVP), and Polyvinylidene fluoride (PVDF), have been electrospun so far by means of needless and centrifugal techniques, providing high-rate productivity compared to the conventional ones.

However, the use of large amounts of harmful solvents, such as DMF, can require a high cost in recycling, thus limiting the large-scale production of these synthetic membranes. Safer bio-sources, deep eutectic, and ionic liquids solvents have been recently proposed as low toxic solution to allow a proper spinnability and processability for these synthetic polymers, but further investigations should be done to extend their use to pilot scale manufacturing [118,119]. On the other hand, the formulation of alternative solvents, including water and ethanol, with biopolymer materials, such as Polyvinyl acid (PVA), polylactic acid (PLA), and polyethylene oxide (PEO), have been used in both these ES techniques, showing high productivity rate [97,103,106,109,114,115] (Table 2). These polymers are nowadays widely implemented in health industry application, including personal protective-clothing, tissue engineering and drug delivery, due to their biocompatibility and biodegradable characteristics [120–122]. Unlike these solvent based methods, the melt ES is an eco-friendly and solvent free process [95, 123]. Given the absence of solvents to solubilize the polymer in the spinning solution, the viscosity of the polymer melt is higher than that usually obtained for standard solution ES with single needle. Therefore, a strong electric field, three or five times higher than that used in conventional ES, is applied to the melt polymer to guarantee the fiber formation. Among the different types of melt ES set-ups designed so far, the needleless melt differential ES proved to be a promising method to start mass production of fiber. Like needleless ES, the needleless melt differential process avoids the use of capillarity needle and make use of very high voltage to produce multiple jets from free melt polymer surface. The set-up is provided with five principal components, including both a melt inlet and distributor, umbellate nozzle spinneret, high voltage power supply, and a receiver plate (Fig. 5 d). Firstly, the melt polymer is being channeled by means of a micro inlet toward a melt distributor to be then transformed from a cylindrical flow into a more uniform ring-like shape one. The further distribution of the flow to umbellate nozzle spinneret allows the formation of a uniform melt thin layer on the circumferential surface. The application of a critical high voltage power involves the formation of polymer multiple jets around the circular edge of the umbellate nozzle and their further ejection in the form of fibers to the receiver plate. An increase in the output of the melt polymer fibers is possible by reducing the distance between the multiple jets (interjet distance) forming around the rim of the nozzle, and thus expanding the number of Taylor cones produced (Fig. 5 e, f). Shorter
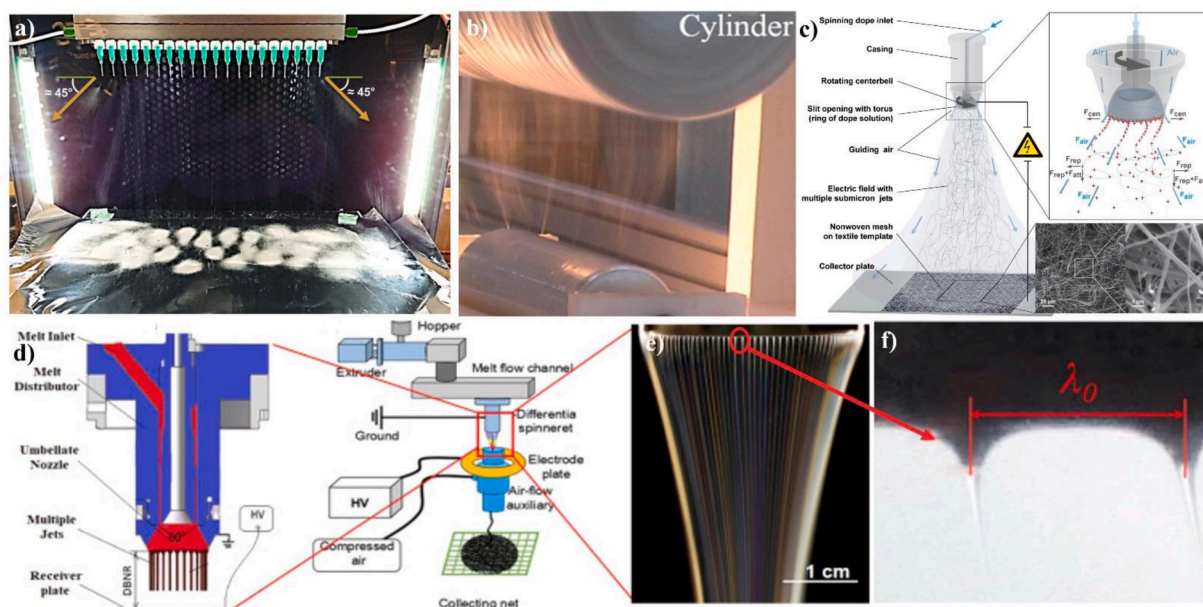

Fig. 5. (a) Multi-needles ES set up; adapted with permission from [96]. (b) Needleless ES using spiral coil spinneret; adapted with permission from [94]. (c) Centrifugal ES set-up; adapted with permission from [97]. (d) Umbrella like spinneret and schematic diagram of melt polymer differential ES; (e) formation of multiple melt polymer jet; (f) definition of interjet distance; adapted with permission from [98].

Table 2

A comparison between scale up electrospinning methods to fiber manufacturing.

Electrospinning Technique	Method	Polymer[1]	Solvent[2]	Productivity	Electrospun fiber size	Application	Refs.
Needleless	Anular spinneret	PAN	DMF	~4.5 g/h	~133- 351 nm	Air filtration	[100]
	Needle roller electrospinner	PVA	DI	~12.8 g /h	~190 nm	–	[103]
	Anular spinneret	PVP PCL Silk fibroin PANI /PAA PAN PVDF/ PEG	DMF/Ethanol/DI TFA Trifluororethylene DMF DMF DMF/DI	~4.8 g/h	< 2 μm	–	[104]
	Yarn spinneret	PAN	DMF	~1.17 g /h	~100–117 nm	–	[105]
	Threaded rod spinneret	PEO	DI and ethanol	~5–6 g/h	~100–500 nm	–	[106]
	Linear flume spinneret	PAN	DMF	~4.8 g/h	~108–210 nm	–	[107]
	Mushroom-spinneret.	PAN	DMF	13.7 g/h	~100–200 nm	–	[108]
	Bullet spinneret	PVA	Water	~1.08–4.55 g/h	~123–546 nm	–	[109]
Multi-needle	–	TPU	–	~50 g/h	~145 nm	Air filtration for PM$_{2.5}$	[110]
High speed (HSES)	Rotational spinneret	SBE-β-CD	VOR and water	~240 g/h	~0.5 – 2 μm	–	[111]
	Rotational spinneret	PVA	DI	~3.6–6 g/h	~271–477 nm	Biopharmaceutical	[112]
Air-blowing assisted Coaxial	–	PVP	DMF	~3.6 g/h	~1–16 μm	–	[113]
Centrifugal	Single subdisk	PS PVP	Chloroform Ethanol	~25 g/h	~263–8372 nm	Mask filter	[114]
	–	PVP TPU	Ethanol DMF	~50 g/h	~2.8–8.9 μm ~1.8 – 5.4 μm	Biomaterial and biomedical	[115]
	–	PEO PLA	Water Chloroform	~38.3 g/h ~12.8 g/h	~180 nm ~525 nm	–	[97]
Melt Differential Centrifugal (MDCE)	Centrifugal differential disk	PP	(Solvent-free)	~124.3 g/h	~790 nm	–	[116]
Melt Differential (PMDES)	Umbrella-like spinneret	PP/PLA	(Solvent-free)	~0.3–0.6 kg/h	~300 nm	Biomedical and tissue engineering	[98]
Melt	600-nozzle spinneret	PLA	(Solvent-free)	~0.9–5.1 kg/h	~1 μm	–	[117]

[1] Polymers abbrevations: PAN (Polyacrylonitrile); PVA (Polyvinyl acid); PVP (Polyvinylpyrrolidone); PCL (Polycaprolactone); PANI (Polyaniline); PAA (polyacrylic acid); PVDF (Polyvinylidene fluoride); PEG (polyethylene glycol); PEO (polyethylene oxide); TPU (Thermoplastic polyurethane); SBE-β-CD (Sulfobutylether-β-cyclodextrin); PS (polystyrene); PLA (polylactic acid); PP (Polypropylene). [2]Solvents abbrevations: DMF (N, N-Dimethylformamide); DI (De-ionized water); TFA (trifluoroacetic acid); VOR (Voriconazole).

interjet distance can be obtained by applying high electric fields during the spinning process as well as by lowering the value of the polymer melt viscosity by varying the nozzle temperature [117,124,125]. Despite the high-rate production, the resulting fibers are still large, exceeding 1 μm in size than those fabricated by means of solution ES methods. To address the drawbacks due to the large diameter limitation, nontoxic additives have been blended with polymer to produce submicron fiber [98,126]. Scale up production line for melt ES providing polymers electrospun membrane sheet of width around 1.6 m with 1–10 m/min speed production have been reported in literature [98]. The productivity efficiency of synthetic PP and biodegradable PLA electrospun membranes were comparable with those reported for standard MB lines, which provided high throughput rate around ~1 kg/h [21]. Also, a scalable set-up for melt Centrifugal ES has been designed with the inclusion of nozzle spinneret to generate multiple jets from the rim disk and enhance the throughput rate of nanofibers [116] (Table 2). A list of international companies that supply several ES equipment based on needleless and centrifugal technologies for industrial production of nanofibers, has been reviewed in other works [127,128]. The advantage of melt ES processes, including the Needleless and Centrifugal ones, is due to a reduction in cost of solvent recovery that brings to a more sustainable manufacturing process of polymer membranes. However, the high processing temperatures ensure that only thermoplastic

polymer showing high decomposition temperature can be processed [95]. On the other hand, less toxic solvent-based ES methods can be a solution to high productivity of biopolymer membranes, due to their low impact on environmental waste, life cycle and health assessment [119]. Further assessment on environmental cost and impact for many alternative green solvents is necessary to reduce the risk caused by using hazardous solvents and to allow a more sustainable manufacturing process for large scale polymer membranes.

3.3. Electrospinning parameters and filtration efficiency

ES technique has shown to be a low expensive approach to design nanofiber with controlled size. Many processing ES parameters, including applied voltage, distance between the two electrodes, nozzle tip (needle) diameters, and flow rate, as well as polymer concentration in the solution, can be properly tuned to control structural morphology and orientation distribution of the fibers [129–133]. Among these parameters, the polymer concentration strongly affects the fibers diameter. It was observed that lower viscosity in the ES solution involves the formation of finer fibers in the electrospun membrane [134–137]. A reduction of the fiber size in the range of nanofiber is required to obtain high filtration efficiency against submicron particles [138–140]. Indeed, the probability of fine aerosols to impact the ultrafine fibers increase due

to the high surface area, whereas small interstitial sites between the fibers improves the ability of the membranes to remove particles bigger than the pores size because of the sieving effect [141]. Also, an increase of the basis weight for a given surface or thickness obtained with a longer deposition time during the ES process has proven to be a good strategy to improve filtration efficiency of the filters [142–144]. However, the use of thicker layers as well as that of small fibers can negatively affect the air permeability of the fabric resulting in an increase of the pressure drop with consequences on the breathability. Therefore, the overall performance of the filter can be estimated by means of the calculation of the quality factor (QF), which takes into account both the pressure drop (ΔP) and the filtering efficiency towards particles (η) [141]:

$$QF = -\frac{\ln(1 - \eta)}{\Delta P} \tag{1}$$

Better filter performance can be obtained for high QF values, which means to keep low pressure drop and high particles filtering efficiency.

One strategy to obtain effective filtration is that to fabricate electrospun fibers with high interconnectivity or porosity. An enhanced porosity can involve a proper airstream across the electrospun membrane with a significant reduction in the pressure drop, without affecting the ability of capture of the nanofibers against submicron particles [62,141].

4. The use of electrospun nanofibers in surgical mask and respirator applications

4.1. Improvement of the face mask's performance by using nanofibers

In recent years many synthetic and thermoplastic polymers such as PVDF, PAN, PP, Polyimide (PI), and polystyrene (PS), have been electrospun in fibers to improve the prevention of infection from expiration of airborne contaminants [4,18,27]. A reduction of the fiber diameter as well as of the interstitial space between the fibers has been observed to lead to a significant improvement in mechanical adsorption of fine particles in several polymer based electrospun membranes [145–148].
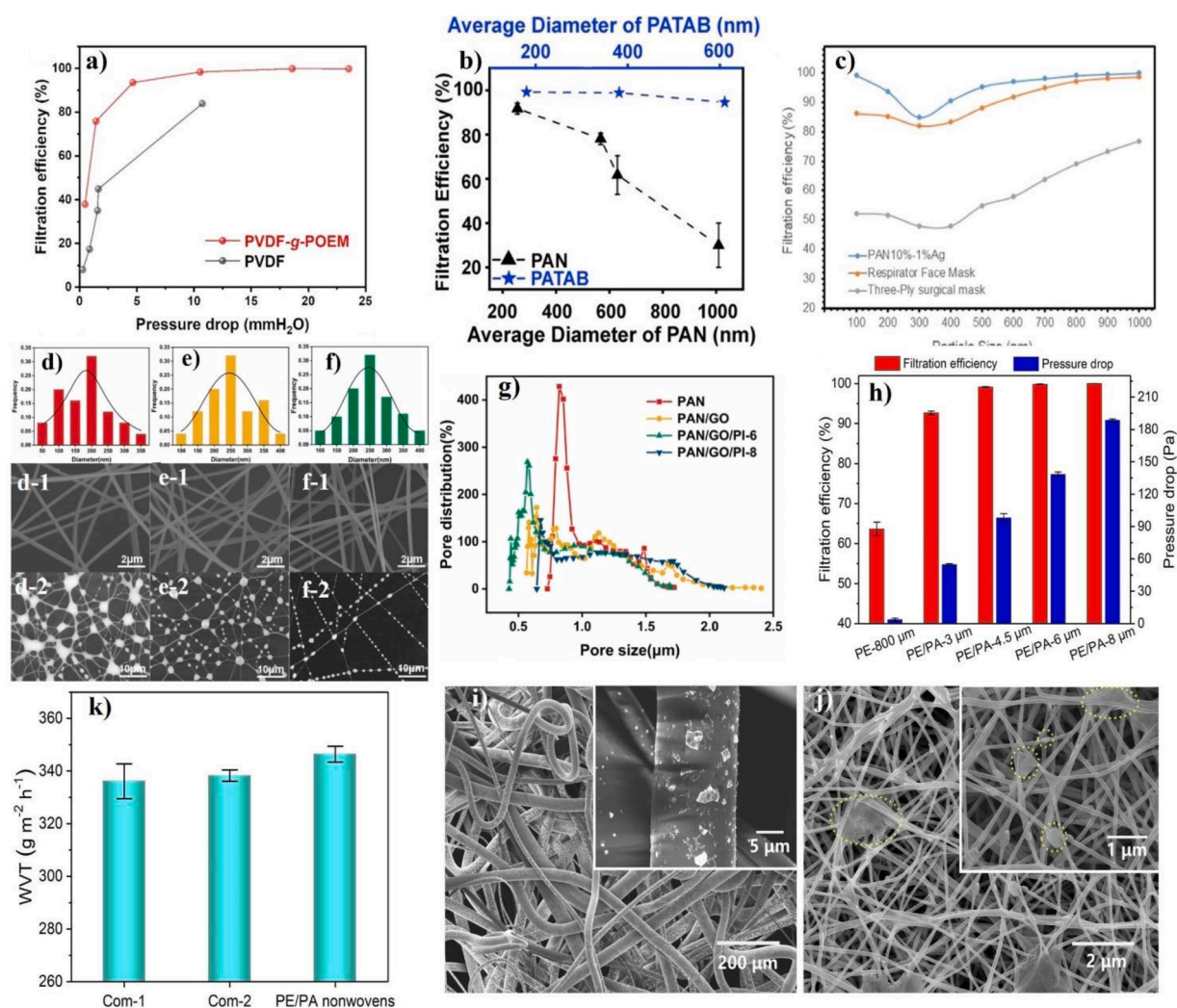

Fig. 6. (a) Comparison between the filtration efficiency measured for PVDF and amphiphilic PVDF-*g*-POEM double comb copolymer for different pressure drop values; adapted with permission from [146]. (b) Filtration efficiency values measured for PAN electrospun fibers as function of different average diameter; adapted with permission from [148]. (c) Filtration efficiency measured for PAN10%−1%Ag (1.50 g/m2), Respirator Face Mask and Three-Ply surgical as function of aerosol particle size; adapted with permission from [147]. Diameter statistics of (d) PAN, (e) PAN/ (Graphene oxide) GO, and (f) PAN/GO/PI-6 nanofibers; SEM images of (d-1) PAN, (e-1) PAN/GO, and (f-1) PAN/GO/PI-6; SEM images and illustration of (d-2) PAN, (e-2) PAN/GO, and (f-2) PAN/GO/PI-6 nanofibers after PM$_{2.5}$ adsorption; (g) pore size distribution measured for PAN, PAN/GO, and PAN/GO/PI electrospun membranes; adapted with permission from [149]. (h) Filtration efficiency and pressure drop measured for multilayer PE/PA with different PA electrospun membrane thickness; SEM images obtained for (i) PE meltblown nonwoven membrane and (j) PA electrospun one after filtering the PM; (k) water vapor transmission rate test measured for the PE/PA and two different commercial face masks, namely com-1 and com-2; adapted with permission from [150].

Ultrathin PVDF-*g*-POEM electrospun fibers exhibited higher performance in capturing NaCl particle (≤ 0.3 um) compared to PVDF nanofibers with larger diameter (Fig. 6 a) [146].

When the small fibers and the mean free path of air become comparable, a slip flow regime occurs for the nanofibers, resulting in a low pressure drop for the electrospun membranes as well. Moreover, from an analysis of the filtration test performed on PAN nanofibers prepared at different fiber size, a significant drop in both particle capture of $PM_{2.5}$ (particle size < 2.5 μm) and pressure drop has been observed and attributed to the presence of large diameter fiber and wide pore size in the electrospun membranes (Fig. 6 b) [148]. Additionally, small pore size in electrospun membranes improved the capture of particles of greater dimension because of the sieving effect. The measures of minimum efficiency values obtained from particle filtration curves performed on several PAN nanofibers have proven to be comparable with the average pore size, thus indicating that particles slightly smaller in size were the most penetrating in the filters [147]. Nevertheless, because of the small inter-fiber space, the least efficiency measured for PAN electrospun membranes were shifted to a lower particle size range, providing a better interception of submicron particles compared to those observed for commercial filters used in face masks (Fig. 6 c). Also, Dai et al. reported that a decrease in pore size leads to a better capture of aerosols particles [149]. From an analysis of the Scanning Electron Microscopy (SEM) images performed on the PAN, PAN/ Graphene oxide (GO), and PAN/GO/PI membranes they noted that within the same adsorption time the amount of $PM_{2.5}$ particles, present with the shape of beads, were more uniformly adsorbed on the nanofibers composed of PAN/GO/PI and in greater amount than those found on PAN (Fig. 6 d–f). The best interaction occurred between nanofibers and submicron particles has been attributed to the uniform inter-fiber space distribution observed at 0.5 μm, which was lower in size and narrower compared to those observed for other PAN and PAN/GO electrospun membranes (Fig. 6 g). In Table 3 a summary of the performances obtained from recent electrospun membranes-based face masks is provided for a comparison.

As it can be seen in Table 3, the measurements performed so far on several natural and synthetic polymer-based electrospun filters demonstrate that in addition to small fiber size also the area of the pores results to be lower compared to those reported for commercial face mask [191–193]. These results therefore indicate that the optimization of both fibers and inter-fiber space in electrospun membranes can be beneficial to achieve proper nanofibers filters with high filtration effectiveness to remove submicron particles. The application of electrospun fibers as filter to improve performance in commercial face mask has been also investigated. The inclusion of PS/PVDF nanofiber membranes inside a N95 respirator has been observed to provide higher filtration performance compared to the standard one, showing also low pressure drop at ~ 72 Pa, well below the maximum limit imposed by the NIOSH standard (Table 1) [172]. On the other hand, the application of electrospun PAN/ based microporous carbon nanofibers (MCNFs) in face masks proved a significant reduction in facial temperature recording during exhalation and inhalation test, thus making them more comfortable during the breathing compared to a common mask [194]. Combining electrospun fibers and melt blowing fabric with different pore and fiber morphology in masks turned out to be an excellent way to fabricate new face masks with excellent filtration performance and more comfortable wearability. From a comparison between the filtration curve measured for the pristine MB based polyethylene (PE) membranes and those obtained for multilayer designed at different thickness of electrospun Nylon-6 (PA) fibers, it is shown that the addition of ultrathin PA significantly improved the capture of fine particles in the multilayer PE/PA (Fig. 6 h). This analysis was in accordance with what was observed in the SEM images performed on PA and PE membranes, where an evident capture of low particle size prevalently occurred in the PA membranes due to the smaller fiber and micro-pore size (Fig. 6 i, j). A similar result has been reported in the work carried out by Yuanqiang Xu et al. where a

higher capture of fine particles with size below 0.5 μm was attributed to the addition of electrospun nanofiber with smaller inter-fiber space on MB-based PE membrane, which was made instead of larger pores [160]. Furthermore, experimental evidence based on water vapor transmission rate (WVT) revealed that multilayer membranes based on electrospun and MB fabric provided higher values of WVT compared to that observed in commercial face masks, thus proving a better passage of moisture air during exhalation, and therefore a less human discomfort in wearing the mask [150,160] (Fig. 6 k). Also, the measures obtained from the air permeability test, which is related to the pressure drop of the fabric and is defined as the rate of the air passing through the membrane under a certain pressure, were found to be comparable and in accordance with the standard required for commercial face masks, thus ensuring a proper breathability in the multilayer fabric [150]. These results indicate that a combination of micro and nanofibers in a multilayer membrane can involve a better breathability over commercial face mask, while providing an effectiveness capture of PM. It is worth noting that electrospun of thin polymeric nanofibers on thicker MB membranes allow to address the drawback due to the poor mechanical properties. Furthermore, the addition of nanofiber with sub-micron pores structures in MB based face mask can face the issues of discharge dissipation in a high humidity exposure for used charged fibers and ensure a more stable filtration performance, without the need of further electrostatic treatment for the membranes.

4.2. Eco-sustainable polymer materials for nanofiber masks

The polymers employed for membrane manufacturing are non-degradable and even worse their production as well as their disposal is not sustainable environment-wise, in most cases [195]. The outbreak of pandemic has revealed these environmental issues, given the large amount of plastic pollution due to the improper disposal of discarded masks [196–198]. It was estimated that just the 1% of the total disposed masks, which is around 10 million of mask for month, corresponds to a plastic weight ranging between 30 – 40 tons dumped in the environment [199]. The plastic fibers composing the inner and outer layers of waste masks, such as PP and PE, can be broken down in smaller parts, also defined as microplastics (MPs), and remain in the environment for a very long time [200]. Besides, these MPs can further decompose due to a series of potential aging process, including physical abrasion, ultraviolet (UV) radiation, and chemical oxidation, and so release toxic additives as well as provide attachment points for microorganism with negative consequences for ecosystem and human health [201]. The enhancement of the ecotoxicity of the MPs released in open sea, which is provoked by the continuous accumulation of plastic coming from disposable masks at the landfills, is rising up nowadays a global concern [202,203]. Therefore, the urgent need to implement more sustainable development has become a relevant issue to address in the increasing demand of face masks [156]. To reduce the environmental impact due to the massive use of disposable masks, some researchers explored the fabrication of high efficiency filter material by employing recycled polyethylene terephthalate (PET) [164] (Fig. 7 a).

Investigation on ES of recycled PET filter have been carried out with satisfactory results on PM removal efficiency and low pressure drop [189]. The latest works have shown how filters based on PET waste nanofiber can be achieved by optimization of the ES parameters and can additionally be redissolved and reprocessed, without losing their performance in filtration [164]. The use of recycled expanded polystyrene (EPS) for the manufacturing of multilayer electrospun filter mask with different fibers size provided promising performances for both submicron particles filtration ($\sim 99.4\%$) and optimal pressure drop, ranging between 48 and 58 Pa [165] (Fig. 7 b, c). Therefore, the feasibility in using recycled materials such as PET and EPS for the fabrication of face mask could be considered to implement a circular economy and a significantly lowering in the environmental impact in terms of resources consumption and environmental pollution for future policies [205,206].

Table 3

Performance of electrospun filter for face mask application.

Tested aerosols particles	[1]Electrospun fiber composition	PFE	BFE	Pressure drop	Quality Factor (QF)	Electrospun fiber size (Pore size)	Refs.
		(%)	(%)	(Pa)	(Pa^{-1})		
NaCl	Nylon-6 onto PE MB nonwovens (Face velocity 5.33 cm s^{-1})	>99	–	<100	~0.0486	~126 nm (6 µm)	[150]
	PMMA-EVOH onto spunbonded PP	~99	–	~44	–	~319 nm	[151]
	PVA (Needleless electrospinning)	~99	–	~78	~0.0593	~273 nm	[152]
	PAN/PVDF-PDMAEMA	<96	–	~78	~0.398	~190/525 nm	[153]
	PVDF-Si NPs[2]	99%	–	~392	~0.02	~1 µm	[145]
	PVDF/TTVB[3]	~99	–	~350	–	~479 nm	[154]
	PVDF-g-POEM (Face velocity 5.3 cm s^{-1})	>93%	–	–	~0.06	~77 nm	[146]
	(ABC)-type terpolymer (Face velocity 5.3 cm s^{-1})	~99	–	~177	~0.025	~400 nm	[155]
	PLA	~95	–	–	~0.014	~630 nm	[156]
	PLA	~99	–	~104	~0.094	~37.4 nm (0.73 µm)	[157]
	PA6/PVP/CS	~99	–	~54	~0.118	~130 nm	[158]
	CA-TiO$_2$	~99	–	~31	–	~278 nm	[159]
	PP/PLA-Ag NPs (Face velocity 10.67 cm s^{-1})	~99	–	~105	~0.048	~820 nm (5 µm)	[160]
	PS/Ag NPS	>97	–	<147	–	~ 3 µm-	[161]
	PAN/Ag NPs	~99	–	~65	~0.15	~320 nm (0.3–0.9 µm)	[147]
	PAN/Ag NPs/*Bontioides*/g-C$_3$N$_4$ (Face velocity 0.29 m s^{-1})	~99	–	~65	~0.097	~727 nm	[162]
	PVA/PEO/CNF/N-TiO$_2$	~98	–	–	–	~0.79 µm	[163]
	Recycled PET	>98	–	~36	–	~1.2 µm	[164]
	Recycled EPS (Face velocity 5.3 cm s^{-1}) (Needleless Electrospinning)	~99	–	~48	~0.099	~1.04 µm	[165]
	PVA/AG NPS (Face velocity 5.5 cm s^{-1})	97.7		~59	~0.09	~434 nm	[166]
	PVA/WS-CS[4] (Needleless electrospinning)	~97	–	~57	~0.0825	~217 nm (12–22 nm)	[167]
	PVA/SBE-βCD (Face velocity 5.3 cm s^{-1})	~99	–	~57	~0.82	~2.26 µm	[168]
	PAMAM/PAN/TEO (Needleless Electrospinning)	~98	–	~388	–	440 nm	[169]
Murine hepatitis virus A59 (MHV-A59) used in NaCl	PVDF-RB[5]	~99	–	~40	–	~200 nm (1.5–2.0 µm)	[170]
Polystyrene latex sphere (PSL) Virus surrogate used in PSL:influenza A (H1N1); coronavirus 229E;SARS-CoV-2(Delta variant);	PLA and Manuka oil	>99 ~99 ~99 ~99	~99	<58	–	~168 nm	[171]
–	PS/PVDF	~99	–	~72	–	–	[172]
–	PLA & phytochemical-based herbal-extracts (Needleless Electrospinning)	–	~97	~35	~0.097	~8 µm (20 µm)	[173]
–	PVB-Thymol	~83	~99	~46	–	~375 nm	[174]
–	Nylon 6 (Needleless Electrospinning)	–	~97	–	–	110–400 nm (0.6 µm)	[175]
Dioctyl sebacate (DEHS)	CA/TPU-LiCl	~99	–	~52	~0.12	~280 nm (0.9 µm)	[176]
	PVA-TA	~99	–	~35	~0.15	~430 nm	[177]
	PVA-LS	~99	–	~24	~0.212	~439 nm	[178]
PM$_{0.3}$	PAN	>97	–	~ 50–500	–	~430 nm (0.5–1.2 µm)	[179]
	PAN/ZnO NPs	~98.8	–	~48	~0.092	< 420 nm	[180]
	CA/AC/TiO$_2$ (Face velocity 0.8 m s^{-1})	~82	–	~63	~0.0271	–	[181]
	PAN/FPVDP@CNTs[6] (Face velocity 5.33 m s^{-1})	~99	–	~49	~0.1984	~113 nm (1.5 µm)	[182]
	Gelatin/β–Cyclodextrin (Face velocity 6 cm s^{-1})	>95	–	~148	~0.029	~130–247 nm (1–1.4 µm)	[183]
	SP/PS	>95	–	<343	–	–	[184]
	Zein on cellulose paper towel	99%	–	109	–	0.6–2.4 µm (0.2–0.3 µm)	[185]
PM$_{1.0}$	PLA	~98	–	~29	–	~274 nm (2.5 µm)	[186]

(continued on next page)

Table 3 (*continued*)

Tested aerosols particles	[1]Electrospun fiber composition	PFE	BFE	Pressure drop	Quality Factor (QF)	Electrospun fiber size (Pore size)	Refs.
	PLA-PA11	~89	–	~6.5	–	~76 nm	[187]
	PAN/silane/ZnO NPs	~99	–	~44	~0.137	1 < μm (19 nm)	[188]
PM$_{2.5}$	PAN/PI/GO[7]	~99	–	~92	~0.0576	~244 nm (0.5 μm)	[149]
	Recycled PET (Face velocity 4.8 cm s^{-1})	~100	–	~212	–	~1.27–3.25 μm	[189]
	PAN/CTAB[8]	>99	–	~11	~0.469	~150–200 nm (2–4 μm)	[148]
	PASS/Ag/ZnO	~99	–	~42	~0.07	~330 nm (2 μm)	[190]

[1] Electrospun fibers abbreviations: PE (Polyethylene); PMMA (poly(methyl methacrylate)); EVOH (ethylene vinyl alcohol); PVA (Polyvinyl acid); PAN (Poly-acrylonitrile); PVDF (Polyvinylidene fluoride); PDMAEMA (poly [2-(N,N-dimethyl amino) ethyl methacrylate]); g-POEM (graft-poly(oxyethylene methacrylate); (ABC)-type terpolymer (Poly(styrene-co-2-(dimethylamino)ethyl methacrylate-co-acrylonitrile))); PLA (polylactic acid); PA6 (polyamide 6); PVP (Poly-vinylpyrrolidone); CS (Chitosan); CA (cellulose acetate); PP (Polypropylene); PEO (polyethylene oxide); CNF (cellulose nanofibers); PET (polyethylene terephthalate); Polyarylene sulfide sulfone (PASS); EPS (expanded polystyrene); SBE-β-CD (Sulfobutylether-β-cyclodextrin); PAMAM (polyamidoamine dendritic polymers); TEO (tea tree essential oil); PS (polystyrene); PVB (polyvinyl butyral); CA (cellulose acetate); TPU (Thermoplastic polyurethane); TA (Tannic acid); LS (lignosulfonate); AC (activated charcoal); FPVDP (fluorinated polyvinylpyrrolidone); SP (Spiropyran); PS (polystyrene); PA11 (Polyamide-11); PI (Polymide).
[2] NPs (Nanoparticles).
[3] TTVB (organic photosensitizer).
[4] WS (water soluble).
[5] RB (Rose Bengal).
[6] CNTs (Carbon nanotubes).
[7] GO (Graphene oxide).
[8] CTAB (Cetyltrimethylammonium bromide-Br^{-}).

Also, the utilization of renewable and biodegradable thermoplastic polymers, such as PLA and polyvinyl butyral (PVB), has shown to be a sustainable alternative to produce effective filters comparable to many commercial face mask [156,157,173,174,207]. Wang et al. designed a biodegradable face mask entirely formed of PLA polymer [157]. The assembly of nanofibers layers with different diameter size, provided a multi-scale structure in the membrane with high porosity and small pore size, which was able to maintain high filtration performance against PM$_{0.3}$ also after a prolonged exposure in high humidity environment (Fig. 7 d, e). Besides, from a study on the weight loss in degradation (WL), they observed that the PLA-based face mask was completely decomposed from microorganism present in soil after being buried in for 150 days (Fig. 7 f, g). A similar result in biodegradation performance has been reported also by Patil et al. [173]. The SEM images performed on the 3-ply cotton-PLA-cotton layered face mask after 20 days of pre-treatment with a slurry consisting of fresh cow-dung microflora, revealed an extensive growth of bacteria colonies on the PLA nanofiber surface, thus suggesting an effective biodegradation process occurring on the membrane (Fig. 7 h). The filtration performance of green PLA face masks result to be comparable with that obtained for multilayer membranes of MB and synthetic electrospun nanofibers seen above [150,160] (Table 3). On the other hand, the biodegradable PLA-based face mask can be easily decomposed trough biological process in a reasonable time, thus resulting in less pollution for the environment. In addition to synthetic and biodegradable polymers, the cellulose nanofibers have been receiving attention as emerging raw materials because of their abundant availability and for their properties, such as biodegradability, renewability, high mechanical strength, porosity, etc. [208–210]. Recent works have focused on the ES of polymers and cellulose blends for the development of filter materials, reporting promising performances for face mask/ respirators [158,211,212]. Additionally, the cellulose acetate (CA) has shown to be an eco-friendly alternative to petroleum-based non-biodegradable polymers for the fabrication of electrospun nanofiber filters [159,181,213]. Wang et al. investigated the application of CA by means of ES technique to design new biodegradable filter for face mask [176]. The electrospun membrane based on CA, thermoplastic polyurethanes (TPU), and lithium chloride (CA/TPU-LiCl) showed high filtration efficiency (99.8%) against dioctyl sebacate (DEHS) aerosol micro particles with low pressure drop (~ 52 Pa). To test the reusability, a standard disinfection method

involving alcohol has been performed on the biodegradable CA/TPU-LiCl membrane. The disinfection test revealed a high resistance of the electrospun filter to alcohol soaking, such that after ten repeated cycles both the filtration performance and the pressure drop remained quite stable around 98.2% and 34 Pa, respectively. The degradation of CA can occur in the soil surface as well as by means of microorganism and enzymes treatments, but the rate is strictly dependent on the environmental conditions in which the natural polymer is subjected [214]. A recent study carried out by Samadian *et al.*, demonstrated that the inclusion of berberine in a CA/gelatin based electrospun nanofibers enhanced the degradation rate of the membrane, which resulted in a high weight loss around ~ 80% after only 14 days of exposition in PBS solution [215]. Also, Oldal et al. observed that CA electrospun nanofibers membrane can be easily degraded by means of natural enzymes, such as cellulase and esterase [204]. Compared to pristine CA nanofibers, a faster response in the degradation process has been observed for CA membranes pretreated in solution with green surfactant (Fig. 7 i–l). The use of tetrabutylammonium bromide (TBAB) and High-foaming Honey Surf (HS) made the access to the polymer chain of CA-based membrane easier for both enzymes, thus improving the biodegradation process in the observed elapsed time of 16 h. These results indicate that electrospun membranes based on natural polymers, such as PLA and CA, can be a valid solution to fabricate more sustainable and high-performance face mask, to relieve the high consumption of petroleum-derived plastics polymers, which is used in the manufacturing of disposable commercial face mask, and to prevent possible effect on environmental hazard in the long run.

4.3. Nanoparticles surface modification for better antibacterial and antiviral electrospun face masks

Face masks provide a useful physical resistance to the transmission of aerosol carriers of either viruses or bacteria, but a high risk of contamination occurs on the fabric for long time usage. Considering therefore the current COVID-19 pandemic, the importance of providing stable self-cleanable filters with strong antibacterial and antiviral activity has led to the development of nanoparticles (NPs) embedded electrospun nanofibers, in the past few years. The ES of hybrid materials has shown to be a straightforward and innovative approach to process and stabilize NPs either onto or into the electrospun nanofibers membranes. The
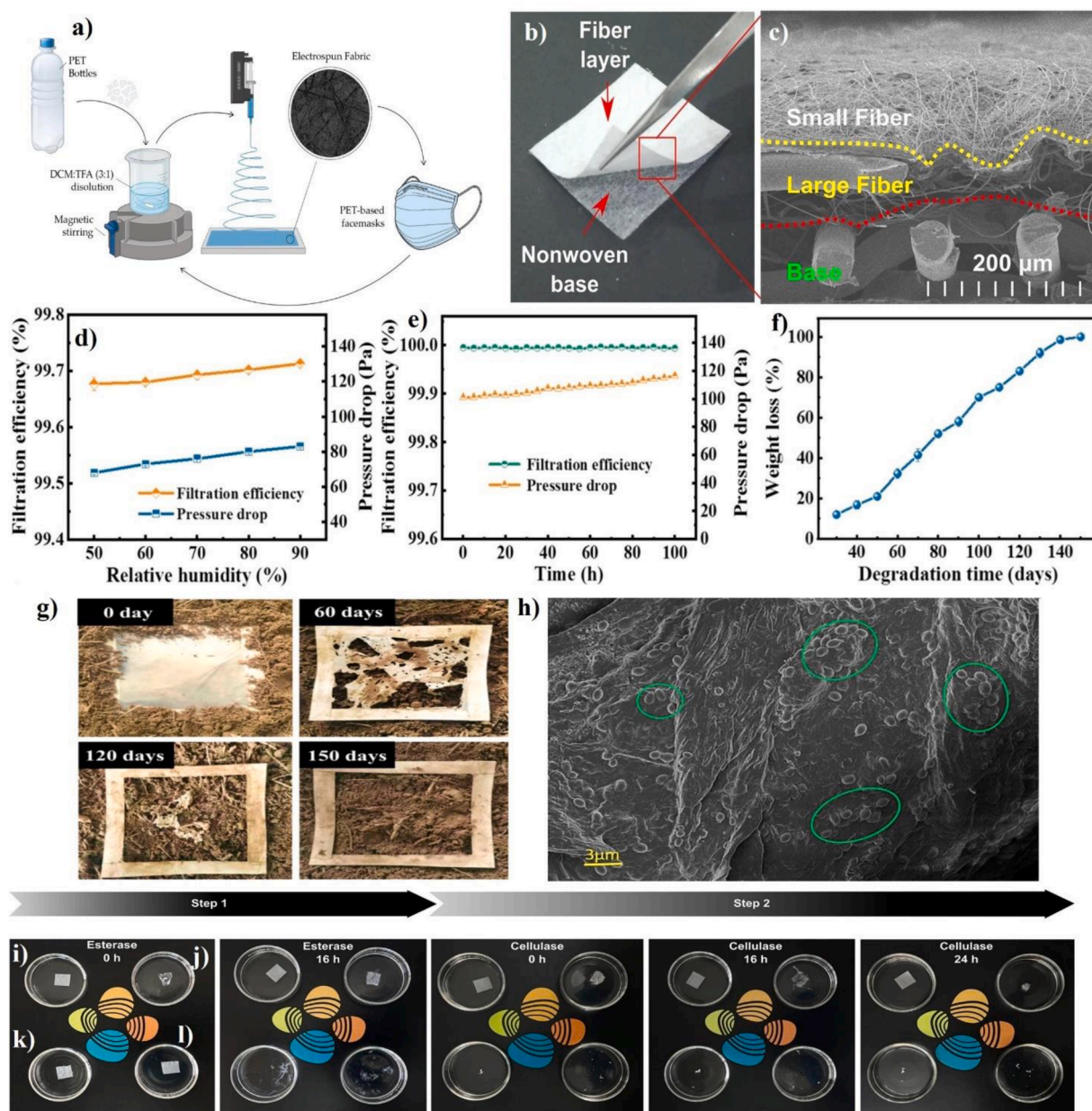
Fig. 7. (a) Schematic diagram of a face mask obtained by bottle recycled PET; adapted with the permission from [164]. (b) Example of nonwoven base with multiple EPS fiber layers for air filter; and (c) SEM image of the membrane cross-section, indicating the three different fiber sizes; adapted with the permission from [165]. (d) Filtration performance measure for the three-layer face mask based on PLA electrospun membranes at different relative humidity and the (e) long-term filtration stability test carried out, under 90% humidity; (f) weight loss measure for the for the three-layer face mask based on PLA electrospun membranes after being buried in outdoor soil; (g) images taken to the three-layer face mask based on PLA electrospun membranes showing the soil burial degradation within the 150 days; adapted with permission from [157]. (h) SEM image showing the bacteria growth on PLA surface after 20 days of treatment in cow-dung, jaggery and water containing biodegradation slurry; adapted with permission from [173]. Biodegradability tests performed on the CA electrospun based membranes by employing esterase and cellulase enzymes: (i) Polypropylene fibrous membrane used as control, given its non-susceptibility to degrade under enzymes conditions; (j) CA nanofibers tissue; (k) CA nanofibers tissue processed with tetrabutylammonium bromide (TBAB); and (l) CA nanofibers tissue processed with High-foaming HoneySurf (HS); adapted with permission from [204].

antimicrobial effectiveness of metal NPs, such as Au and Ag, as well as metal oxide NPs, such as, TiO_2, CuO, ZnO, and MgO, have been studied with several human pathogens bacteria such as *Escherichia coli* (*E. coli*) and *S. aureus* [216–220]. Most of these inorganic NPs exhibit bactericidal properties either through photocatalytic activity, where reactive oxygens species (ROS) are induced by visible or UV light to affect the cell viability by hindering principal mechanisms of protein and enzymes, or by electrostatic interaction with the bacteria cell wall, where NPs bind electrostatically the cell membranes causing their alteration in both potential and depolarization thus involving respiratory disfunction and

eventually the cell death [221]. Several studies reported about the efficacy of ZnO as antimicrobial coating for surfaces exposed to possible contamination of either bacteria or SARS-COV-2 [222–225]. It is well known that both Zn and ZnO are of particular interest as supportive treatment in therapy of COVID-19 infection [226–230]. The fabrication of several based polymers electrospun embedded with low-cost ZnO NPs have been investigated and proposed for protective clothing application. Nanofibers made of Polyvinyl pyrrolidone (PVP) and PVA with the addition of ZnO NPs showed antimicrobial activity against *S. aureus, E. coli, Klebsiella pneumonia* and *Streptococcus aeruginosa* tested bacterial

strains [231]. The incorporation of ZnO NPs at 10 wt.% in the poly- L-lactic acid (PLLA, or polylactide) electrospun membrane was observed to improve the mechanical properties as well as the bacteriostatic action against *S. aureus* [232]. A noticeably enhancement of the mechanical strength occurs also for PVDF nanofiber loaded with 5 wt.% of ZnO NPs, since an elongation-at-break equal to $(30 \pm 2)\%$ was observed compared to the pristine PVDF nanofibers, which owns $(24 \pm 0.5)\%$ [233]. Cytotoxicity test proved the nontoxicity for 5% ZnO—NPs@ PVDF nanofibers. Besides, for these NPs loading the hybrid PVDF nanofiber exhibits a high antiviral activity against human adenoviruses type-5 (ADV5) in both the adsorption and virucidal mechanisms; therefore, the fabric has shown to easily prevent both the entry and the replication of the virus in the cells. An activity increase against colistin resistant bacteria, such as *K. pneumoniae* strain 10, has been observed for thermoplastic polyurethane (TPU) nanofibers with 4% ZnO [234]. Moreover, it has been shown that a higher presence of ZnO on the nanofibers membrane involves a lower ability of the SARS-CoV-2 spike protein to engage with the human cell receptor (ACE2). Therefore, the concentration of the metal oxide in the TPU nanofibers resulted to be crucial to inactivate the virus. Abdul Salam et al. [235] have investigated both the antibacterial and antiviral properties of hybrid PAN nanofibers with 5 wt.% ZnO as function of the HeiQ Viroblock (VB) concentration. They observed that the higher the amount of VB in the PAN/ZnO electrospun the higher is the antibacterial efficiency of the hybrid membrane against both *S. aureus* and *Pseudomonas aeruginosa,* with efficiency values equal to

92.59% and 88.64% respectively. Besides, the PAN/ZnO sample loaded with the maximum concentration of VB (5%) showed a significant antiviral activity against avian influenza virus compared to the pristine PAN sample. The antiviral mechanism behind the VB technology has been attributed to the combined action of the vesicle component and the inside silver ions. Indeed, the cosmetic grade liposomes forming the vesicle are expected to weaken the envelope membrane of the influenza thus allowing the silver ions to directly attack the inner core to destroy the virus (Fig. 8 a).

From the Transmission Electron Microscope (TEM) analysis performed on the PAN/ZnO samples fabricated at different concentration of VB is possible to observe the distribution of ZnO NPs on the nanofiber surface as well as the roughness of the single fiber due to the presence of VB (Fig. 8 b–e). As can be seen in Fig. 8 d, the surface of the nanofibers become more rougher by increasing the VB doping concentration in the electrospun solution, thus indicating that a greater amount of this viscous liquid being evenly deposited on the nanofiber matrix. These studies revealed that the presence on the fiber surface of ZnO NPs alone or with other active materials can be effective in preventing the spread of bacteria and viruses on the electrospun membranes. Their application as filters would allow to address the issues of bacteria proliferation observed in commercial face mask after prolonged use by removing possible contamination, which can represent a health risk especially for severe disease cases [66,68]. It is worth noting that the morphological changes occurring at the fiber surface level due to the inclusion of NPs
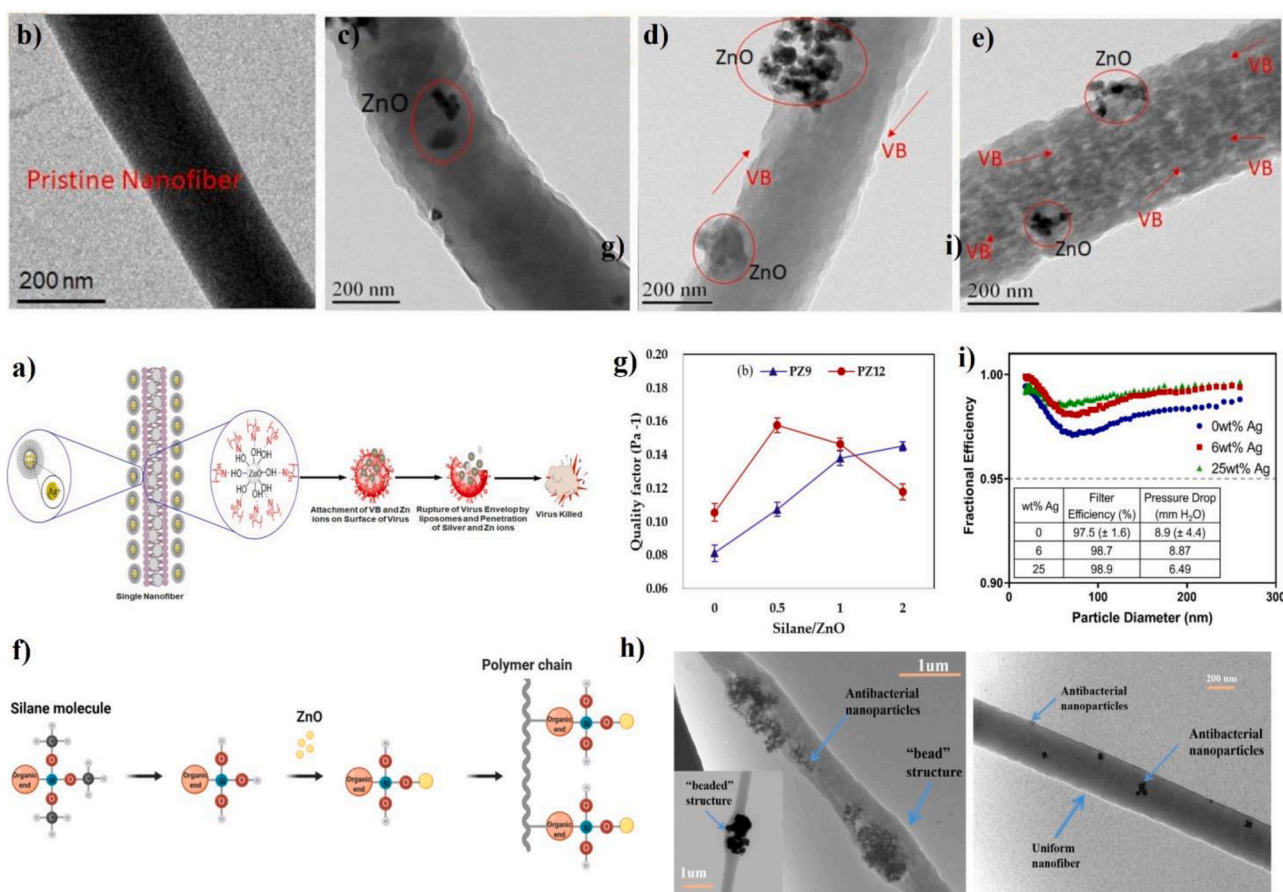

Fig. 8. (a) Schematic picture of antiviral activity of VB-loaded PAN/ZnO electrospun nanofibers; TEM analysis of VB-loaded ZnO/PAN electrospun nanofibers: (b) pristine PAN nanofibers; (c) ZnO/PAN nanofibers; (d) 2.5% VB-loaded ZnO/PAN electrospun nanofibers; (e) 5% VB-loaded ZnO/PAN nanofibers; adapted with permission from [235]. (f) Schematic diagram modification process for of ZnO NPs by means of the reaction with silane coupling agent MPTMS; (g) comparison between the QF measured for PAN nanofibers obtained at 9 wt% (PZ9) and 12 wt% (PZ12) for different silane/ZnO NPs mass ratio; adapted with permission from [188]. (h) TEM images obtained for PASS/ZnO/sulfide electrospun membrane showing both agglomerated (left) and more uniform NPs (right) distribution on the fiber surface; adapted with permission from [190]. (i) Filtration curves measured for PS electrospun membranes fabricated at different Ag concentrations and tested at different aerosol particle size; adapted with permission from [161].

materials also significantly affect the PM capture efficiency in electrospun membranes, in addition to the antibacterial and antiviral activity. Hanaa Aamer *et al.* observed a better filtration performance for PAN nanofibers functionalized with ZnO NPs compared to the pristine membrane ones [180]. They stated that the addition of ZnO NPs induced an increasing in surface roughness, with consequent reduction in stream of $PM_{0.3}$ through the membrane. In another work, they reported that a modification of the ZnO NPs obtained by means of the reaction with 3-methacryloxypropyltrimethoxysilane (MPTMS) led to a more uniform distribution of NPs on the PAN nanofibers surface, thus resulting in a better capture of both pathogens and aerosols contaminants (Fig. 8 f, g) [188]. On the other hand, a high content of ZnO NPs in polyarylene sulfide sulfone (PASS) electrospun membrane previously functionalized with Ag was reported to induce a gradually increase in mean pore size [190]. The addition of 2 wt% ZnO NPs provided a maximum filtration performance in PASS membrane, whereas with a further increase at 3 wt % the structures resulted in larger pore size that exceeded $PM_{2.5}$ size and brought to a drastic drop in particle capture efficiency. From the TEM image in Fig. 8 h is clear that the formation of two distinct distribution of NPs on the fiber surface, one more discontinuous with large and extended agglomerations and the other more evenly distributed, may explain the different overall filtration behavior occurring as consequences of the different contents of ZnO NPs added in the PASS membrane Moreover, the integration of Ag NPs proved to significantly increase the fibers diameter in PS electrospun membrane [161]. However, the even surface roughness formed from the addition of Ag NPs brought to a slighter increase in particle filtration and a low decrease in pressure drop, thus resulting in an enhancement in performance for the PS membrane (Fig. 8 i). Chen et al. observed that despite the addition of *M.bontioides* and Ag-CN compound made the fiber larger, the even increase of the roughness occurred at the fiber surface level led to an enhancement of the contact with both pathogens and aerosols contaminants thus involving a higher interception for tiny NaCl particles with size around 70–80 nm as well as a strong inhibitory activity against *E. coli, S. aureus,* and influenza A H3N2 [162]. The large amount of Mg, Ag, C, N, and O elements observed by the analysis of the SEM-EDX (Energy Dispersive X-ray Analysis) clearly indicated that *M. bontioides* and Ag-CN NPs were dispersed uniformly during the ES process (Fig. 9 a,
c).

This result was also in accordance with the TEM image in Fig. 9 b, which revealed the presence of heterogeneous Ag-CN NPs aggregates both above and inside the single nanofiber surface. As seen so far, a proper optimization of the ES process allows a stable and uniform distribution of NPs as well as for other active materials at single fiber surface level. This method can be beneficial compared to other recent approach adopted to functionalize commercial face mask, which may result instead in a coating instability for the surface functionalization over the time with an undesired effect on antimicrobial and antiviral properties [236–238]. Additionally, recent studies proved that several NPs materials with antimicrobial and antiviral properties, including MgO and CuO, are compatible when embedded in electrospun membranes based on natural polymers, such as CA and poly(ε-caprolactone) (PCL) [239,240]. Because of the incorporation of MgO NPs, the PCL-based electrospun showed a pronounced antibacterial activity against both *E. coli* and *S. aureus* as well as a remarkable improvement in filtration efficiency against polystyrene particles of 1 μm size [239]. Also, the addition of CuO in CA based electrospun membrane provided similar result in terms of antibacterial efficacy [240]. However, only the addition of $CUSO_4$ metal salts and thymol caused a drastically reduce of SARS-COV-2 virus, observed only after 1 h of contact with the functionalized CA membrane. Hence, the development of antiviral and antimicrobial face mask obtained from biodegradable materials could be also advantageous to prevent the transmission of SARS-COV-2 virus, as well as other potential hospital infections caused by bacteria, and to further reduce the impact on the environment, which is already put at risk due to the huge use of disposable mask. The functionalization of electrospun membranes by the addition of relatively nontoxic and low-cost NPs as well as other active compound can therefore be an affordable method to produce advanced electrospun membranes in view of large-scale production. These electrospun filters can provide desirable properties in terms of both particle filtration and antibacterial effectiveness, and significantly reduce the risk due to the handling and reuse of contaminated mask.
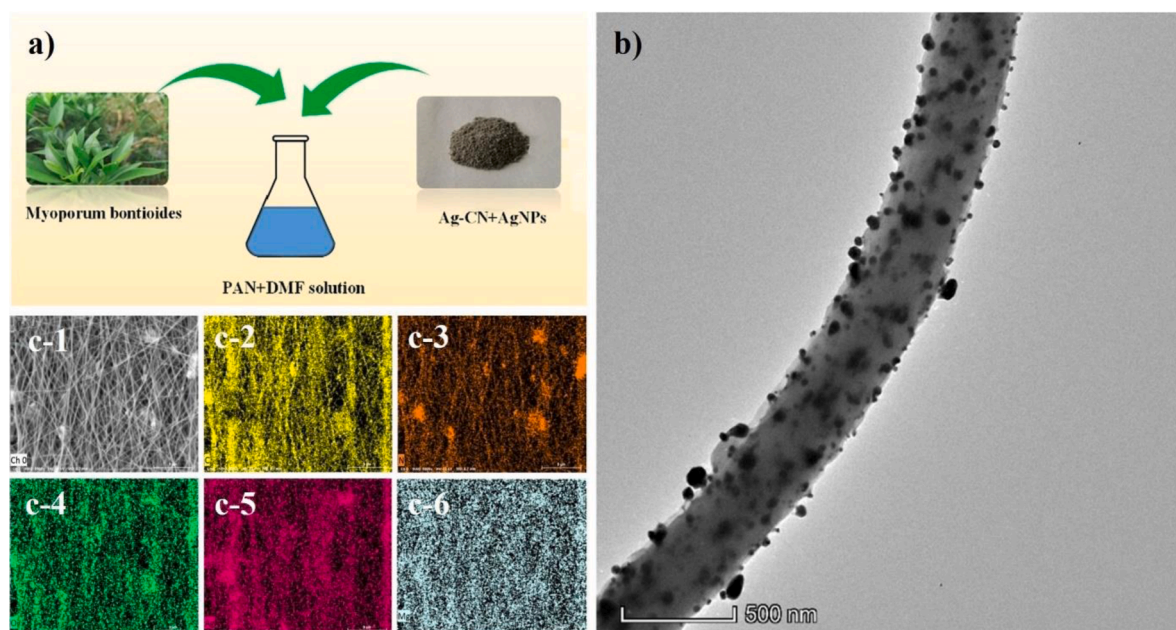

Fig. 9. (a) Electrospun solution for the fabrication of the PAN/*M.bontioides*/Ag-CN/Ag nanofibrous membrane; (b) TEM image of PAN/*M.bontioides*/Ag-CN/Ag nanofiber; SEM image of the PAN/*M.bontioides*/Ag-CN/Ag nanofibrous membrane (c-1) and with respective EDX analysis performed for C (c-2), N (c-3), O (c-4), Ag (c-5), Mg (c-6); adapted with permission from [162].

4.4. Electrospun nanofiber for self-powered wearable masks application

Electrostatic nanofibers are widely utilized in air filtration application. Polymer-based nanofibers with spontaneous dipole moment or optimal polarity provide an efficient electrostatic surface charge, which promotes the capture of opposite charged particles during the process of air filtering [145,146,148,172,184,241,242]. Experimentally it has been observed that an exposition of electrostatic nanofibers to external electric field involves a better capture of submicron particles than uncharged nanofibers, which rely only on interception and diffusion mechanical capture [243,244]. In addition to electrostatic induction, a large polarization and optimal formation of electrical charge have also been successfully achieved either by exposing polymers with piezoelectric property to mechanical stress [245] or through rubbing adjacent polymer membranes with opposite electronegativity, thus resulting in triboelectric effect on the interface [246]. Because of the high capacity to retain electrical charge, active polymer nanofibers have been used as triboelectric nanogenerators (TENGs) and Piezoelectric nanogenerators (PENGs) materials to develop energy harvesting air filters [247–250]. So far, several Respiration-driven TENGs (R-TENGs) designed with polymer-based electrospun nanofibers, including PVDF, PI, and PAN, have provided an effective electrostatic adsorption of submicron particles by harvesting electrical energy from human breathing [251–254]. The triboelectrification mechanism behind a R-TENG is based mainly on the contact-separation mode occurring between two different materials, showing distinct electron affinity [255]. To explain the working principle, a schematic diagram of the R-TENG fabricated by Fu et al. with PVDF electrospun membrane and cellulose aerogel/MOF (CA/Ni-HITP) composite is reported in Fig. 10 a, b [251].

Because of the tight contact occurring between the two layers, electrostatic charges of opposite sign can be induced by triboelectrification on the respective surfaces. This process can be seen in Fig. 10 b-(i), where a possible case of air exhalation during breathing can lead to the contact between the two materials, thus involving the generation of a negative triboelectric charge on the high electronegative PVDF based membrane and a positive one on the CA/Ni-HITP. When the two layers are separated, for instance during a further air inhalation, a potential difference is generated due to the electrostatic induction and a

transfer of charges occurs form PVDF to CA/Ni-HITP (Fig. 10 b-(ii)). This process occurs as long as the distance between them does not induce a neutralization of the charges, which would then result in an interruption of the current (Fig. 10 b-(iii)). After exhaling, the layers get closer again, thus inducing a positive charge on CA/Ni-HITP which balances the former negative triboelectric charge present on PVDF. This results in a reverse current, which is detected from the CA/Ni-HITP to PVDF (Fig. 10 b-(iv)). Therefore, the air pressure exerted during a continuously breathing cycle led to an alternate current, which constantly can charge the membranes (Fig. 10 c). From a comparison of the quality factors obtained for CA, CA/Ni-HITP, CA/Ni- HITP+PVDF, commercial face mask, and R-TENG, it can be noted that due to the triboelectric effect a significantly enhancement in capture of PM with size ranging between 0.3 −1 um occurred in the self-powered filter (Fig. 10 d). An improvement in filtration efficiency induced by triboelectric effect have been reported for other self-powered electrostatic adsorption face mask based on electrospun as well [249,250,252–254,256]. In Table 4, a comparison between the performances obtained for recent Piezoelectric and Triboelectric electrospun system is reported.

In particular, Hao et al. recently designed a self-powered triboelectric filter system based on PAN nanofibers doped with poly-(tetrafluoroethylene) PTFE nanofibrils and electroplated polyurethane (PU), which provided a high electrostatic adsorption of submicron particles, also after a prolonged use over the time [254]. Unlike the single electrospun filter, the $PM_{0.5}$ removal efficiency measured for the self-powered triboelectric remained quite stable, after one month of continuous filtration (Fig. 11 a, c).

Additionally, the measured pressure drop proved not to be drastically affected by the addition of an extra electrospun membrane and resulted also to be lower in value compared to that of commercial masks, thus proving a considerable advantage in breathability (Fig. 11 b). Nevertheless, the durability test performed on several self-powered air system revealed that in presence of different humid environment the submicron particles removal efficiency decreased, due to a possible dissipation of triboelectric charge on the fibers surface [250–252]. In particular, the experimental study of Guoxu Liu *et al.* carried out for PVDF electrospun based R-TENG clearly showed that the effect of triboelectric charge decay, which were caused by the humid
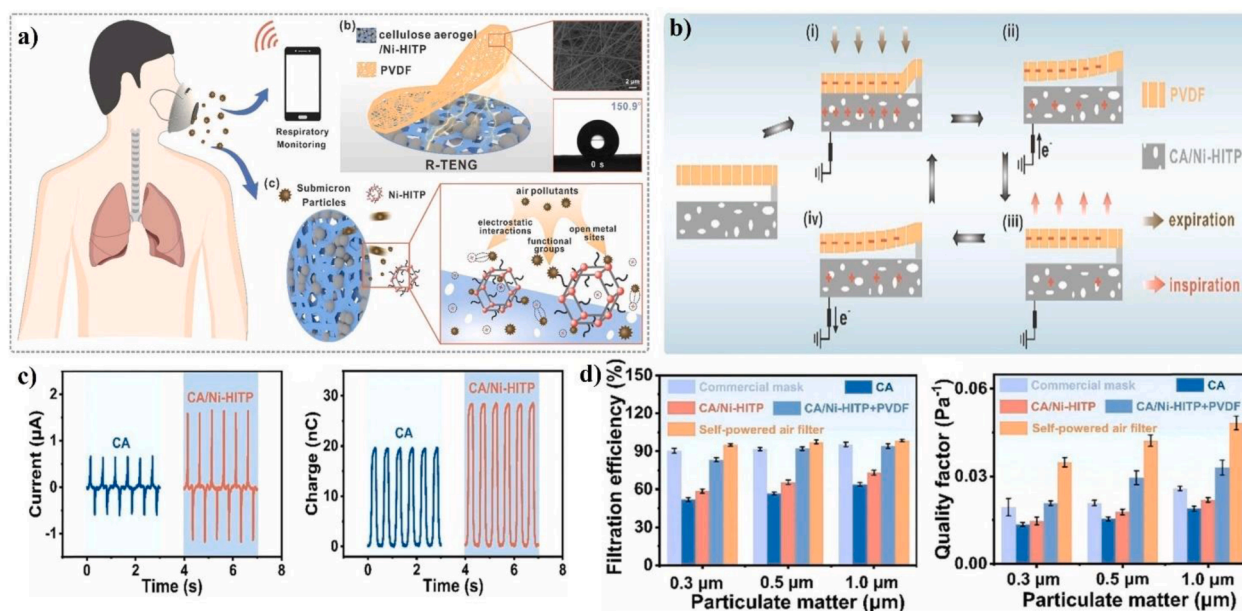

Fig. 10. (a) Self-powered air filter for respiratory monitoring and removal of submicron particles; (b) schematic diagram of the triboelectric effect of R-TENG; (c) short-circuit current and transferred charges of R-TENG before and after *in situ* growth of conducting metal organic- framework (Ni-HITP); (d) a comparison of PM removal efficiencies of commercial mask, CA, CA/Ni-HITP, CA/Ni-HITP+PVDF and self-powered air filter obtained at different submicron particle sizes; adapted with permission from [251].

Table 4

Piezoelectric and Triboelectric electrospun system for smart face masks application.

Pollutants	PFE	Pressure drop	Quality factor	[1]Polymer materials	Electrospun fiber size	Application	Refs.
	(%)	(Pa)	(Pa^{-1})				
PM$_{1.0}$ PM$_{0.5}$ PM$_{0.3}$	~98.4 ~97.3 ~95	~86	~0.03 – 0.05	PVDF	<1 μm	Self-powered face mask (R-TENG)	[251]
PM$_{0.5}$ PM$_{1.0}$ PM$_{2.5}$ PM$_{5.0}$ PM$_{10}$	>86.9	~57 (Face velocity 10 cm s^{-1})	–	PVDF	<2 μm	Self-powered face mask (R-TENG)	[252]
PM$_{0.3}$ PM$_{0.5}$ PM$_{1.0}$ PM$_{2.5}$ PM$_{5.0}$ PM$_{10}$	>90	~10–60	–	PI	<1 μm	Self-powered face mask (R-TENG)	[253]
PM$_{0.3}$ PM$_{5.0}$	~99	~797	>0.005	PVDF/PAN	~572/244 nm	Monitoring self-powered face mask (RM-TENG)	[257]
PM$_{0.5}$ PM$_{2.5}$	~91.5 ~98	~98	–	PAN doped with PTFE and electroplated PU sponge	~150–200 nm	Self-Powered Filter for Respirator device	[254]
PM$_{0.3}$	~99.5	~200 (Face velocity 18.6 cm s^{-1})	~0.019	PVDF on nylon mesh	~260 nm	Self-charging triboelectric/piezoelectric face mask filter	[256]
PM$_{0.3}$	~99.7	~38	~0.154	PEO	~764 nm	Monitoring self-powered filter for face mask	[258]
PM$_{1.0}$ PM$_{2.5}$	>91 >99	91 (Face velocity 5.83 cm s^{-1})	~0.02–0.05	PLLA	–	Self-charging piezoelectric face mask filter	[259]
PM$_{1.0}$ PM$_{2.5}$ PM$_{10}$	~100	~65 (Face velocity 0.1 m s^{-1})	–	EC with PTFE spheres	~400 nm	Triboelectric PM capture filter	[249]
PM$_{0.3}$	~98	~40	~0.094	PBAT@CTAB-MMT	~300 nm	Self-powered filter for face mask	[260]

[1] Polymers materials abbreviations: PVDF (Polyvinylidene fluoride); PI (Polymide); PAN (Polyacrylonitrile); PTFE (polytetrafluoroethylene); PU (polyurethane); PEO (polyethylene oxide); PLLA (poly(l-lactic acid)); EC (Ethylcellulose); PBAT (polybutylene adipate terephthalate); CTAB (cetyltrimethylammonium bromide); MMT (montmorillonite).

environment, mainly affected the filtration of tiny particles (Fig. 11 d, e) [252]. Therefore, the dissipation of triboelectric charge may result in a lower adsorption of either potential bacteria or virus carriers. In this perspective, Dong Hee Kang et al. designed a multilayer system with triboelectric/piezoelectric properties made of PVDF nanofibers and nylon mesh, which provided highly efficient charges retention for long period of time with optimal performance both in terms of PM$_{0.3}$ submicron filtration and pressure drop [256] (Fig. 11 f). Under humid air condition, the filtration efficiency of tiny particles measured for the system of triple or more level filters slightly decreased compared to that observed in dry air condition (Fig. 11 g), pointing out that the triboelectric charge can be preserved during breathing, without having a significant impact on the effectiveness of the filter. The self-powered membrane also showed suitable properties to be employed as a reusable filter in face mask. In fact, the performances of the charged filter remained quite unaltered after ten cycles of both ethanol dipping process and further oven drying, without any sign of PM aggregated on the nanofibers surfaces (Fig. 11 h–j). Also, Lin et al. developed a smart hybrid perfluorinated electret nanofibrous membrane (HPFM) by electrospinning of Polytetrafluoroethylene (PTFE) and Fluorinated ethylene propylene (FEP), which showed high capacity in electric charge storage under high humidity environment [258]. The presence of an amorphous and crystalline surface occurring at the fiber surface level between the low crystallinity of FEP and the higher one of PTFE brings to a low mobility of the charges, which resulted therefore in a more stabilized charge on the fiber surface (Fig. 12 a).

Because of the high electric charge stabilization, the face mask using HPFM membrane provided a stable filtration efficiency against PM$_{0.3}$, even after 48 h of exposition to at high humidity ~ 100% RH. A

quantitative confirmation of the high capacity in charge storage was given by the Surface potential curves analysis, which revealed a more stable and higher number of charges trapped in HPFM compared to those measured for single electret filters (Fig. 12 b). This result also agreed with the analysis carried out by the Kelvin Probe Force Microscopy (KPFM) that measured a high intensification in surface potential observed on the nanofibers for HPFM, which was ascribed to the formation of well-localized space charges stored at the nanoscale interface on the fiber surface (Fig. 12 c). Hence, these studies clearly proved that advanced face mask based on electret electrospun filter polymers material and TENG technology can prevent the quick dissipation of electric charge caused by the high amount of vapor water increasing inside the mask during continuous breathing and provide a suitable filtration performance against small aerosols particles, also after prolonged wearing. Furthermore, the use of Triboelectric system can address the loss in efficiency observed in MB based electret filters charged by corona caused by a prolonged contact of the MB membranes with high humidity [23,87]. In addition, to provide an optimal filtration efficiency for submicron particles, these R-TENG based electrospun can also exhibit good accuracy in detecting parameters, such as respiratory rate, inhalation, and exhalation time, which are necessary to identify possible respiratory diseases in patients [248,251,257]. The harvest of mechanical energy from ambient environment by means of the TENG technology can therefore be advantageous to manufacture low-cost self-powered mask, especially now in the modern Internet of the Thing (IoT) where an incessant request of energy supply is required due to the large use of wearable electronic devices and monitoring sensors [255]. Also, several biodegradable polymers materials were found to be suitable for the manufacturing of TENG devices. The smart face mask
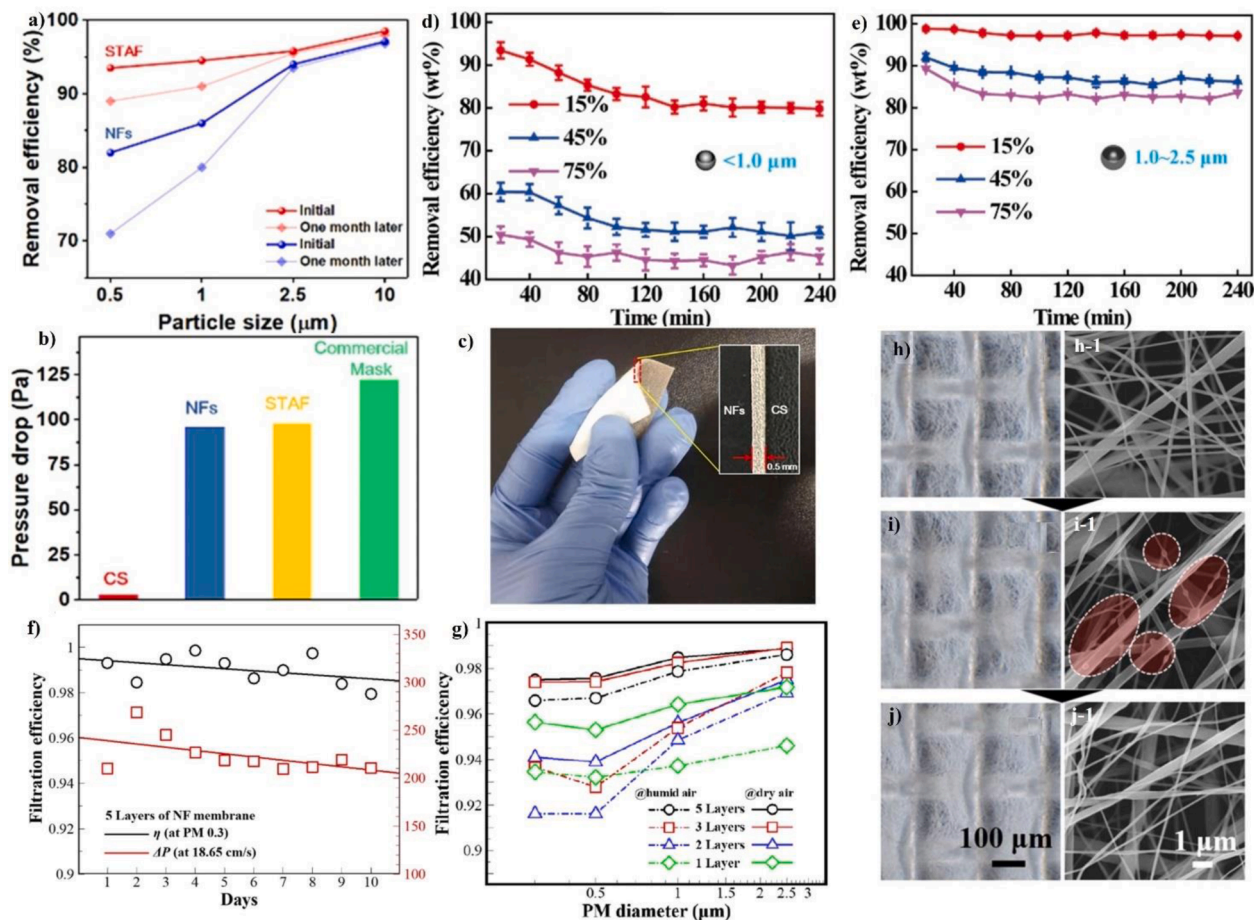
Fig. 11. (a) A comparison between the filtration efficiency obtained for the self-powered triboelectric filter based on PAN/PTFE/PU and that of PAN electrospun nanofibers (NFs), before and after one month of continuous filtration; (b) pressure drop measured for the for different materials, including the self-powered triboelectric filter, NFs, PTFE conductive sponges (CS), and commercial mask; (c) picture taken to a small piece of the STAF system; adapted with permission from [254]. Durability removal efficiency test performed on PVDF electrospun based R-TENG in different external humidities and for particle sizes lower than 1.0 μm (d) and ranging between (e) 1.0 and 2.5 μm; adapted with permission from [252]. (f) Filtration efficiency and pressure drop variation of a quintuple-layer of PVDF/nylon system filter after 10 days; (g) durability filtration efficiency test of the multilayer PVDF/Nylon system after continuous dry or humid air penetration for 0.5 h at different PM sizes; optical microscope and SEM images of PVDF/nylon-based nanofiber multilayers before (h, h-1) and after filtration (i, i-1); and regeneration (j, j-1) by means of oven drying due to ethanol dipping treatment; adapted with permission from [256].

designed by Yujang Cho *et al.* based on biodegradable polybutylene adipate terephthalate (PBAT) electrospun filter, functionalized with ecofriendly nanoclay mineral montmorillonite (MMT), and cetyltrimethylammonium bromide (CTAB) surfactant, provided higher filtration performance for PM$_{0.3}$, compared to commercial face mask [260] (Fig. 12 d). After 10 cycles of repetitive charging and discharging step by mechanical compression and release, the performance remained unaltered, thus indicating a continuous generation of triboelectric charges during the entire friction test. Besides, because of the incorporation of CTAB-MMT, the functionalized membrane showed high antiviral activity against influenza and Human coronavirus (Fig. 12 e). Also, new type of medical self-powered mask based on PVA and PLLA biodegradable polymers provided high charge retention as well as better optimal self-charging performance, under high relative humidity [259, 261]. After water exposure, the self-charging piezoelectric nanofiber membrane based on biodegradable PLLA designed by Le et al. showed a limited loss in both PM$_{2.5}$ and PM$_{1.0}$ removal compared to both surgical and N95 masks [259]. Furthermore, the electric filter performance remained stable after post annealing treatment for a period of eight weeks, thus showing long durability for prolonged use. Moreover, an antibacterial activity against both *S. aureus* and *P. aeruginosa* has been observed by exposing the piezoelectric membrane to 90 min of ultrasound sonication (Fig. 12 f, g). After sterilization procedure, the residual

contaminant that adhered the fibers surface were easily removed by means of water immersion and further air blowing, thus making it reusable. It is important to note that these biodegradable TENG showed comparable and in some cases higher QF values to those reported for other inorganic polymer based devices (Table 4) as well as a better biodegradation rate when they are either buried in composting soil or exposed to optimal degradation condition [259,260]. In view of their importance for innovative biomedical application, many of these biodegradable polymers are available on the market nowadays and can be easily dissolved into solution to be used for scalable manufacturing process [128,262,263]. These current studies revealed that high performance in particle filtration, self-charging, and charge retention can be achieved by implementing both synthetic and biodegradable polymers-based electrospun membranes. In particular, the manufacture of biodegradable based TENG represent a new design of self-powered air filter device that can meet the emerging demand of electrical energy and promote a more sustainable green circular economy.

4.5. Reusable filter material under visible light

The importance of disinfecting the disposable surgical facemasks for reuse has become, from the start of the pandemic, an essential issue to overcome the negative impacts on the environment due to the plastic
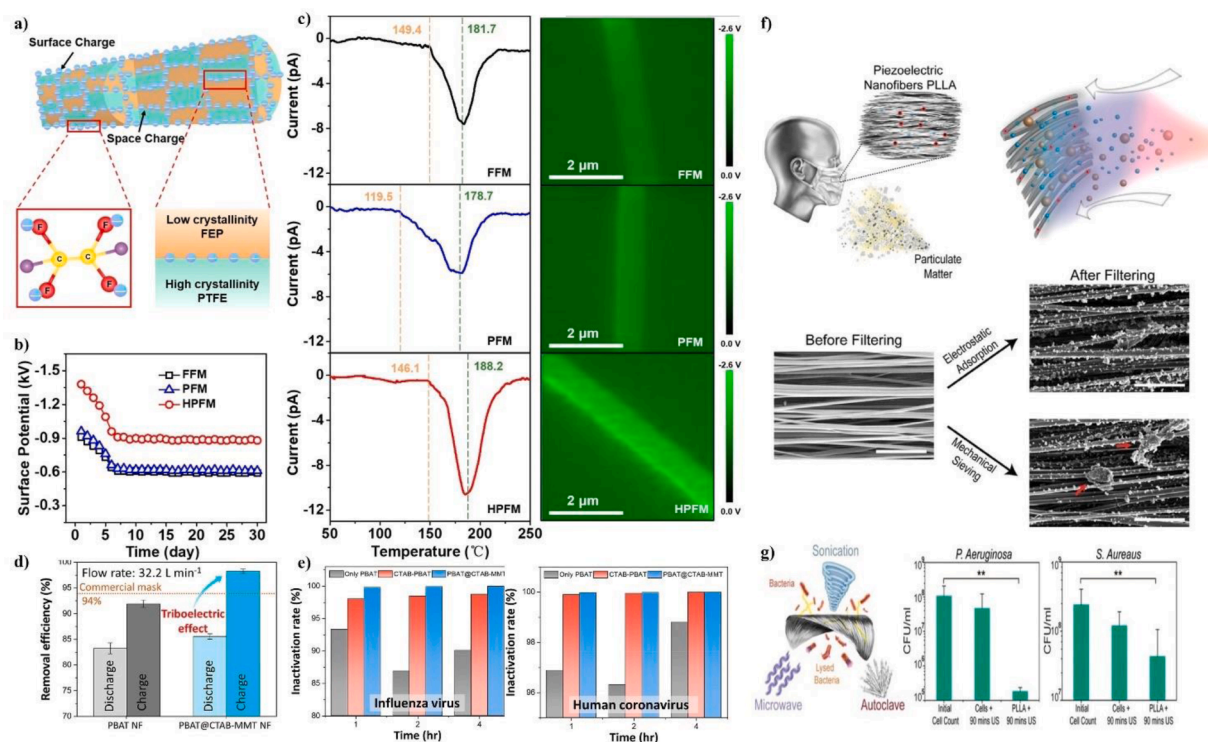
Fig. 12. (a) A picture for the charge-trapping mechanism of HPFM electrospun membrane; (b) surface potential variation as function of time obtained for the HPFM system, FEP electret nanofibrous membrane, and PTFE electret nanofibrous membrane; (c) thermally stimulating discharge current spectra (left) and corresponding KPFM images measured for the nanofibers of FFM, PFM, and HPFM (right); adapted with permission from [258]. (d) Filter efficiency evaluation obtained or the PBAT/CTAB/MMT and PBAT triboelectric membranes; (e) a comparison between the Inactivation rates of both influenza virus (left) and Coronavirus (right) obtained for PBAT/CTAB, PBAT, and PBAT/CTAB/MMT; adapted with permission from [260]. (f) A picture of a face mask made of electrospun piezoelectric PLLA nanofibers showing SEM images for the combined effect in PM capturing due to mechanical sieving and piezoelectrically enhanced electrostatic adsorption; (g) decontamination of the PLLA air filter from *P. aeruginosa* (gram-negative) and *S. aureus* (gram-positive) bacteria via ultrasound stimulation; adapted with permission from [259].

waste as well as to avoid further contamination from bacteria or virus which have been left on the mask [264,265]. Despite some strategies have been studied to sanitize a contaminated mask, the sterilization processes can negatively affect the particle filtration performance thus making the device ineffective to further use [266,267]. Recent advances in environmental-friendly mask development focused on the use of either photocatalytic or photothermal material to deactivate, after an exposition to light sources, bacteria and viruses extending the lifetime quality of face masks and making them reusable. In this perspective, Li et al. designed a reusable, biodegradable, and antibacterial electrospun membrane based on PVA, PEO, and cellulose nanofiber containing photocatalytic materials [163]. Since the limitation in absorbance of TiO_2 in the UV range, the membrane has been functionalized also with nitrogen-doped TiO_2 (N-TiO_2) to enhance the photocatalysis under visible light irradiation (Fig. 13 a).

The irradiation of photocatalyst materials such as TiO_2 with light of energy equal or greater than its band gap, observed to be around ∼ 3.06 eV, can promote the excitation of electrons from the valence band (VB) to the conductive band (CB), thus resulting in the formation of excited electron-hole pairs [268]. The interaction between excited electron–hole pairs and ambient air molecules through oxidation and reduction process induce the generation of ROS, such as hydroxyl (•OH) and superoxide anion (O_2^-) radicals, and hydrogen peroxide (H_2O_2), which during photocatalytic process can damage the walls and the membranes of cells, protein, RNA, DNA, bacteria, and virus [269]. By doping the TiO_2 NPs with nitrogen, the energy band gap of the TiO_2 NPs was observed to decrease at 2.77 eV, thus resulting in a shift in the absorption spectrum to longer wavelengths (Fig. 13 b). Because of the extended adsorption of light in both the UV and near visible region, the count of the bacteria survived by the N-TiO_2 mask were significantly lower compared to that measured for N-TiO_2 mask (Fig. 13 c). An exposition of

the face mask with TiO_2 (N-TiO_2) NPs mixture to only 10 min of light was sufficient to obtain a complete bacteria disinfection efficiency (100% bactericidal activity), in both *E. Coli* and *S. aureus* (Fig. 13 d, e). Moreover, the antibacterial activity remained stable after three sterilization cycles, without any significant decrease in filtration efficiency. Notably, the generation of ROS induced by visible-UV light involved a complete inactivation of bacteria on the functionalized membrane. In contrast, most bacteria remained alive on the same membrane in absence of light exposition, due to the limited antibacterial efficiency caused by the electrostatic interaction between the active TiO_2 (N-TiO_2) NPs mixture with the negatively charged bacteria. Li et al. used an organic photosensitizer (TTVB) in Poly (vinylidene fluoride-*co*-hexafluoropropylene) (PVDF-H) polymer-based electrospun membrane to enhance the generation of ROS under light irradiation (Fig. 13 f) [154]. From a comparison between the fluorescence emission intensities measured at 525 nm for the functionalized membrane and the pristine one, it was noted that the presence of TTVB led to a high generation of ROS for longer exposition time to light source (Fig. 13 g). In addition to optimal filtration performance against NaCl particle (≤ 0.3 um), the membrane functionalized with TTVB showed a high inactivation rate of a least ∼99% against several pathogens, including *S. aureus, E. coli,* and M13 bacteriophage vector, after only 5 min of visible light exposition (Fig. 13 h). Also, the effect of ROS in viral decontamination for face masks has been investigated by Shen et al., that recently designed a photosensitized electrospun nanofibrous membrane with good filtration performances in capturing and rapidly deactivating coronavirus strain surrogates, under visible light radiation (Fig. 14 a) [170]. In their previous study they evaluated the filtration efficiency of PVDF electrospun nanofibers by testing the Murine hepatitis virus A59 (MHV-A59) as coronavirus strain aerosols, because of their similarity in size and structure with SARS-CoV-2 (size ∼85 nm) [19]. The high dominant
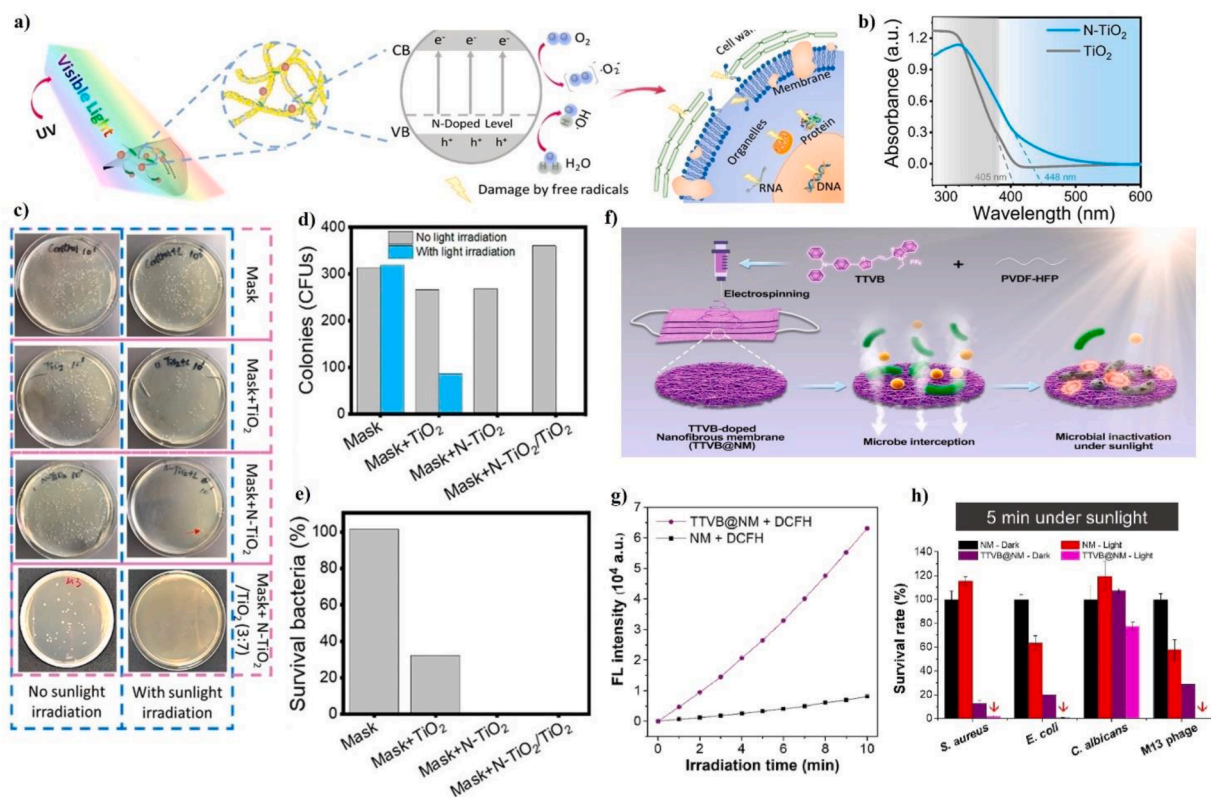
Fig. 13. (a) Schematic diagram that represents how N-TiO2 embedded in face masks can sterilize bacteria under light irradiation; (b) UV−vis spectra obtained for TiO2 and N-TiO2; (c) photo images of plate incubation for E. coli and S. aureus after washing the mounted bacteria on masks with and without light irradiation; (d) CFU count and percentage of survival bacteria (e) for the respective plates; adapted with permission from [163]. (f) Schematic illustration of the preparation of PVDF electrospun fibers functionalized with TTVB for microbe interception and further inactivation under sunlight exposition; (g) comparison between the fluorescence intensity obtained for the PVDF/TTVB electrospun membrane and that without dopant (NM); (h) a comparison between the survival rate for several bacteria obtained for both PVDF/TTVB and NM under 5 min of light exposition and dark condition; adapted with permission from [154].

capture of both airborne corona virus and submicron aerosol particles observed for PVDF-based electrospun membranes indicated that electrospun filter with lower fiber diameter and smaller pore size provided a better prevention for the transmission of COVID, compared to commercial filter of larger fiber size.

Besides the observed high retention of MHV-A59 aerosols, the addition of a photoreactive dye additive, the Rose Bengal (RB) one, to the PVDF based electrospun nanofiber membrane allowed the production of highly reactive singlet oxygen ($^1O_2$) that inactivated the 97.1% of the MHV-A59 coronavirus droplets, after a short exposure time to visible light of ∼ 15 min (Fig. 14 b). To compromise the viability, also the ORF5 gene copy number of MHV-A59 was drastically reduced from the generation of ROS during photosensitization, in both droplet and aerosol test with surrogate coronavirus. Moreover, after 4 days of light exposition in outdoor a significant decrease in both corona virus inactivation and generation of $^1O_2$ have been observed for the PVDF-RB membranes (Fig. 14 c). In contrast, a longer exposition under indoor light of 7 days did not compromise the photoreactivity of the functionalized membrane, which maintained a significant performance in both filtration and inactivation of coronavirus. These studies showed that the implementation of photocatalytic inorganic and organic compound in electrospun polymer membranes can be an easy solution to involve a proper sterilization process, under visible light source, by means of the generation of ROS. Moreover, the manufacturing cost for these photocatalytic membranes are economic and easily available on commercial scale [270], and the highly efficient catalyst obtained from low energy irradiation under visible light makes use of functionalized membranes energetically safer as well as easily implemented, compared to other methods commonly used for pathogens removal [271,268]. The use of photothermal nanomaterials, including graphene, carbon nanotubes

(CNTs), and other metal NPs, have been also considered for the manufacture of sunlight self-sterilization face mask [272]. Under exposition to sunlight source, these nanocomposites can absorb light energy and convert it in heat to provoke a significant increase of the local temperature, which may result in a thermal denaturation of cells, bacteria, and viruses [273]. Xiong et al. designed a novel needleless ES/spraying-netting technology to fabricate a hierarchical system based on CNTs network welded on PAN nanofiber (NF) layer with good filtration performances, both photothermal and electrothermal self-sterilization, and recycling performance [182] (Fig. 15 a).

The configurations obtained for the NF/CNT filter showed high efficiency in PM$_{0.3}$ removal (∼ 99.9%) with low pressure drop (∼ 49 Pa). Since the small micron scale pores and multi-scale structure enhance the photon absorption in the full wave band between (500–2500) nm, the NF/CNT filter showed a fast photothermal response ($T > 70$ °C within 5 s of sunlight exposition) that involves an excellent antibacterial activity against E. Coli (> 99.8%) only after a sun exposure time of three minutes (Fig. 15 b–d). The authors stated that since the COVID-19 can be deactivated within few minutes of heat treatment higher than or equal to 65 °C [274], the high equilibrium temperature of NF/CNTs ($T > 60$ °C after 0.5 sun) would allow to kill the virus after 15 min of sun exposition. A faster high-temperature response with better antibacterial performance (> 99.9%) has been obtained by providing an electrical current of 61 mA for two minutes (Fig. 15 e, f). The photothermal response showed to be comparable or higher with those observed for other self-sterilizing face masks, recently designed with different sunlight-responsive materials [275–277]. However, due to the small average pore size and small fiber diameter the multi scale nanoarchitecture of NF/CNTs provided better performance in both filtration and pressure drop, especially after 50 wetting-drying cycles, thus suggesting its potentiality as a reusable
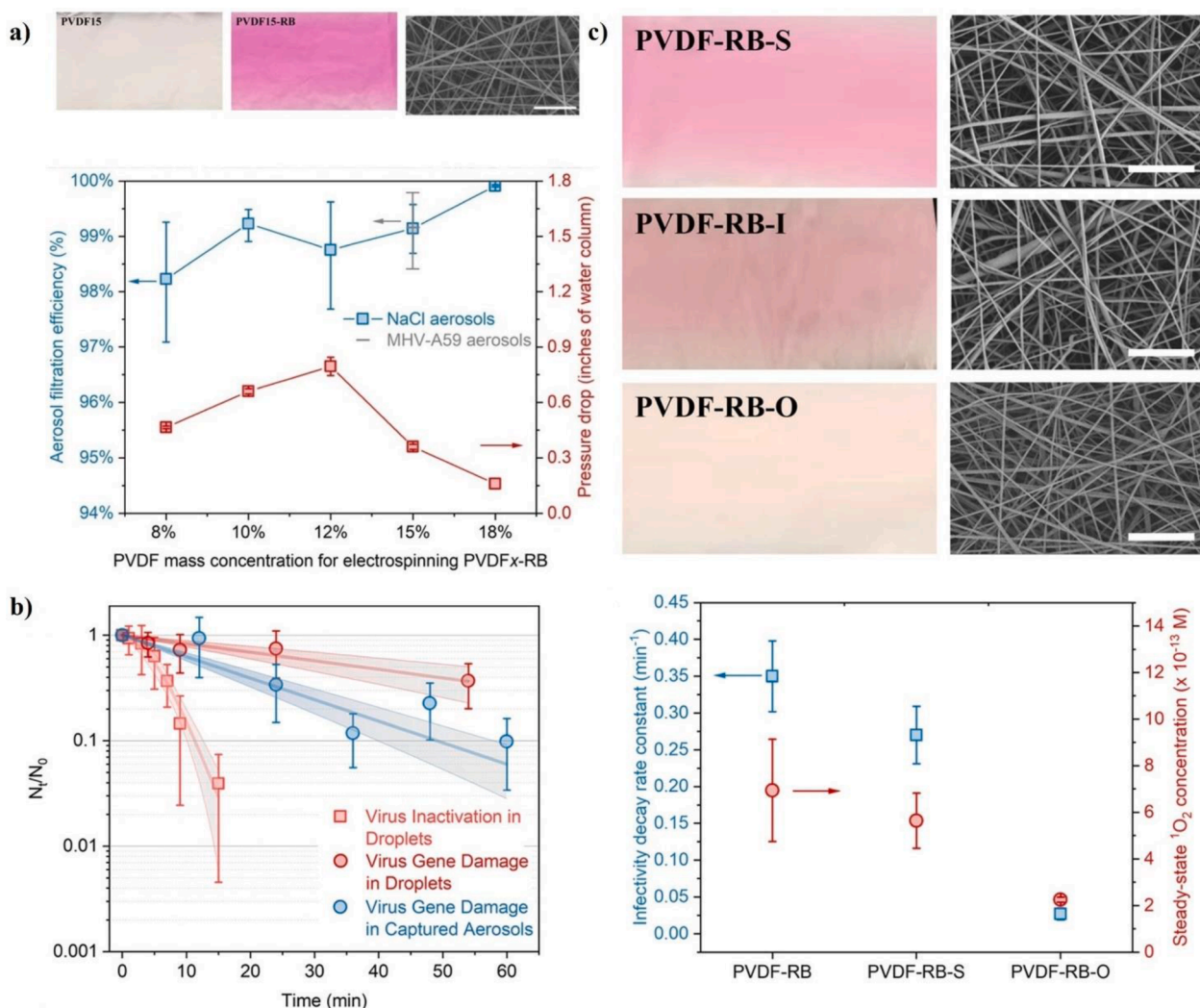
Fig. 14. (a) (top panel) Photos of PVDF15 (15 wt% of PVDF), PVDF15- RB, and SEM image of PVDF15- RB nanofibrous membrane; (below) NaCl, MHV-A59 aerosol filtration efficiency, and pressure drop observed for RB-sensitized electrospun membranes with different PVDF concentrations (PVDFx-RB); (b) kinetics of MHV-A59 infectivity decay obtained in both droplets and aerosol test; the N_t/N_0 ratio represents the ORF5 gene copy numbers, which is measured by the ICC-RT-qPCR, about infectivity, or RT-qPCR, about gene damage, during a light exposition time given by *t* to that obtained at the initial instant of zero. (c) Optical photos and SEM images (top panels) of PVDF15-RB membranes obtained after different aging test: indoor fluorescent light in laboratory (PVDF-RB-I) and simulated indoor light (PVDF-RB-IS) up to seven days of light exposition; and outdoor light (PVDF-RB-O) exposition up to four days. Scale bars in the SEM images are 5 μm; (below) first-order decay rate constants of MHV-A59 infectivity in droplets test and related $^1O_2$ formation on pristine and light simulated exposed PVDF15-RB membranes. adapted with permission from [170].

filter to reduce disease spread and consumption of resources (Fig. 15 g). Moreover, due to the large-area deposition and to the structural stability of the CNT network on scaffold polymer nanofibers, the needleless electrospinning coupled with spraying-netting has proven to be an easy and accessible technique to produce self-sterilizing filter membranes on large scale. These studies clearly show that electrospun membranes functionalized with either photocatalytic or photothermal nano-materials can be advantageous to produce low-cost high-filtering per-formance face masks with suitable self-sterilization properties. The fast sterilization response obtained under low exposition time in visible light/sunlight would allow to overcome the drawback of efficiency degradation observed in commercial face masks, caused by a long time-exposure to conventional heating and UV-C radiation disinfection methods [193,278–280]. Furthermore, the easy decomposition of biopolymer self-sterilizing face masks in water and soil may be a new promising line of research to substitute nonrenewable synthetic poly-mers and relieve the plastic waste pollution at the landfills [163].

5. Future perspectives for sustainability of membrane technology

The demand for green chemistry is increasing, due to the growing awareness on the negative environment and health impacts associated with traditional industrial processes, and special attention has been given to electrospun nanofibers membranes, since their wide-spread applications in biomaterial industry and scale-up in commercial pro-duction of filtering layers in face masks [281,282]. The electrospinning solutions often involve the use of halogenated compounds, such as 1,1,1, 3,3,3- hexafluoro-2-propanol (HFIP), tetrahydrofuran (TFH), N,Ndi-methyl- formamide (DMF), 1-methyl-2-pyrrolidinone (NMP),and dime-thylacetamide (DMAC), because of their high solvation power for hydrophobic polymers and low boiling points which ensure a proper viscosity of the commonly used high molecular weight polymers, necessary properties for the ES process to convert the solution into fibers [283]. However, the most used solvents in the ES process, as well as for other methods adopted in the ultrafiltration membranes manufacturing processes, are toxic and their usage has been recently restricted by the
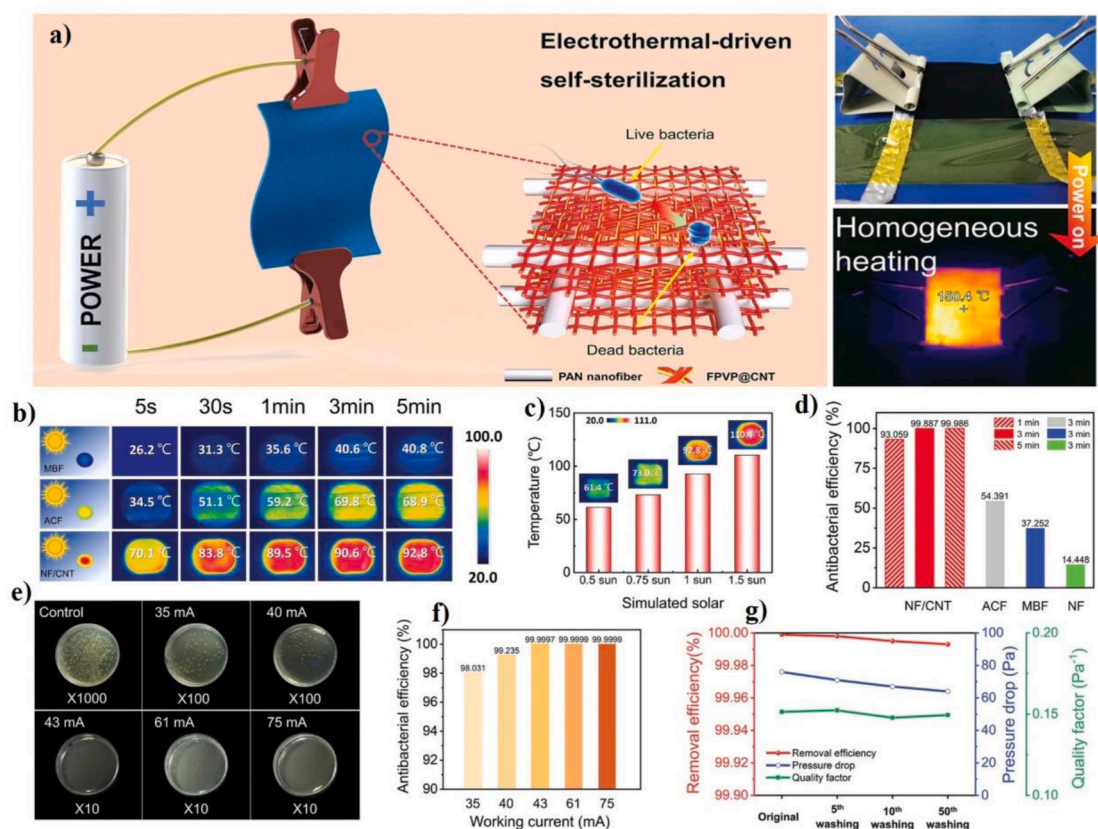
Fig. 15. (a) Schematics of self-sterilization of NF/CNT fibrous due to electrothermal; (b) IR images recording the temperature changes of carbon fiber layer (ACF), melt-blown fabric layer (MBF), and NF/CNT fibrous masks; (c) equilibrium temperatures of the NF/ CNT fibrous network under different simulated solar; (d) sterilization performance of ACF, MBF, and NF/CNT fibrous network masks under 1 sun; (e) photographs of the distributions of *E. coli* colonies on nutrient agar solid plates when applied small currents for 2 min; (f) sterilization performance of the electrothermal NF/CNT filter under different applied currents for 2 min; (g) filtration performance, pressure drop, and quality factor of the NF/CNT filter after repeating wetting-drying process; adapted with permission from [182].

Chemical Control Regulation in the European Union (REACH) [119, 282]. A strategy to improve the sustainability of the ultrafiltration membranes manufacturing process would consist in using greener/low-toxicity solvents from renewable resources. To date, bio-based nontoxic solvents have been attracting attention due to their decreased impacts on human health and environment [119,284]. The Hansen solubility parameters (HSP) calculated for these green solvents reveal a high polymer-solvent compatibility with the typical polymers employed for membrane applications, thus suggesting feasibility for these non-hazardous solvents in the fabrication process [119,284]. In literature, some studies reported first steps in eco-friendly alternative ES employed to spin common polymers for membranes manufacturing [285,286]. Green solvents based nanofibrous membranes have been also electrospun to be used as breathable and comfortable materials for application of protective clothing or as an additional protective layer within existing cartridges as well as in fluid filtration and separation of nanomaterials [185,287–289,186,183]. In particular, the applicability of water as a green solvent for environmental-friendly membrane processing has been recently investigated for several polymer materials [119]. Since it has good cost-effectiveness and environmental compatibility, the fabrication of environmental electrospun membranes based on water-soluble and biodegradable PVA polymer has been recently considered to replace non-degradable materials and toxic solvent in different biomedical application, including drug delivery and tissue engineering [120,290]. However, the mechanical properties of pristine PVA membrane are poor, and the filtration performance in the long run may be affected by possible breakage of nanofibers. In this perspective, Cui et al. observed that the addition of Tannic Acid (TA) to water-soluble precursor solution provides better mechanical properties to the

membrane compared with that observed for pristine PVA [177] (Fig. 16 a).

A similar result was also found in a previous work by adding ligno-sulfonate (LS) to PVA electrospinning solution [178]. The PVA-TA nanofiber showed high filtration efficiency against $PM_{1.0}$ (~ 99.5%) with pressure drop about 35 Pa. In comparison with medical surgical face masks, the fiber interception mechanism of PVA-TA filter proved to be unaltered showing an excellent fine particle filtration after twenty consecutive tests performed (Fig. 16 b, c). Furthermore, PVA nanofibers prepared with water-soluble chitosan (WS-CS) by means of needleless ES showed a small average pore size ranging between 12.06 and 22.48 nm and provided antibacterial activity against *S. aureus* as well as high filtration efficiency in removal $PM_{2.5}$ (~ 93.1 - 97%), with optimal pressure drop (~ 41 – 44 Pa) [167] (Table 3). In another work, it has been observed that the addition of TiO_2 nanotubes to the water pre-cursor solution of CS/PVA provided high mechanical strength to nano-fibers product thus showing less tendency to degrade over time. Moreover, under dark conditions the $CS/PVA/TiO_2$ membrane showed a bacterial inhibition growth of ~ 44.8%, higher than that observed for the control sample [291]. Also, the addition of Ag NPs has shown to enhance proper depletion of both *S. aureus* and *E. coli* on PVA-water based electrospun [166]. Therefore, the addition of active compound proved to be beneficial to address the poor mechanical properties issue in water soluble PVA membrane and enhance its antibacterial effectiveness. Furthermore, morphological changes occurring at the fiber surface level due to the inclusion of active materials in blend solution ES have been observed to significantly improve the removal of PM for the electrospun membranes, as well. In a recent study, Deng et al. reported that the addition of Sodium sulphobutylether-β-cyclodextrin (SBE-βCD)
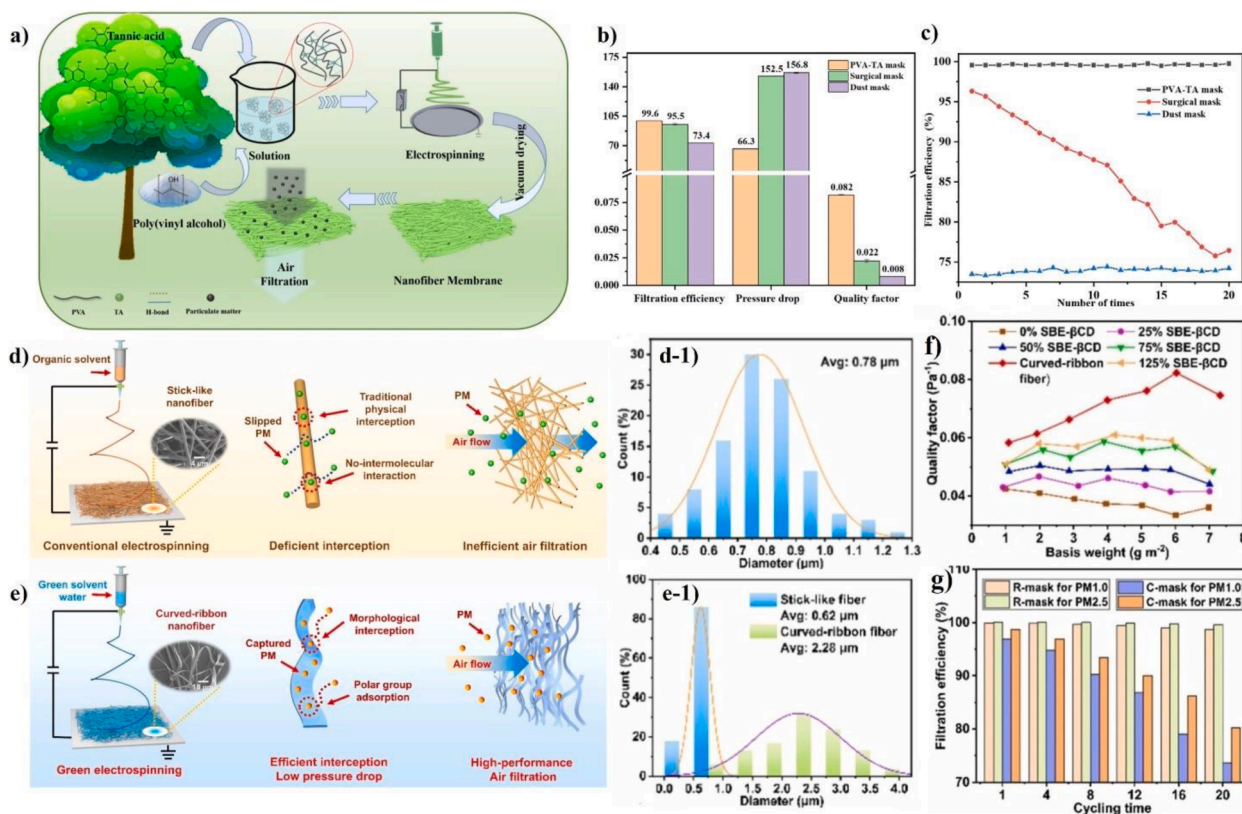
Fig. 16. (a) Schematic diagram showing the preparation of PVA-TA nanofiber membrane; (b) a comparison between PVA-TA, surgical and dust masks on filtration efficiency, pressure drop, and quality factor properties; (c) $PM_{1.0}$ capture of the PVA-TA masks after 20 consecutive filtration tests; adapted with permission from [177]. (d) Schematic illustration of conventional stick-like nanofiber and (e) curved-ribbon nanofiber based on green ES for eco-friendly breathable and high-performance air filtration; fiber diameter distribution of (d-1) pristine PVA and (e-2) 100%SBE-βCD/PVA; (f) Quality factor of nanofiber membranes for PM1.0 under 5.3 cm s^{-1}; (g) cycling filtration performance of re-assembled curved-ribbon mask and common medical mask for removing $PM_{1.0}$ and $PM_{2.5}$; adapted with permission from [168].

in PVA ultrapure water solution resulted in the formation of curved-ribbon fibers, with high mechanical properties as well as better filtration performance compared to pristine PVA membrane [168]. Compared to the stick-like fibers obtained by conventional ES, the green electrospun fibers provided a more efficient interceptor mechanism capture for $PM_{1.0}$ around 99.12% due to the combination of morphological interception and electrostatic mechanisms as well as a higher tensile strength and strain, which can be ideal to stabilize the breathable filter under external air stress (Fig. 16 d–f). Furthermore, after 20 cycling filtrations test the filter maintained both filtration stability against $PM_{1.0}$ and proper pressure drop of 59.5 Pa, thus making it reusable for most applications (Fig. 16 g). A similar result has been reported also in the work carried out by Hu et al., where a higher capture of $PM_{0.3}$ was observed for zein based electrospun membranes with flat ribbon structure, obtained by ethanol/ deionized water mixture solvent [185] (Fig. 17 a).

The simulated 3D structure model also confirmed that a larger contact surface in flat zein fibers leads to an improvement in filtration, due to a higher interaction occurring between the pollutant particles and the numerous functional groups owing to zein protein (Fig. 17 c). Notably, both the filtration and the pressure drop were observed to remain stable, also when varying the relative humidity in the range between 20% and 80% (Fig. 17 b). Furthermore, the face mask based on zein filter completely degraded after 42 h under cellulase enzyme, thus proving to be biodegradable and environmental-friendly (Fig. 17 d, e). These studies clearly showed that nanofibers based on biopolymers and natural materials can be easily dissolved in greener solvents and being optimized by means of ES to address the lack of mechanical properties and to improve filtration performance for submicron particles. Such

customizability makes the green ES methods commercially attractive to produce eco-friendly face mask, since it would relieve the high consumption of non-renewable plastic resources and that of hazardous solvents in large-scale commercial production.

5.1. Electrospun nanofibers in bio-textiles for potential biomedical application

Due to the high versatility in producing a wide range of continuous polymer based nanofibers, ES has attracted much interest in recent years as a potential solution for the development and the design of textile-based scaffold for tissue engineering [30,31,35]. Scaffold in tissue engineering is used to mimic the extracellular matrix (ECM) of the native tissue. To restore the functionality of the damaged tissues, ECM provide biochemical and physical cues by enabling cellular physiological activities and diffusion of vital cells as well as promoting cell adhesion, morphogenesis, and migration on the tissue structure [292]. Since the structural similarities between the electrospun nanofibers and the complex network forming native tissues, different electrospun based scaffolds have been fabricated to reproduce both the morphological and biochemical characteristic of ECM for cardiac, nerve, muscle, tendons, and connective tissue regeneration [293]. The combination of several natural and synthetic polymers by means of Coaxial ES have been found to be a useful approach to tailor and customize the biochemical and physical properties of electrospun based scaffold for the specific requirement of medical implants [294]. Natural biomaterials, including collagen, chitosan, and gelatin, provided suitable biocompatibility to the electrospun mats, but showed disadvantages in bio mechanical properties. On the other hand, the addition of synthetic biopolymers, such as
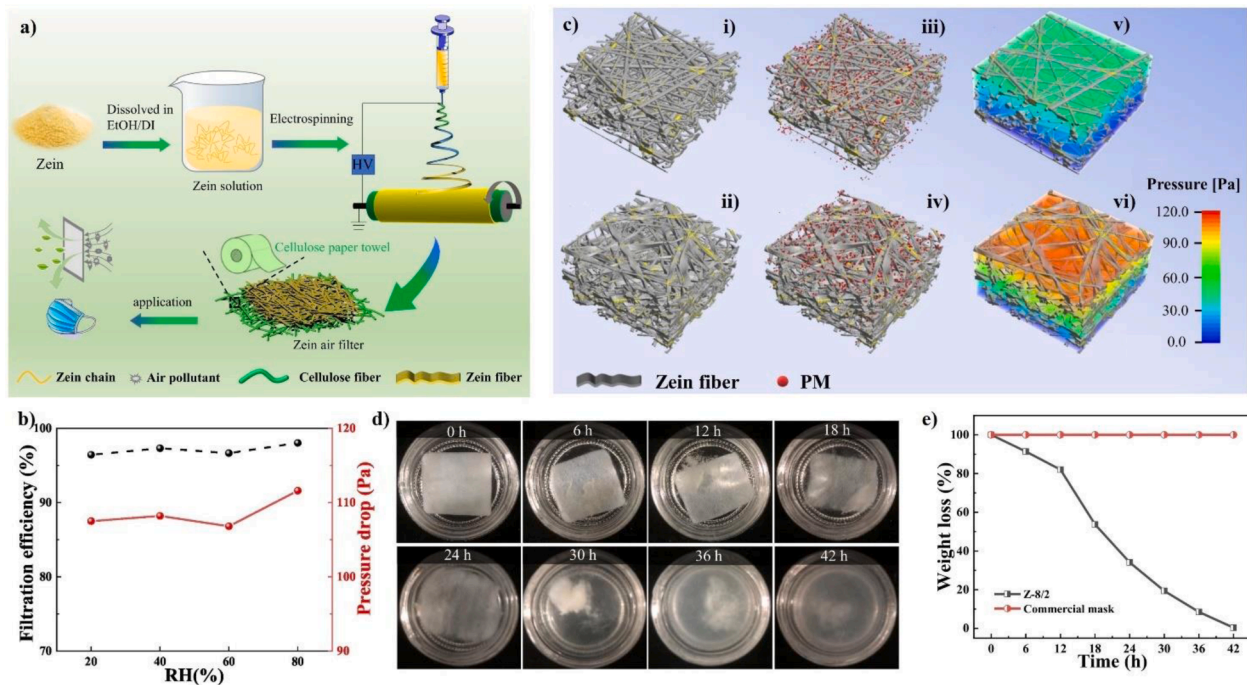
Fig. 17. (a) Schematic diagram showing the fabrication of the zein electrospun filter on cellulose membrane; (b) the filtration and pressure drop performance stability under different humidity conditions; (c) the model depicted shows (i) Stick-like zein and (ii) flat ribbon-like zein mat; (iii, iv) filtering simulation calculated from the two different fiber structures, respectively; (v, vi) pressure field simulations for the two distinct model, respectively; (d) images of the Biodegradability test for the zein based electrospun filter under enzymatic degradation in time, and (e) the measure of the related weight loss; adapted with permission from [185].
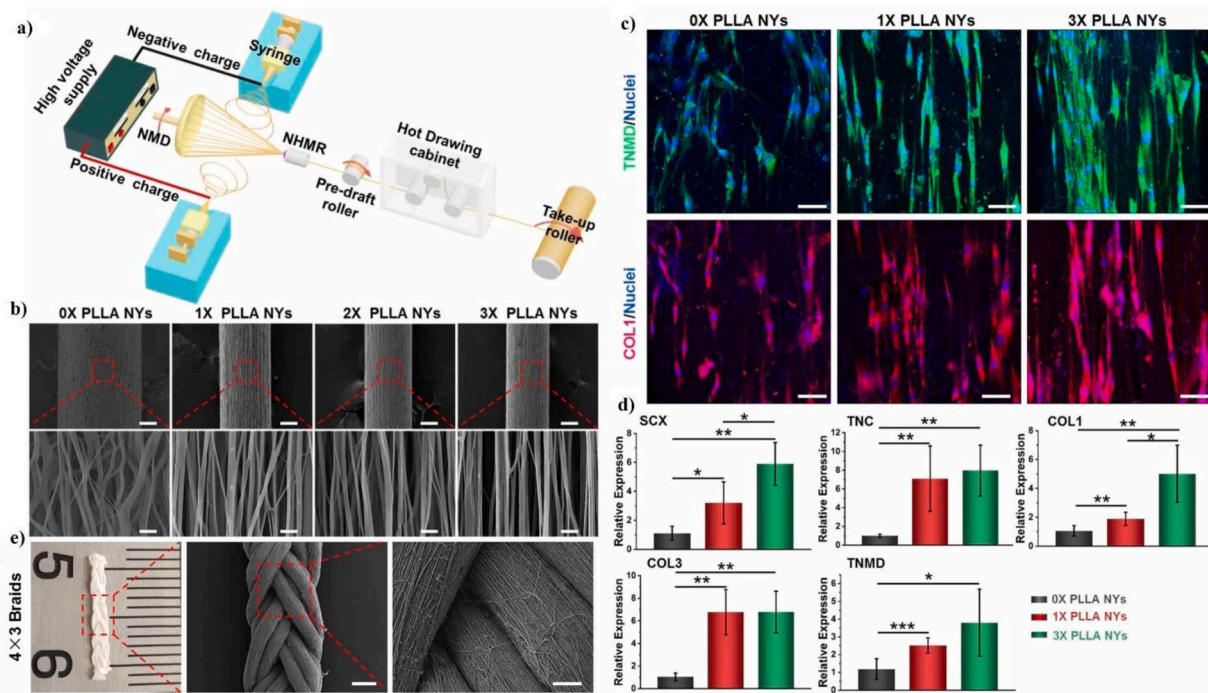

Fig. 18. (a) A schematic illustration of the modified ES system for the fabrication of PLLA NYs with and without the hot drawing process; (b) SEM images obtained for the PLLA NYs without hot drawing process (0X PLLA NYs), and three thermally drawn PLLA NYs processed with several stretching degrees, i.e., 1X PLLA NYs, 2X PLLA NYs and 3X PLLA NYs. Scale bars: 100 μm for top panel and 2.5 μm for down panel; (c) images of immunofluorescent staining taken of hADMSCs present on the 0X PPLA NYs, 1X PPLA NYs and 3X PPLA NYs after 14 days of culture. Tenomodulin (TNMD), antibody to collagen type I (COL1), and nuclei were marked with green, red, and blue, respectively. Scale bars are equal to 50 μm. (d); the qPCR analysis obtained for five tendon-specific gene markers such as SCX, TNC, COL1, COL3 and TNMD for hADMSCs cultured after 24 days on the 0X PPLA NYs, 1X PPLA NYs and 3X PPLA NYs; (e) photograph and SEM images of braids fabricated with 12 electrospun based PLLA NYs, named as 4 × 3 braids. Scale bars: 0.5 mm for left image and 100 μm for right one; adapted with permission from [297].

PVA, PLLA, PCL, ensured a better structural stability to natural/-synthetic based scaffold, thus satisfying requirement for ECM in tissue engineering [295]. However, due to random orientation of conventional nanofibers, the electrospun based scaffold cannot correctly mimic the oriented features of native ECMs, such as nerve, and tendons, thus limiting cells migration and its large application to tissue engineering. In comparison, scaffold based on more aligned nanofibers proved to be more efficient to guide and accelerate both the differentiation and infiltration of *in vitro* cell tissue regeneration, but due to the poor mechanical properties and the low thickness they resulted in insufficient structural support for some native tissue [293,296]. The assembling of electrospun nanofibers into ordered textile nanoyarns (NYs) has been found to be advantageous to overcome the poor mechanical properties of electrospun mats and involve a better bioactivity properties in scaffold by promoting cell proliferation, migration, and differentiation *in vivo* microenvironment [30,31]. In particular, the modified conjugated ES technique designed by Wu et al. proved to be an innovative method for the fabrication of aligned polymer based NYs with suitable mechanical strength and high biocompatibility [297]. A schematic picture of the modified electrospinning system is reported in Fig. 18 a, to illustrate the generation of PLLA based NYs.

The polymer jets of opposite charge are electrospun by two needles, located opposite to each other, and collected between a steady neutral hollow metal rod (NHMR) and a rotating neutral metal disk (NMD) to be subsequently bundled in NYs by means of a hot drawing cabinet. The single PLLA based NYs obtained with hot drawing process showed a higher alignment degree, a higher strength, and a higher Young's modulus compared to that obtained without hot stretching treatment, thus indicating a better mechanical property (Fig. 18 b). Furthermore, CCK assays carried out on hot stretched PLLA based NYs also showed a high proliferation of human Adipose Derived Mesenchymal Stem Cells (hADMSCs). This result was in accordance with the images of immunofluorescences for phalloidin and DAPI double staining that revealed a significantly elongation and alignment for cytoskeletal protein and nuclei of the cells, respectively, thus suggesting that aligned nanofibers in NYs with hot drawing process can induce a better cell attachment and proliferation enhancement. Indeed, both protein secretion and formation of nuclei along yarn longitudinal direction of aligned PPLA NYs have been observed in the immunofluorescences analysis carried out for tenogenic differentiation of hADMSCs (Fig. 18 c). The quantitative PCR (qPCR) analysis also revealed a high relative expression for tendon-specific gene markers, including SCX, TNC, COL1, COL3 on hot stretched PLLA based NYs, thus indicating that high alignment of nanofibers in PLLA based NYs can be beneficial to tenogenic differentiation of hADMSCs (Fig. 18 d). Importantly, NYs can be furthermore braided by means of traditional textile engineering methods, such as weaving, knitting, and braiding to manufacture different woven fabric nanotextiles with controlled structures and shapes, which are able to meet the requirements for the different tissue engineering applications (Fig. 18 e) [30]. Woven textiles interlaced with silk fibroin (SF)/PLLA based NYs by means of weaving method proved to be beneficial to drive the growth activity of HADMSCs [298]. From a comparison between the SEM images and the quantitative MTT analysis performed on scaffolds interlaced with SF/PLLA NYs at different mass ratio, it was noted that the higher the presence of bioactive SF, the higher the proliferation capacity of the HADMSCs. Moreover, after *in vivo* subcutaneous implantation of SF/PLLA NYs based scaffolds, the low immunofluorescence staining intensity of CD68 protein, a general marker for macrophages, which was measured in presence of high amount of SF indicated a drastically reduction of the inflammatory response, thus suggesting that SF/PLLA NYs based woven fabrics can effectively induce cellular infiltration and tissue regeneration.

A similar result has been observed also in the recent work of Ye Qi et al., where the low number of macrophages obtained by the measure of the immunofluorescence staining intensity of CD68 protein for woven textiles interlaced with aligned SF/PCL based NYs was clearly attributed

to the presence of SF in the NYs units forming the scaffold [299]. Therefore, NYs based woven fabrics can maintain the characteristic properties given from the original NYs, including mechanical, biocompatibility, and biostability properties, and can be adjusted in several shape and structure, to satisfy the several request for medical implantation (Fig. 19 a). Moreover, recent scaffold based NYs functionalized with active nanomaterials showed excellent biocompatibility and demonstrated to be appropriate to manufacture nerve guidance conduit (NGC) for the repair of injured nerves [31]. Zhang et al. designed an innovative PCL based NYs functionalized by means of PCL microparticles embedded with bioactive nerve growth factor (NFG), which was able to promote both topological and biochemical signals for the manipulation of axon growth cells [300]. Compared to aligned PCL based NYs, the inclusion of PCL microparticles was observed to effectively promote the axon growth for PC12 and SH-SY5Y cells. Additionally, the load of bioactive NFG in the core of PCL microparticles induced a longer migration distance of neural stem cells on the NYs environment, thus proving that such combination promotes both a better axonal extension and a subsequently migration of the stem cells (Fig. 19 b–e). Also, a multifunctional tube-filling material fabricated with aligned NYs based on poly(p-dioxanone) (PPDO) biopolymer and different concentrations CNTs has been designed to improve the performances of the NGCs in the repair of long-gap peripheral nerve (PN) injuries [301]. The addition of CNTs at 5% in PPDO based NYs proved to support both elongation and alignment for hADMSCs as well as to enhance both electrical conductivity and mechanical properties. Besides, under the combination of both electrical stimulation and chemical induction the expressions of the myelination-associated proteins and other genes markers for hADMSCs measured by means of QRT-PCR analysis were higher in the conductive functionalized PPDO based NYs compared to those observed in growth medium (GM), thus indicating a significant improvement in the differentiation of hADMSCs into myelinating Schwann cell-like cells (Fig. 19 f, g). Hence, these results demonstrated that the development of electrospun NYs functionalized with active materials can be determinant to promote the neuronal differentiation of stem cells. Furthermore, the addition of natural and synthetic biopolymers in electrospun based NYs allows to adjust the biodegradability rate, thus making the production of nanotextile woven fabric more suitable for the fabrication of bio textiles implants [297,298]. In addition, the high fracture strength and tensile elongation provided by nanotextiles woven fabric plays an important role in the production of flexible and smart textile for healthcare wearable applications [30,302]. Recent electrospun nanofibers prepared by using polypyrrole (PPy) and covered with PAN-KCZ/ZnO nanofibers were twisted to prepare composite NYs with both photothermal and electrothermal properties for self-sterilization application [303]. The fabricated nanotextile woven provided a faster high-temperature response under the exposition to both light irradiation and electrical power, which promoted the continuous release of active KCZ in preventing the infection from bacteria pathogens. Also, thermoplastic polyurethanes (TPU) based NYs functionalized with silver nanowires and MXene exhibited a fast electromechanical performance under mechanical deformations as well as a photothermal and electrothermal response under external stimuli, including electricity and light, that resulted to be advantageous for the realization of wearable healthcare sensors [304]. Hence, the combination of ES with traditional textile processing methods can be a feasible approach to design and develop advanced nanotextile for several potential applications in various biomedical fields. It is worth noting that electrospun based NYs with high degree of alignment and lengths of the order of hundreds of meters can be produced in a continuous manner [30]. Therefore, thanks to the utilization of automated and programmable textile machines the structure, shape, and mechanical features can be tuned for the large-scale production, thus making the manufacturing of nanotextile woven fabric based on electrospun NYs expandable for a future commercialization.
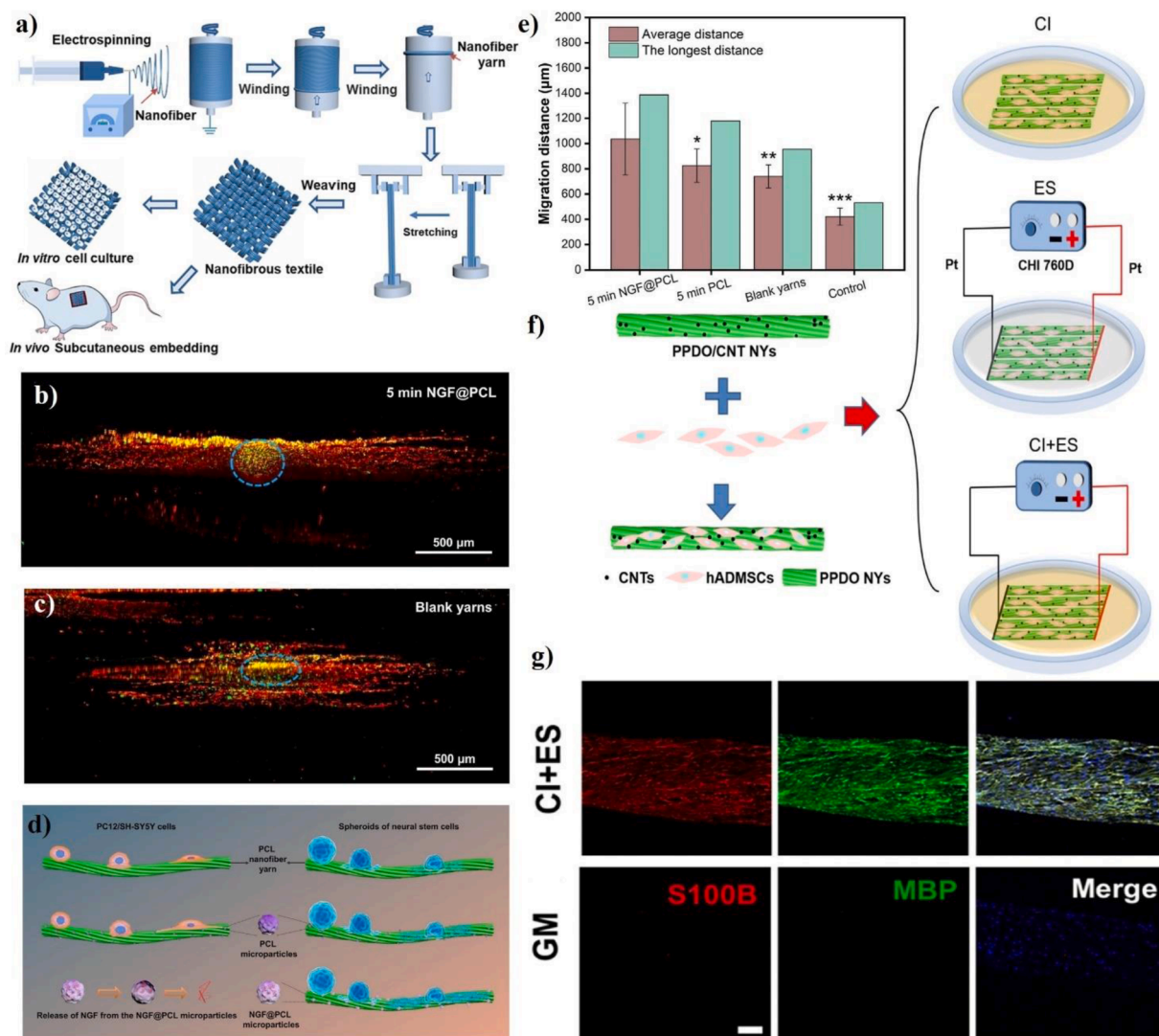
Fig. 19. (a) Schematic diagram of the fabrication process of electrospun based NY and its further production in woven textile, as functional scaffold for *in vivo* tissue engineered application; adapted with permission from [299]. A comparison between the fluorescence images showing the cell migration from the spheroids of neural stem cells after 7 days of culture on (b) PCL NYS functionalized with NGF@PCL microparticles, obtained at a deposition time of 5 min, and that on (c) PCL NYs (blank yarns); (d) schematic picture showing the axonal growth of both PC12 and SH-SY5Y cells and their further migration from the initial spheroids forms of neural stem cells on PCL NYs, PCL NYs functionalized with PCL microparticles, and PCL NYs functionalized with NGF@PCL microparticles; (e) migration distance measured for the neural stem cells after culturing on the different PCL NYs classes for 7 days;; adapted with permission from [300]. (f) Experimental design of the hADMSCs differentiation towards myelinating Schwann cell-like cells by means of electrical stimulation (ES), chemical induction (CI), and their combination; (g) images of the immunofluorescent staining for S100B (red), MBP (green), and nuclei (blue) of hADMSCs seeded on PPDO/5%CNT NYs by using GM and the combination of ES and CI (ES+CI), after 14 days of culture; scale bar equal to 100 μm; adapted with permission from [301].

6. Overview on nanofibers market and conclusions

The great advantages of obtaining fibers with tailored diameter sizes and surface characteristic properties, down to the nano scale, has made the ES a versatile technique to produce promising electrospun membranes with high filtering performances. So far, a great variety of synthetic and natural polymers have been electrospun with the addition of either active natural compounds or nano materials to design functionalized filters that can significantly prevent transmission of infection by viral and bacterial pathogens. Important advances have been achieved in the development of reusable and self-sterilizing biodegradable polymers-based electrospun membranes. The manufacturing of more sustainable electrospun filtering devices can address current issues originating from the outbreak of COVID-19 pandemic, including the improper disposal of surgical mask and the remotion of possible bacterial contamination present on PPE surfaces after their use. Although

most of electrospun research have been carried out at lab-scale, the electrospinning process can be easily up-scaled, thus enabling a promising perspective on rapid production of nanofiber mats to industrial scale. In recent years, many companies have patented and marketed industrial set-up machines for large scale nanofiber production [70,128, 305,306]. Among them, some leading textile industries, such as INO-VENSO (www.inovenso.com), E-SPIN Nanotech (www.espinnanotech. com), and ELMARCO (www.elmarco.com), developed industrial-scale technology to fabricate high production polymers-based electrospun membranes, as advanced filters materials for face mask and respirators application. Since the shortage of face mask during the COVID emergency, several international companies such as ske (www.ske.it), nask (www.nask.hk), sncfibers (www.sncfibers.com), fnm (www.fnm.ir), respilon (www.respilon.com), and nano4fiber (www.nano4fiber.com), have been starting to produce electrospun nanofiber mask with optimal filtration performance, according either to European or USA standard

mask protocols. Performance and characteristics of some face masks based on electrospinning technology, which are currently available on the market, are reported in literature [28]. Several smaller companies and start-ups, including 4C-Air, Maryland-based DiPole Materials, and Spanish Bioinicia, also have reacted to the COVID-19 pandemic by employing ES technology to develop advanced nanofibers-based filter with better performance in both aerosols capture and breathability [307]. The Bioinicia company (www.bioinicia.com) in collaboration with the National Scientific Research Council (CSIC) developed the first world compostable nanofiber respiratory mask for protection against COVID-19 to the market with FFP2 breathability and filtration capacity, based on ES technology. Conversely to commercial mask, the nanofiber-based face mask is made of compostable biomaterial that can easily decompose in 22 days, thus preventing further dissemination of infection plastic waste. NanoLayr company (www.nanolayr.com), formerly known as Revolution fibres Ltd, recently developed a compostable and eco PLA based electrospun filter integrated with manuka oil that meet international standard of N95 respirators providing both bactericidal and virucidal properties as well as the ability to restore filtration performance, after several washing cycles [171]. Biodegradable polymer materials proved to be an eco-friendly resource for the manufacturing of high-efficiency face masks, but the absence of an alternative fiber fabrication protocol to replace common hazardous solvents with less toxic ones in large-scale manufacturing has not been yet established. Since the electrospinning research is leading to industrial application, new strategies for the introduction of alternative and environmental-friendly solvents should be investigated. In this perspective, the use of greener solvents should be a more effective solution to both reduce the environmental impact of hazardous solvents, which are restricted by the REACH regulation, and improve a more sustainable ultrafiltration membranes manufacturing process on large scale in the future.

Declaration of Competing Interest

The authors declare that they have no known competing financial interests or personal relationships that could have appeared to influence the work reported in this paper.

Data availability

No data was used for the research described in the article.

References

[1] M. Ippolito, F. Vitale, G. Accurso, P. Iozzo, C. Gregoretti, A. Giarratano, A. Cortegiani, Medical masks and respirators for the protection of healthcare workers from SARS-CoV-2 and other viruses, Pulmonology 26 (2020) 204–212, https://doi.org/10.1016/j.pulmoe.2020.04.009.
[2] L. Bandiera, G. Pavar, G. Pisetta, S. Otomo, E. Mangano, J.R. Seckl, P. Digard, E. Molinari, F. Menolascina, I.M. Viola, Face coverings and respiratory tract droplet dispersion, R. Soc. Open Sci. 7 (2020), 201663, https://doi.org/10.1098/rsos.201663.
[3] A. Bałazy, M. Toivola, A. Adhikari, S.K. Sivasubramani, T. Reponen, S.A. Grinshpun, Do N95 respirators provide 95% protection level against airborne viruses, and how adequate are surgical masks? Am. J. Infect. Control 34 (2006) 51–57, https://doi.org/10.1016/j.ajic.2005.08.018.
[4] K. O'Dowd, K.M. Nair, P. Forouzandeh, S. Mathew, J. Grant, R. Moran, J. Bartlett, J. Bird, S.C. Pillai, Face masks and respirators in the fight against the COVID-19 pandemic: a review of current materials, advances and future perspectives, Materials 13 (2020) 3363, https://doi.org/10.3390/ma13153363.
[5] N. Zhu, D. Zhang, W. Wang, X. Li, B. Yang, J. Song, X. Zhao, B. Huang, W. Shi, R. Lu, P. Niu, F. Zhan, X. Ma, D. Wang, W. Xu, G. Wu, G.F. Gao, W. Tan, A novel Coronavirus from patients with pneumonia in China, 2019, N. Engl. J. Med. 382 (2020) 727–733, https://doi.org/10.1056/NEJMoa2001017.
[6] L. Setti, F. Passarini, G. De Gennaro, P. Barbieri, M.G. Perrone, M. Borelli, J. Palmisani, A. Di Gilio, P. Piscitelli, A. Miani, Airborne transmission route of COVID-19: why 2 Meters/6 feet of inter-personal distance could not be enough, IJERPH 17 (2020) 2932, https://doi.org/10.3390/ijerph17082932.
[7] M.C. Jarvis, Aerosol transmission of SARS-CoV-2: physical principles and implications, Front. Public Health 8 (2020), 590041, https://doi.org/10.3389/fpubh.2020.590041.
[8] J.K. Mutuku, W.C. Hou, W.H. Chen, An overview of experiments and numerical simulations on airflow and aerosols deposition in human airways and the role of bioaerosol motion in COVID-19 transmission, Aerosol Air Qual. Res. 20 (2020) 1172–1196, https://doi.org/10.4209/aaqr.2020.04.0185.
[9] T.M. Cook, Personal protective equipment during the coronavirus disease (COVID) 2019 pandemic – a narrative review, Anaesthesia 75 (2020) 920–927, https://doi.org/10.1111/anae.15071.
[10] A.D. Workman, D.B. Welling, B.S. Carter, W.T. Curry, E.H. Holbrook, S.T. Gray, G.A. Scangas, B.S. Bleier, Endonasal instrumentation and aerosolization risk in the era of COVID-19: simulation, literature review, and proposed mitigation strategies, Int. Forum Allergy Rhinol. 10 (2020) 798–805, https://doi.org/10.1002/alr.22577.
[11] W. Chen, N. Zhang, J. Wei, H.L. Yen, Y. Li, Short-range airborne route dominates exposure of respiratory infection during close contact, Build. Environ. 176 (2020), 106859, https://doi.org/10.1016/j.buildenv.2020.106859.
[12] N. Zhang, W. Chen, P. Chan, H. Yen, J.W. Tang, Y. Li, Close contact behavior in indoor environment and transmission of respiratory infection, Indoor Air 30 (2020) 645–661, https://doi.org/10.1111/ina.12673.
[13] R. Zhang, Y. Li, A.L. Zhang, Y. Wang, M.J. Molina, Identifying airborne transmission as the dominant route for the spread of COVID-19, Proc. Natl. Acad. Sci. USA 117 (2020) 14857–14863, https://doi.org/10.1073/pnas.2009637117.
[14] E. Mathieu, H. Ritchie, E. Ortiz-Ospina, M. Roser, J. Hasell, C. Appel, C. Giattino, L. Rodés-Guirao, A global database of COVID-19 vaccinations, Nat. Hum. Behav. 5 (2021) 947–953, https://doi.org/10.1038/s41562-021-01122-8.
[15] H. Brüssow, S. Zuber, Can a combination of vaccination and face mask wearing contain the COVID-19 pandemic? Microb. Biotechnol. 15 (2022) 721–737, https://doi.org/10.1111/1751-7915.13997.
[16] S.M. Bartsch, K.J. O'Shea, K.L. Chin, U. Strych, M.C. Ferguson, M.E. Bottazzi, P.T. Wedlock, S.N. Cox, S.S. Siegmund, P.J. Hotez, B.Y. Lee, Maintaining face mask use before and after achieving different COVID-19 vaccination coverage levels: a modelling study, Lancet Public Health 7 (2022) e356–e365, https://doi.org/10.1016/S2468-2667(22)00040-8.
[17] K.L. Andrejko, J.M. Pry, J.F. Myers, N. Fukui, J.L. DeGuzman, J. Openshaw, J.P. Watt, J.A. Lewnard, S. Jain, , California COVID-19 Case-Control Study Team, California COVID-19 Case-Control Study Team, Y. Abdulrahim, C.M. Barbaduomo, M.I. Bermejo, J. Cheunkarndee, A.F. Cornejo, S. Corredor, N. Dabbagh, Z.N. Dong, A. Dyke, A.T. Fang, D. Felipe, P.M. Frost, T. Ho, M.H. Javadi, A. Kaur, A. Lam, S.S. Li, M. Miller, J. Ni, H. Park, D.J. Poindexter, H. Samani, S. Saretha, M. Spencer, M.M. Spinosa, V.H. Tran, N. Walas, C. Wan, E. Xavier, Effectiveness of face mask or respirator use in indoor public settings for prevention of SARS-CoV-2 infection-California, February–December 2021, MMWR Morb. Mortal. Wkly. Rep. 71 (2022) 212–216, https://doi.org/10.15585/mmwr.mm7106e1.
[18] W. Essa, S. Yasin, I. Saeed, G. Ali, Nanofiber-based face masks and respirators as COVID-19 protection: a review, Membranes 11 (2021) 250, https://doi.org/10.3390/membranes11040250.
[19] H. Shen, Z. Zhou, H. Wang, M. Zhang, M. Han, D.P. Durkin, D. Shuai, Y. Shen, Development of electrospun nanofibrous filters for controlling Coronavirus aerosols, Environ. Sci. Technol. Lett. 8 (2021) 545–550, https://doi.org/10.1021/acs.estlett.1c00337.
[20] A. Brochocka, A. Nowak, K. Majchrzycka, M. Puchalski, S. Sztajnowski, Multifunctional polymer composites produced by melt-blown technique to use in filtering respiratory protective devices, Materials 13 (2020) 712, https://doi.org/10.3390/ma13030712.
[21] Y. Kara, K. Molnár, A review of processing strategies to generate melt-blown nano/microfiber mats for high-efficiency filtration applications, J. Ind. Text. 51 (2022) 137S–180S, https://doi.org/10.1177/15280837211019488.
[22] Y. Pu, J. Zheng, F. Chen, Y. Long, H. Wu, Q. Li, S. Yu, X. Wang, X. Ning, Preparation of polypropylene micro and nanofibers by electrostatic-assisted melt blown and their application, Polymers 10 (2018) 959, https://doi.org/10.3390/polym10090959.
[23] M.C. Han, H.W. He, W.K. Kong, K. Dong, B.Y. Wang, X. Yan, L.M. Wang, X. Ning, High-performance electret and antibacterial polypropylene meltblown nonwoven materials doped with boehmite and ZnO nanoparticles for air filtration, Fibers Polym. 23 (2022) 1947–1955, https://doi.org/10.1007/s12221-022-4786-8.
[24] J. Wu, H. Zhou, J. Zhou, X. Zhu, B. Zhang, S. Feng, Z. Zhong, L. Kong, W. Xing, Meltblown fabric vs nanofiber membrane, which is better for fabricating personal protective equipments, Chin. J. Chem. Eng. 36 (2021) 1–9, https://doi.org/10.1016/j.cjche.2020.10.022.
[25] S. Ullah, A. Ullah, J. Lee, Y. Jeong, M. Hashmi, C. Zhu, K.I. Joo, H.J. Cha, I.S. Kim, Reusability comparison of melt-blown vs nanofiber face mask filters for use in the Coronavirus pandemic, ACS Appl. Nano Mater. 3 (2020) 7231–7241, https://doi.org/10.1021/acsanm.0c01562.
[26] J. Xu, X. Xiao, W. Zhang, R. Xu, S.C. Kim, Y. Cui, T.T. Howard, E. Wu, Y. Cui, Air-filtering masks for respiratory protection from PM2.5 and pandemic pathogens, One Earth 3 (2020) 574–589, https://doi.org/10.1016/j.oneear.2020.10.014.
[27] Z. Zhang, D. Ji, H. He, S. Ramakrishna, Electrospun ultrafine fibers for advanced face masks, Mater. Sci. Eng. R Rep. 143 (2021) 100594, https://doi.org/10.1016/j.mser.2020.100594.
[28] V.S. Naragund, P.K. Panda, Electrospun nanofiber-based respiratory face masks-a review, Emerg. Mater. 5 (2022) 261–278, https://doi.org/10.1007/s42247-022-00350-6.

[29] A. Zakrzewska, M.A. Haghighat Bayan, P. Nakielski, F. Petronella, L. De Sio, F. Pierini, Nanotechnology transition roadmap toward multifunctional stimuli-responsive face masks, ACS Appl. Mater. Interfaces 14 (2022) 46123–46144, https://doi.org/10.1021/acsami.2c10335.

[30] S. Wu, T. Dong, Y. Li, M. Sun, Y. Qi, J. Liu, M.A. Kuss, S. Chen, B. Duan, State-of-the-art review of advanced electrospun nanofiber yarn-based textiles for biomedical applications, Appl. Mater. Today 27 (2022), 101473, https://doi.org/10.1016/j.apmt.2022.101473.

[31] Y. Li, T. Dong, Z. Li, S. Ni, F. Zhou, O.A. Alimi, S. Chen, B. Duan, M. Kuss, S. Wu, Review of advances in electrospinning-based strategies for spinal cord regeneration, Mater. Today Chem. 24 (2022), 100944, https://doi.org/10.1016/j.mtchem.2022.100944.

[32] L. Sethuram, J. Thomas, Therapeutic applications of electrospun nanofibers impregnated with various biological macromolecules for effective wound healing strategy – a review, Biomed. Pharmacother. 157 (2023), 113996, https://doi.org/10.1016/j.biopha.2022.113996.

[33] F.D. Al-Shalawi, M.A. Azmah Hanim, M.K.A. Ariffin, C. Looi Seng Kim, D. Brabazon, R. Calin, M.O. Al-Osaimi, Biodegradable synthetic polymer in orthopaedic application: a review, Mater. Today Proc. 74 (2023) 540–546, https://doi.org/10.1016/j.matpr.2022.12.254.

[34] M. Kumar, Ayah.R. Hilles, Y. Ge, A. Bhatia, S. Mahmood, A review on polysaccharides mediated electrospun nanofibers for diabetic wound healing: their current status with regulatory perspective, Int. J. Biol. Macromol. 234 (2023), 123696, https://doi.org/10.1016/j.ijbiomac.2023.123696.

[35] M. Gruppuso, G. Turco, E. Marsich, D. Porrelli, Polymeric wound dressings, an insight into polysaccharide-based electrospun membranes, Appl. Mater. Today 24 (2021), 101148, https://doi.org/10.1016/j.apmt.2021.101148.

[36] X. Zhang, L. Xie, X. Wang, Z. Shao, B. Kong, Electrospinning super-assembly of ultrathin fibers from single- to multi-Taylor cone sites, Appl. Mater. Today 26 (2022), 101272, https://doi.org/10.1016/j.apmt.2021.101272.

[37] M.S. Islam, P. Larpruenrudee, S.C. Saha, O. Pourmehran, A.R. Paul, T. Gemci, R. Collins, G. Paul, Y. Gu, How severe acute respiratory syndrome Coronavirus-2 aerosol propagates through the age-specific upper airways, Phys. Fluids 33 (2021), 081911, https://doi.org/10.1063/5.0061627.

[38] K.A. Prather, C.C. Wang, R.T. Schooley, Reducing transmission of SARS-CoV-2, Science 368 (2020) 1422–1424, https://doi.org/10.1126/science.abc6197.

[39] I. Armentano, M. Barbanera, E. Carota, S. Crognale, M. Marconi, S. Rossi, G. Rubino, M. Scungio, J. Taborri, G. Calabrò, Polymer materials for respiratory protection: processing, end use, and testing methods, ACS Appl. Polym. Mater. 3 (2021) 531–548, https://doi.org/10.1021/acsapm.0c01151.

[40] S. Das, S. Sarkar, A. Das, S. Das, P. Chakraborty, J. Sarkar, A comprehensive review of various categories of face masks resistant to Covid-19, Clin. Epidemiol. Glob. Health 12 (2021), 100835, https://doi.org/10.1016/j.cegh.2021.100835.

[41] S. Rossettie, C. Perry, M. Pourghaed, M. Zumwalt, Effectiveness of manufactured surgical masks, respirators, and home-made masks in prevention of respiratory infection due to airborne microorganisms, Chronicles 8 (2020) 11–26, https://doi.org/10.12746/swrccc.v8i34.675.

[42] C. Boi, F. Borsetti, T.M. Brugo, M. Cappelletti, M.G. De Angelis, S. Fedi, S. Di Giacomo, T. Fabiani, G. Foli, A. Garelli, U. Genchi, D. Ghezzi, C. Gualandi, E. Lalli, M. Magnani, A. Maurizzi, F. Mazzi, N. Mehrabi, M. Minelli, R. Montalbano, L. Morelli, S. Nici, R. Onesti, A. Paglianti, K. Papchenko, S. Pappalardo, N.F. Parisi, S. Rapino, M. Reggio, M. Roselli, E. Ruggeri, L. Sabatini, E. Saracino, G.E. Scarponi, L. Serra, V. Signorini, A. Storione, M. Torsello, E. Tugnoli, C.M. Vargiu, G. Vidali, F.S. Violante, One year of surgical mask testing at the University of Bologna labs: lessons learned from data analysis, Sep. Purif. Technol. 294 (2022), 121180, https://doi.org/10.1016/j.seppur.2022.121180.

[43] R.J. LaRue, P. Morkus, S. Laengert, S. Rassenberg, M.A. Halali, J. W. Colenbrander, C.M. Clase, D.R. Latulippe, C. Lannoy, Navigating performance standards for face mask materials: a custom-built apparatus for measuring particle filtration efficiency, Glob. Chall. 5 (2021), 2100052, https://doi.org/10.1002/gch2.202100052.

[44] B. Illés, P. Gordon, Filtering efficiency measurement of respirators by laser-based particle counting method, Measurement 176 (2021), 109173, https://doi.org/10.1016/j.measurement.2021.109173.

[45] M.Z. Rahman, M.E. Hoque, M.R. Alam, M.A. Rouf, S.I. Khan, H. Xu, S. Ramakrishna, Face masks to Combat Coronavirus (COVID-19)-processing, roles, requirements, efficacy, risk and sustainability, Polymers 14 (2022) 1296, https://doi.org/10.3390/polym14071296.

[46] H.E. Whyte, Y. Montigaud, E. Audoux, P. Verhoeven, A. Prier, L. Leclerc, G. Sarry, C. Laurent, A. Le Coq, A. Joubert, J. Pourchez, Comparison of bacterial filtration efficiency vs. particle filtration efficiency to assess the performance of non-medical face masks, Sci. Rep. 12 (2022) 1188, https://doi.org/10.1038/s41598-022-05245-4.

[47] Centers for Disease Control and Prevention (CDC). Interim infection prevention and control recommendations for patients with suspected or confirmed Coronavirus Disease 2019 (COVID-19) in healthcare; updated Sept. 23, 2022. https://www.cdc.gov/coronavirus/2019-ncov/hcp/infection-control-recommendations.html#print, (n.d.).

[48] World Health Organization (WHO). Clinical Management of COVID-19, Living guideline; updated Jan. 13 2023. https://www.who.int/publications-detail-redirect/WHO-2019-nCoV-clinical-2023.1., (n.d.).

[49] C.R. MacIntyre, Q. Wang, B. Rahman, H. Seale, I. Ridda, Z. Gao, P. Yang, W. Shi, X. Pang, Y. Zhang, A. Moa, D.E. Dwyer, Efficacy of face masks and respirators in preventing upper respiratory tract bacterial colonization and co-infection in hospital healthcare workers, Prev. Med. 62 (2014) 1–7, https://doi.org/10.1016/j.ypmed.2014.01.015.

[50] C.R. MacIntyre, Q. Wang, H. Seale, P. Yang, W. Shi, Z. Gao, B. Rahman, Y. Zhang, X. Wang, A.T. Newall, A. Heywood, D.E. Dwyer, A randomized clinical trial of three options for N95 respirators and medical masks in health workers, Am. J. Respir. Crit. Care Med. 187 (2013) 960–966, https://doi.org/10.1164/rccm.201207-1164OC.

[51] L.J. Radonovich, M.S. Simberkoff, M.T. Bessesen, A.C. Brown, D.A.T. Cummings, C.A. Gaydos, J.G. Los, A.E. Krosche, C.L. Gibert, G.J. Gorse, A.C. Nyquist, N. G. Reich, M.C. Rodriguez-Barradas, C.S. Price, T.M. Perl, for the ResPECT investigators, N95 respirators vs medical masks for preventing influenza among health care personnel: a randomized clinical trial, JAMA 322 (2019) 824, https://doi.org/10.1001/jama.2019.11645.

[52] M. Loeb, N. Dafoe, J. Mahony, M. John, A. Sarabia, V. Glavin, R. Webby, M. Smieja, D.J.D. Earn, S. Chong, A. Webb, A.D. Walter, Surgical mask vs N95 respirator for preventing influenza among health care workers: a randomized trial, (2023). (Reprinted), JAMA 302 (2009), https://doi.org/10.1001/jama.2019.11645.

[53] T.U. Rashid, S. Sharmeen, S. Biswas, Effectiveness of N95 masks against SARS-CoV-2: performance efficiency, concerns, and future directions, ACS Chem. Health Saf. 29 (2022) 135–164, https://doi.org/10.1021/acs.chas.1c00016.

[54] J.J. Bartoszko, M.A.M. Farooqi, W. Alhazzani, M. Loeb, Medical masks vs N95 respirators for preventing COVID-19 in healthcare workers: a systematic review and meta-analysis of randomized trials, Influenza Other Respir. Viruses 14 (2020) 365–373, https://doi.org/10.1111/irv.12745.

[55] S. Adanur, A. Jayswal, Filtration mechanisms and manufacturing methods of face masks: an overview, J. Ind. Text. 51 (2022) 3683S–3717S, https://doi.org/10.1177/1528083720980169.

[56] A. Tcharkhtchi, N. Abbasnezhad, M. Zarbini Seydani, N. Zirak, S. Farzaneh, M. Shirinbayan, An overview of filtration efficiency through the masks: mechanisms of the aerosols penetration, Bioact. Mater. 6 (2021) 106–122, https://doi.org/10.1016/j.bioactmat.2020.08.002.

[57] A.M. Todea, F. Schmidt, T. Schuldt, C. Asbach, Development of a method to determine the fractional deposition efficiency of full-scale HVAC and HEPA filter cassettes for nanoparticles ≥3.5 nm, Atmosphere 11 (2020) 1191, https://doi.org/10.3390/atmos11111191.

[58] I.A. Borojeni, G. Gajewski, R.A. Riahi, Application of electrospun nonwoven fibers in air filters, (2022) 27.

[59] Y. Gao, E. Tian, Y. Zhang, J. Mo, Utilizing electrostatic effect in fibrous filters for efficient airborne particles removal: principles, fabrication, and material properties, Appl. Mater. Today 26 (2022), 101369, https://doi.org/10.1016/j.apmt.2022.101369.

[60] Department of Materials Science and Engineering, The University of Tennessee, Knoxville, TN 37996 USA P. Tsai, Performance of masks and discussion of the inactivation of SARS-CoV-2, Eng. Sci. (2020), https://doi.org/10.30919/es8d1110.

[61] S.A. Grinshpun, M. Yermakov, M. Khodoun, Autoclave sterilization and ethanol treatment of re-used surgical masks and N95 respirators during COVID-19: impact on their performance and integrity, J. Hosp. Infect. 105 (2020) 608–614, https://doi.org/10.1016/j.jhin.2020.06.030.

[62] H. Shen, M. Han, Y. Shen, D. Shuai, Electrospun nanofibrous membranes for controlling airborne viruses: present status, standardization of aerosol filtration tests, and future development, ACS Environ. Au 2 (2022) 290–309, https://doi.org/10.1021/acsenvironau.1c00047.

[63] L.H. Kwong, R. Wilson, S. Kumar, Y.S. Crider, Y.R. Sanchez, D. Rempel, A. Pillarisetti, Review of the breathability and filtration efficiency of common household materials for face masks, ACS Nano 15 (2021) 5904–5924, https://doi.org/10.1021/acsnano.0c10146.

[64] R.M. Jones, D. Rempel, Standards for surgical respirators and masks: relevance for protecting healthcare workers and the public during pandemics, Ann. Work Expo. Health 65 (2021) 495–504, https://doi.org/10.1093/annweh/wxab008.

[65] A. Scarano, F. Inchingolo, F. Lorusso, Facial skin temperature and discomfort when wearing protective face masks: thermal infrared imaging evaluation and hands moving the mask, IJERPH 17 (2020) 4624, https://doi.org/10.3390/ijerph17134624.

[66] X. Guan, J. Lin, J. Han, X. Gao, Y. Zhang, B. Hu, R. Guidoin, L. Wang, Prolonged use of surgical masks and respirators affects the protection and comfort for healthcare workers, Materials 15 (2022) 7918, https://doi.org/10.3390/ma15227918.

[67] M. Liao, H. Liu, X. Wang, X. Hu, Y. Huang, X. Liu, K. Brenan, J. Mecha, M. Nirmalan, J.R. Lu, A technical review of face mask wearing in preventing respiratory COVID-19 transmission, Curr. Opin. Colloid Interface Sci. 52 (2021), 101417, https://doi.org/10.1016/j.cocis.2021.101417.

[68] A. Buzzin, G. Domènech-Gil, E. Fraschetti, E. Giovine, D. Puglisi, D. Caputo, Assessing the consequences of prolonged usage of disposable face masks, Sci. Rep. 12 (2022) 16796, https://doi.org/10.1038/s41598-022-20692-9.

[69] Q. Armand, H.E. Whyte, P. Verhoeven, F. Grattard, L. Leclerc, N. Curt, S.P. Ragey, J. Pourchez, Impact of medical face mask wear on bacterial filtration efficiency and breathability, Environ. Technol. Innov. 28 (2022), 102897, https://doi.org/10.1016/j.eti.2022.102897.

[70] F. Russo, R. Castro-Muñoz, S. Santoro, F. Galiano, A. Figoli, A review on electrospun membranes for potential air filtration application, J. Environ. Chem. Eng. 10 (2022), 108452, https://doi.org/10.1016/j.jece.2022.108452.

[71] W. Gilbert, P.F. Mottelay, De magnete, unabridged republ. of the 1893 ed, Dover, New York, 1991.

[72] X.X. Lord Rayleigh, On the equilibrium of liquid conducting masses charged with electricity, Lond. Edinb. Dublin Philos. Mag. J. Sci. 14 (1882) 184–186, https://doi.org/10.1080/14786448208628425.

[73] J. Zeleny, Instability of electrified liquid surfaces, Phys. Rev. 10 (1917) 1–6, https://doi.org/10.1103/PhysRev.10.1.

[74] Cooley, J.F., Improved methods of and apparatus for electrically separating the relatively volatile liquid component from the component of relatively fixed substances of composite fluids. Patent number GB 06385, 1900, n.d.

[75] A. Formhals, "Process and apparatus for preparing artificial threads," US Patent 1975504, 1934, n.d.

[76] A. Formhals, "Method and apparatus for spinning," US Patent 2160962, 1939, n.d.

[77] A. Formhals, "Artificial thread and method of producing same," US Patent 2187306, 1940, n.d.

[78] N. Bhardwaj, S.C. Kundu, Electrospinning: a fascinating fiber fabrication technique, Biotechnol. Adv. 28 (2010) 325–347, https://doi.org/10.1016/j.biotechadv.2010.01.004.

[79] T. Geoffrey, Disintegration of water drops in an electric field, Proc. R. Soc. Lond. A 280 (1964) 383–397, https://doi.org/10.1098/rspa.1964.0151.

[80] J. Xue, T. Wu, Y. Dai, Y. Xia, Electrospinning and electrospun nanofibers: methods, materials, and applications, Chem. Rev. 119 (2019) 5298–5415, https://doi.org/10.1021/acs.chemrev.8b00593.

[81] X. Yang, J. Wang, H. Guo, L. Liu, W. Xu, G. Duan, Structural design toward functional materials by electrospinning: a review, e-Polymers 20 (2020) 682–712, https://doi.org/10.1515/epoly-2020-0068.

[82] Y. Zhou, Y. Liu, M. Zhang, Z. Feng, D.G. Yu, K. Wang, Electrospun nanofiber membranes for air filtration: a review, Nanomaterials 12 (2022) 1077, https://doi.org/10.3390/nano12071077.

[83] I. Shepa, E. Mudra, J. Dusza, Electrospinning through the prism of time, Mater. Today Chem. 21 (2021) 100543, https://doi.org/10.1016/j.mtchem.2021.100543.

[84] M. Cai, H. He, X. Zhang, X. Yan, J. Li, F. Chen, D. Yuan, X. Ning, Efficient synthesis of PVDF/PI side-by-side bicomponent nanofiber membrane with enhanced mechanical strength and good thermal stability, Nanomaterials 9 (2018) 39, https://doi.org/10.3390/nano9010039.

[85] D. Han, A.J. Steckl, Coaxial electrospinning formation of complex polymer fibers and their applications, ChemPlusChem 84 (2019) 1453–1497, https://doi.org/10.1002/cplu.201900281.

[86] H. Zhang, N. Liu, Q. Zeng, J. Liu, X. Zhang, M. Ge, W. Zhang, S. Li, Y. Fu, Y. Zhang, Design of polypropylene electret melt blown nonwovens with superior filtration efficiency stability through thermally stimulated charging, Polymers 12 (2020) 2341, https://doi.org/10.3390/polym12102341.

[87] H. Zhang, J. Liu, X. Zhang, C. Huang, X. Jin, Design of electret polypropylene melt blown air filtration material containing nucleating agent for effective PM2.5 capture, RSC Adv. 8 (2018) 7932–7941, https://doi.org/10.1039/C7RA10916D.

[88] J. Zhang, G. Chen, G.S. Bhat, H. Azari, H. Pen, Electret characteristics of melt-blown polylactic acid fabrics for air filtration application, J. Appl. Polym. Sci. 137 (2020) 48309, https://doi.org/10.1002/app.48309.

[89] P.J. Espinoza-Montero, M. Montero-Jiménez, S. Rojas-Quishpe, C.D. Alcívar León, J. Heredia-Moya, A. Rosero-Chanalata, C. Orbea-Hinojosa, J.L. Piñeiros, Nude and modified electrospun nanofibers, application to air purification, Nanomaterials 13 (2023) 593, https://doi.org/10.3390/nano13030593.

[90] A. Sanyal, S. Sinha-Ray, Ultrafine PVDF nanofibers for filtration of air-borne particulate matters: a comprehensive review, Polymers 13 (2021) 1864, https://doi.org/10.3390/polym13111864.

[91] W.W.F. Leung, C.H. Hung, Skin effect in nanofiber filtration of submicron aerosols, Sep. Purif. Technol. 92 (2012) 174–180, https://doi.org/10.1016/j.seppur.2011.02.020.

[92] P. Li, C. Wang, Y. Zhang, F. Wei, Air filtration in the free molecular flow regime: a review of high-efficiency particulate air filters based on carbon nanotubes, Small 10 (2014) 4543–4561, https://doi.org/10.1002/smll.201401553.

[93] T. Xia, Y. Bian, L. Zhang, C. Chen, Relationship between pressure drop and face velocity for electrospun nanofiber filters, Energy Build. 158 (2018) 987–999, https://doi.org/10.1016/j.enbuild.2017.10.073.

[94] Y. Li, J. Zhu, H. Cheng, G. Li, H. Cho, M. Jiang, Q. Gao, X. Zhang, Developments of advanced electrospinning techniques: a critical review, Adv. Mater. Technol. 6 (2021), 2100410, https://doi.org/10.1002/admt.202100410.

[95] A. Bachs-Herrera, O. Yousefzade, L.J. del Valle, J. Puiggali, Melt electrospinning of polymers: blends, nanocomposites, additives and applications, Appl. Sci. 11 (2021) 1808, https://doi.org/10.3390/app11041808.

[96] É.J. Beaudoin, M.M. Kubaski, M. Samara, R.J. Zednik, N.R. Demarquette, Scaled-up multi-needle electrospinning process using parallel plate auxiliary electrodes, Nanomaterials 12 (2022) 1356, https://doi.org/10.3390/nano12081356.

[97] F. Müller, S. Jokisch, H. Bargel, T. Scheibel, Centrifugal electrospinning enables the production of meshes of ultrathin polymer fibers, ACS Appl. Polym. Mater. 2 (2020) 4360–4367, https://doi.org/10.1021/acsapm.0c00853.

[98] C. Mingjun, Z. Youchen, L. Haoyi, L. Xiangnan, D. Yumei, M.M. Bubakir, Y. Weimin, An example of industrialization of melt electrospinning: polymer melt differential electrospinning, Adv. Ind. Eng. Polym. Res. 2 (2019) 110–115, https://doi.org/10.1016/j.aiepr.2019.06.002.

[99] C. Lyu, P. Zhao, J. Xie, S. Dong, J. Liu, C. Rao, J. Fu, Electrospinning of nanofibrous membrane and its applications in air filtration: a review, Nanomaterials 11 (2021) 1501, https://doi.org/10.3390/nano11061501.

[100] L. Wei, R. Sun, C. Liu, J. Xiong, X. Qin, Mass production of nanofibers from needleless electrospinning by a novel annular spinneret, Mater. Des. 179 (2019) 107885, https://doi.org/10.1016/j.matdes.2019.107885.

[101] H. Niu, T. Lin, Fiber generators in needleless electrospinning, J. Nanomater. 2012 (2012) 1–13, https://doi.org/10.1155/2012/725950.

[102] J. Chen, Z. Yu, C. Li, Y. Lv, S. Hong, P. Hu, Y. Liu, Review of the principles, devices, parameters, and applications for centrifugal electrospinning, Macro Mater. Eng. 307 (2022), 2200057, https://doi.org/10.1002/mame.202200057.

[103] Y. Zhang, L. Zhang, L. Cheng, Y. Qin, Y. Li, W. Yang, H. Li, Efficient preparation of polymer nanofibers by needle roller electrospinning with low threshold voltage, Polym. Eng. Sci. 59 (2019) 745–751, https://doi.org/10.1002/pen.24993.

[104] M. Waqas, A. Keirouz, M.K. Sanira Putri, F. Fazal, F.J. Diaz Sanchez, D. Ray, V. Koutsos, N. Radacsi, Design and development of a nozzle-free electrospinning device for the high-throughput production of biomaterial nanofibers, Med. Eng. Phys. 92 (2021) 80–87, https://doi.org/10.1016/j.medengphy.2021.04.007.

[105] H.J. He, C.K. Liu, K. Molnar, A novel needleless electrospinning system using a moving conventional yarn as the spinneret, Fibers Polym. 19 (2018) 1472–1478, https://doi.org/10.1007/s12221-018-8183-2.

[106] G. Zheng, J. Jiang, X. Wang, W. Li, W. Zhong, S. Guo, Self-cleaning threaded rod spinneret for high-efficiency needleless electrospinning, Appl. Phys. A 124 (2018) 473, https://doi.org/10.1007/s00339-018-1892-y.

[107] L. Wei, C. Liu, X. Mao, J. Dong, W. Fan, C. Zhi, X. Qin, R. Sun, Multiple-jet needleless electrospinning approach via a linear flume spinneret, Polymers 11 (2019) 2052, https://doi.org/10.3390/polym11122052.

[108] J. Xiong, Y. Liu, A. Li, L. Wei, L. Wang, X. Qin, J. Yu, Mass production of high-quality nanofibers via constructing pre-Taylor cones with high curvature on needleless electrospinning, Mater. Des. 197 (2021), 109247, https://doi.org/10.1016/j.matdes.2020.109247.

[109] M.A. Hassan, U. Ali, A. Shahzad, M.B. Qadir, Z. Khaliq, A. Nazir, S. Abid, M. Q. Khan, T. Hussain, Bullet-Spinneret based needleless electrospinning; a versatile way to fabricate continuous nanowebs at low voltage, Mater. Res. Express 6 (2018), 025053, https://doi.org/10.1088/2053-1591/aaf137.

[110] Y. Xu, X. Li, H.F. Xiang, Q.Q. Zhang, X.X. Wang, M. Yu, L.Y. Hao, Y.Z. Long, Large-scale preparation of polymer nanofibers for air filtration by a new multineedle electrospinning device, J. Nanomater. 2020 (2020) 1–7, https://doi.org/10.1155/2020/4965438.

[111] P. Vass, B. Démuth, A. Farkas, E. Hirsch, E. Szabó, B. Nagy, S.K. Andersen, T. Vigh, G. Verreck, I. Csontos, G. Marosi, Z.K. Nagy, Continuous alternative to freeze drying: manufacturing of cyclodextrin-based reconstitution powder from aqueous solution using scaled-up electrospinning, J. Control. Release 298 (2019) 120–127, https://doi.org/10.1016/j.jconrel.2019.02.019.

[112] E. Hirsch, P. Vass, B. Demuth, Zs. Petho, E. Bitay, S.K. Andersen, T. Vigh, G. Verreck, K. Molnar, Z.K. Nagy, G. Marosi, Electrospinning scale-up and formulation development of PVA nanofibers aiming oral delivery of biopharmaceuticals, Express Polym. Lett. 13 (2019) 590–603, https://doi.org/10.3144/expresspolymlett.2019.50.

[113] G. Duan, A. Greiner, Air-blowing-assisted coaxial electrospinning toward high productivity of core/sheath and hollow fibers, Macromol. Mater. Eng. 304 (2019), 1800669, https://doi.org/10.1002/mame.201800669.

[114] B.E. Kwak, H.J. Yoo, E. Lee, D.H. Kim, Large-scale centrifugal multispinning production of polymer micro- and nanofibers for mask filter application with a potential of cospinning mixed multicomponent fibers, ACS Macro Lett. 10 (2021) 382–388, https://doi.org/10.1021/acsmacrolett.0c00829.

[115] L. Wang, B. Wang, Z. Ahmad, J.S. Li, M.W. Chang, Dual rotation centrifugal electrospinning: a novel approach to engineer multi-directional and layered fiber composite matrices, Drug Deliv. Transl. Res. 9 (2019) 204–214, https://doi.org/10.1007/s13346-018-00594-y.

[116] Y. Liu, J. Tan, S. Yu, M. Yousefzadeh, T. Lyu, Z. Jiao, H. Li, S. Ramakrishna, High-efficiency preparation of polypropylene nanofiber by melt differential centrifugal electrospinning, J. Appl. Polym. Sci. 137 (2020) 48299, https://doi.org/10.1002/app.48299.

[117] K. Koenig, F. Langensiepen, G. Seide, Pilot-scale production of polylactic acid nanofibers by melt electrospinning, e-Polymers 20 (2020) 233–241, https://doi.org/10.1515/epoly-2020-0030.

[118] B. Araldi da Silva, R. de Sousa Cunha, A. Valério, A. De Noni Junior, D. Hotza, S. Y. Gómez González, Electrospinning of cellulose using ionic liquids: an overview on processing and applications, Eur. Polym. J. 147 (2021), 110283, https://doi.org/10.1016/j.eurpolymj.2021.110283.

[119] S.A. Naziri Mehrabani, V. Vatanpour, I. Koyuncu, Green solvents in polymeric membrane fabrication: a review, Sep. Purif. Technol. 298 (2022), 121691, https://doi.org/10.1016/j.seppur.2022.121691.

[120] W. Song, X. Zhao, Z. Jin, L. Fan, X. Ji, J. Deng, J. Duan, Poly(vinyl alcohol) for multi-functionalized corrosion protection of metals: a review, J. Clean. Prod. 394 (2023), 136390, https://doi.org/10.1016/j.jclepro.2023.136390.

[121] P. Rai, S. Mehrotra, S. Priya, E. Gnansounou, S.K. Sharma, Recent advances in the sustainable design and applications of biodegradable polymers, Bioresour. Technol. 325 (2021) 124739, https://doi.org/10.1016/j.biortech.2021.124739.

[122] A. Kakoria, S. Sinha-Ray, A review on biopolymer-based fibers via electrospinning and solution blowing and their applications, Fibers 6 (2018) 45, https://doi.org/10.3390/fib6030045.

[123] Y. Ibrahim, E. Hussein, M. Zagho, G. Abdo, A. Elzatahry, Melt electrospinning designs for nanofiber fabrication for different applications, IJMS 20 (2019) 2455, https://doi.org/10.3390/ijms20102455.

[124] H. Li, H. Chen, X. Zhong, W. Wu, Y. Ding, W. Yang, Interjet distance in needleless melt differential electrospinning with umbellate nozzles, J. Appl. Polym. Sci. 131 (2014), https://doi.org/10.1002/app.40515 n/a-n/a.

[125] H. Chen, H. Li, X. Ma, W. He, J. Tan, W. Yang, Large scaled fabrication of microfibers by air-suction assisted needleless melt electrospinning, Fibers Polym. 17 (2016) 576–581, https://doi.org/10.1007/s12221-016-5915-z.

[126] Y. Qin, L. Cheng, Y. Zhang, X. Chen, X. Wang, X. He, W. Yang, Y. An, H. Li, Efficient preparation of poly(lactic acid) nanofibers by melt differential electrospinning with addition of acetyl tributyl citrate: research article, J. Appl. Polym. Sci. 135 (2018) 46554, https://doi.org/10.1002/app.46554.

[127] M. Yu, R.H. Dong, X. Yan, G.F. Yu, M.H. You, X. Ning, Y.Z. Long, Recent advances in needleless electrospinning of ultrathin fibers: from academia to industrial production, Macromol. Mater. Eng. 302 (2017), 1700002, https://doi.org/10.1002/mame.201700002.

[128] S. Omer, L. Forgách, R. Zelkó, I. Sebe, Scale-up of electrospinning: market overview of products and devices for pharmaceutical and biomedical purposes, Pharmaceutics 13 (2021) 286, https://doi.org/10.3390/pharmaceutics13020286.

[129] H.M. Ibrahim, A. Klingner, A review on electrospun polymeric nanofibers: production parameters and potential applications, Polym. Test. 90 (2020), 106647, https://doi.org/10.1016/j.polymertesting.2020.106647.

[130] M.S. Islam, B.C. Ang, A. Andriyana, A.M. Afifi, A review on fabrication of nanofibers via electrospinning and their applications, SN Appl. Sci. 1 (2019) 1248, https://doi.org/10.1007/s42452-019-1288-4.

[131] P.K. Szewczyk, U. Stachewicz, The impact of relative humidity on electrospun polymer fibers: from structural changes to fiber morphology, Adv. Colloid Interface Sci. 286 (2020), 102315, https://doi.org/10.1016/j.cis.2020.102315.

[132] T.U. Rashid, R.E. Gorga, W.E. Krause, Mechanical properties of electrospun fibers-a critical review, Adv. Eng. Mater. 23 (2021), 2100153, https://doi.org/10.1002/adem.202100153.

[133] G.B. Medeiros, F. de A. Lima, D.S. de Almeida, V.G. Guerra, M.L. Aguiar, Modification and functionalization of fibers formed by electrospinning: a review, Membranes 12 (2022) 861, https://doi.org/10.3390/membranes12090861.

[134] V. Naragund, P.K. Panda, Electrospinning of polyacrylonitrile nanofiber membrane for bacteria removal, (2018). 10.5281/ZENODO.3344558.

[135] T. Baby, T. Jose E, G. George, V. Varkey, S.K. Cherian, A new approach for the shaping up of very fine and beadless UV light absorbing polycarbonate fibers by electrospinning, Polym. Test. 80 (2019), 106103, https://doi.org/10.1016/j.polymertesting.2019.106103.

[136] S.F. Dehghan, F. Golbabaei, B. Maddah, M. Latifi, H. Pezeshk, M. Hasanzadeh, F. Akbar-Khanzadeh, Optimization of electrospinning parameters for polyacrylonitrile-MgO nanofibers applied in air filtration, J. Air Waste Manag. Assoc. 66 (2016) 912–921, https://doi.org/10.1080/10962247.2016.1162228.

[137] H. He, Y. Kara, K. Molnár, *In situ* viscosity-controlled electrospinning with a low threshold voltage, Macromol. Mater. Eng. 304 (2019), 1900349, https://doi.org/10.1002/mame.201900349.

[138] Y. Bian, S. Wang, L. Zhang, C. Chen, Influence of fiber diameter, filter thickness, and packing density on PM2.5 removal efficiency of electrospun nanofiber air filters for indoor applications, Build. Environ. 170 (2020), 106628, https://doi.org/10.1016/j.buildenv.2019.106628.

[139] L.R. Manea, A.P. Bertea, A. Bertea, Progress in electrospun nanofibres for air filtration, IOP Conf. Ser. Mater. Sci. Eng. 877 (2020), 012043, https://doi.org/10.1088/1757-899X/877/1/012043.

[140] M.K. Selatile, S.S. Ray, V. Ojijo, R. Sadiku, Depth filtration of airborne agglomerates using electrospun bio-based polylactide membranes, J. Environ. Chem. Eng. 6 (2018) 762–772, https://doi.org/10.1016/j.jece.2017.12.070.

[141] Y. Li, X. Yin, J. Yu, B. Ding, Electrospun nanofibers for high-performance air filtration, Compos. Commun. 15 (2019) 6–19, https://doi.org/10.1016/j.coco.2019.06.003.

[142] F. Zuo, S. Zhang, H. Liu, H. Fong, X. Yin, J. Yu, B. Ding, Free-standing polyurethane nanofiber/nets air filters for effective PM capture, Small 13 (2017), 1702139, https://doi.org/10.1002/smll.201702139.

[143] S. Zhang, H. Liu, F. Zuo, X. Yin, J. Yu, B. Ding, A controlled design of ripple-like polyamide-6 nanofiber/nets membrane for high-efficiency air filter, Small 13 (2017), 1603151, https://doi.org/10.1002/smll.201603151.

[144] R. Al-Attabi, L.F. Dumée, J.A. Schütz, Y. Morsi, Pore engineering towards highly efficient electrospun nanofibrous membranes for aerosol particle removal, Sci. Total Environ. 625 (2018) 706–715, https://doi.org/10.1016/j.scitotenv.2017.12.342.

[145] H. Kim, S. Lee, Y.R. Shin, Y.N. Choi, J. Yoon, M. Ryu, J.W. Lee, H. Lee, Durable superhydrophobic poly(vinylidene fluoride) (PVDF)-based nanofibrous membranes for reusable air filters, ACS Appl. Polym. Mater. 4 (2022) 338–347, https://doi.org/10.1021/acsapm.1c01314.

[146] J. Moon, T.T. Bui, S. Jang, S. Ji, J.T. Park, M.G. Kim, A highly efficient nanofibrous air filter membrane fabricated using electrospun amphiphilic PVDF-g-POEM double comb copolymer, Sep. Purif. Technol. 279 (2021), 119625, https://doi.org/10.1016/j.seppur.2021.119625.

[147] M. Sohrabi, M. Abbasi, A. Sadighzadeh, Fabrication and evaluation of electrospun polyacrylonitrile/silver nanofiber membranes for air filtration and antibacterial activity, Polym. Bull. (2022), https://doi.org/10.1007/s00289-022-04311-1.

[148] A. Lakshmanan, D.S. Gavali, R. Thapa, D. Sarkar, Synthesis of CTAB-functionalized large-scale nanofibers air filter media for efficient PM$_{2.5}$ capture capacity with low airflow resistance, ACS Appl. Polym. Mater 3 (2021) 937–948, https://doi.org/10.1021/acsapm.0c01203.

[149] H. Dai, X. Liu, C. Zhang, K. Ma, Y. Zhang, Electrospinning polyacrylonitrile/graphene oxide/polyimide nanofibrous membranes for high-efficiency PM2.5 filtration, Sep. Purif. Technol. 276 (2021), 119243, https://doi.org/10.1016/j.seppur.2021.119243.

[150] Y. Xu, X. Zhang, X. Hao, D. Teng, T. Zhao, Y. Zeng, Micro/nanofibrous nonwovens with high filtration performance and radiative heat dissipation property for personal protective face mask, Chem. Eng. J. 423 (2021), 130175, https://doi.org/10.1016/j.cej.2021.130175.

[151] F.N.H. Karabulut, G. Höfler, N. Ashok Chand, G.W. Beckermann, Electrospun nanofibre filtration media to protect against biological or nonbiological airborne particles, Polymers 13 (2021) 3257, https://doi.org/10.3390/polym13193257.

[152] Z. Yang, X. Zhang, Z. Qin, H. Li, J. Wang, G. Zeng, C. Liu, J. Long, Y. Zhao, Y. Li, G. Yan, Airflow synergistic needleless electrospinning of instant noodle-like curly nanofibrous membranes for high-efficiency air filtration, Small 18 (2022), 2107250, https://doi.org/10.1002/smll.202107250.

[153] J. Jiang, Z. Shao, X. Wang, P. Zhu, S. Deng, W. Li, G. Zheng, Three-dimensional composite electrospun nanofibrous membrane by multi-jet electrospinning with sheath gas for high-efficiency antibiosis air filtration, Nanotechnology 32 (2021), 245707, https://doi.org/10.1088/1361-6528/abeb9a.

[154] M. Li, H. Wen, H. Li, Z.C. Yan, Y. Li, L. Wang, D. Wang, B.Z. Tang, AIEgen-loaded nanofibrous membrane as photodynamic/photothermal antimicrobial surface for sunlight-triggered bioprotection, Biomaterials 276 (2021), 121007, https://doi.org/10.1016/j.biomaterials.2021.121007.

[155] S. Kumar, J. Jang, H. Oh, B.J. Jung, Y. Lee, H. Park, K.H. Yang, Y.C. Seong, J.S. Lee, AntibacteriAL POLYMERIC NANOFIBERS FROM ZWITTERIONIC TERPOLYMERS BY ELECTROSPINNING FOR AIR FILTRATIon, ACS Appl. Nano Mater. 4 (2021) 2375–2385, https://doi.org/10.1021/acsanm.0c02366.

[156] M. Pierpaoli, C. Giosuè, N. Czerwińska, M. Rycewicz, A. Wielozyńska, R. Bogdanowicz, M.L. Ruello, Characterization and filtration efficiency of sustainable PLA fibers obtained via a hybrid 3D-printed/electrospinning technique, Materials 14 (2021) 6766, https://doi.org/10.3390/ma14226766.

[157] L. Wang, Y. Gao, J. Xiong, W. Shao, C. Cui, N. Sun, Y. Zhang, S. Chang, P. Han, F. Liu, J. He, Biodegradable and high-performance multiscale structured nanofiber membrane as mask filter media via poly(lactic acid) electrospinning, J. Colloid Interface Sci. 606 (2022) 961–970, https://doi.org/10.1016/j.jcis.2021.08.079.

[158] Z. Shao, Y. Chen, J. Jiang, Y. Xiao, G. Kang, X. Wang, W. Li, G. Zheng, Multistage-split ultrafine fluffy nanofibrous membrane for high-efficiency antibacterial air filtration, ACS Appl. Mater. Interfaces 14 (2022) 18989–19001, https://doi.org/10.1021/acsami.2c04700.

[159] M. Kwon, J. Kim, J. Kim, Photocatalytic activity and filtration performance of hybrid TiO$_2$-cellulose acetate nanofibers for air filter applications, Polymers 13 (2021) 1331, https://doi.org/10.3390/polym13081331.

[160] Y. Xu, X. Zhang, D. Teng, T. Zhao, Y. Li, Y. Zeng, Multi-layered micro/nanofibrous nonwovens for functional face mask filter, Nano Res. 15 (2022) 7549–7558, https://doi.org/10.1007/s12274-022-4350-2.

[161] M.G. Jensen, P.T. O'Shaughnessy, M. Shaffer, S. Yu, Y.Y. Choi, M. Christiansen, C.O. Stanier, M. Hartley, J. Huddle, J. Johnson, K. Bibby, N.V. Myung, D.M. Cwiertny, Simple fabrication of an electrospun polystyrene microfiber filter that meets N95 filtering facepiece respirator filtration and breathability standards, J Appl. Polym. Sci. 140 (2023), https://doi.org/10.1002/app.53406.

[162] P. Chen, Z. Yang, Z. Mai, Z. Huang, Y. Bian, S. Wu, X. Dong, X. Fu, F. Ko, S. Zhang, W. Zheng, S. Zhang, W. Zhou, Electrospun nanofibrous membrane with antibacterial and antiviral properties decorated with Myoporum bontioides extract and silver-doped carbon nitride nanoparticles for medical masks application, Sep. Purif. Technol. 298 (2022), 121565, https://doi.org/10.1016/j.seppur.2022.121565.

[163] Q. Li, Y. Yin, D. Cao, Y. Wang, P. Luan, X. Sun, W. Liang, H. Zhu, Photocatalytic rejuvenation enabled self-sanitizing, reusable, and biodegradable masks against COVID-19, ACS Nano 15 (2021) 11992–12005, https://doi.org/10.1021/acsnano.1c03249.

[164] M. Baselga-Lahoz, C. Yus, M. Arruebo, V. Sebastián, S. Irusta, S. Jiménez, Submicronic filtering media based on electrospun recycled PET nanofibers: development, characterization, and method to manufacture surgical masks, Nanomaterials 12 (2022) 925, https://doi.org/10.3390/nano12060925.

[165] M.M. Munir, M. Adrian, M. Burhanuddin, F. Iskandar, Fabrication and structure optimization of expanded polystyrene (EPS) waste fiber for high-performance air filtration, Powder Technol. 402 (2022), 117357, https://doi.org/10.1016/j.powtec.2022.117357.

[166] M. Blosi, A.L. Costa, S. Ortelli, F. Belosi, F. Ravegnani, A. Varesano, C. Tonetti, I. Zanoni, C. Vineis, Polyvinyl alcohol/silver electrospun nanofibers: biocidal filter media capturing virus-size particles, J Appl. Polym. Sci. 138 (2021) 51380, https://doi.org/10.1002/app.51380.

[167] C.W. Lou, M.C. Lin, C.H. Huang, M.F. Lai, B.C. Shiu, J.H. Lin, Preparation of needleless electrospinning polyvinyl alcohol/water-soluble chitosan nanofibrous membranes: antibacterial property and filter efficiency, Polymers 14 (2022) 1054, https://doi.org/10.3390/polym14051054.

[168] Y. Deng, T. Lu, X. Zhang, Z. Zeng, R. Tao, Q. Qu, Y. Zhang, M. Zhu, R. Xiong, C. Huang, Multi-hierarchical nanofiber membrane with typical curved-ribbon structure fabricated by green electrospinning for efficient, breathable and sustainable air filtration, J. Memb. Sci. 660 (2022), 120857, https://doi.org/10.1016/j.memsci.2022.120857.

[169] M. Mounesan, S. Akbari, B.E. Brycki, Needleless electrospun mats based on polyamidoamine dendritic polymers for encapsulation of essential oils in personal respiratory equipment, J. Ind. Text. 51 (2022) 6333S–6352S, https://doi.org/10.1177/15280837211048155.

[170] H. Shen, Z. Zhou, H. Wang, J. Chen, M. Zhang, M. Han, Y. Shen, D. Shuai, Photosensitized electrospun nanofibrous filters for capturing and killing airborne coronaviruses under visible light irradiation, Environ. Sci. Technol. 56 (2022) 4295–4304, https://doi.org/10.1021/acs.est.2c00885.

[171] F.N.H. Karabulut, D. Fomra, G. Höfler, N.A. Chand, G.W. Beckermann, Virucidal and bactericidal filtration media from electrospun polylactic acid nanofibres capable of protecting against COVID-19, Membranes 12 (2022) 571, https://doi.org/10.3390/membranes12060571.

[172] Y. Li, X. Yin, Y. Si, J. Yu, B. Ding, All-polymer hybrid electret fibers for high-efficiency and low-resistance filter media, Chem. Eng. J. 398 (2020), 125626, https://doi.org/10.1016/j.cej.2020.125626.

[173] N.A. Patil, P.M. Gore, N. Jaya Prakash, P. Govindaraj, R. Yadav, V. Verma, D. Shanmugarajan, S. Patil, A. Kore, B. Kandasubramanian, Needleless electrospun phytochemicals encapsulated nanofibre based 3-ply biodegradable mask for combating COVID-19 pandemic, Chem. Eng. J. 416 (2021), 129152, https://doi.org/10.1016/j.cej.2021.129152.

[174] W.C. Lu, C.Y. Chen, C.J. Cho, M. Venkatesan, W.H. Chiang, Y.Y. Yu, C.H. Lee, R. H. Lee, S.P. Rwei, C.C. Kuo, Antibacterial activity and protection efficiency of polyvinyl butyral nanofibrous membrane containing thymol prepared through vertical electrospinning, Polymers 13 (2021) 1122, https://doi.org/10.3390/polym13071122.

[175] P.K. Panda, A. Gangwar, A.G. Thite, Optimization of Nylon 6 electrospun nanofiber diameter in needle-less wire electrode using central composite design and response surface methodology, J. Ind. Text. 51 (2022) 7279S–7292S, https://doi.org/10.1177/15280837211058213.

[176] J. Wang, S. Liu, X. Yan, Z. Jiang, Z. Zhou, J. Liu, G. Han, H. Ben, W. Jiang, Biodegradable and reusable cellulose-based nanofiber membrane preparation for mask filter by electrospinning, Membranes 12 (2021) 23, https://doi.org/10.3390/membranes12010023.

[177] J. Cui, Y. Wang, T. Lu, K. Liu, C. Huang, High performance, environmentally friendly and sustainable nanofiber membrane filter for removal of particulate matter 1.0, J. Colloid Interface Sci. 597 (2021) 48–55, https://doi.org/10.1016/j.jcis.2021.03.174.

[178] J. Cui, T. Lu, F. Li, Y. Wang, J. Lei, W. Ma, Y. Zou, C. Huang, Flexible and transparent composite nanofibre membrane that was fabricated via a "green" electrospinning method for efficient particulate matter 2.5 capture, J. Colloid Interface Sci. 582 (2021) 506–514, https://doi.org/10.1016/j.jcis.2020.08.075.

[179] V.S. Naragund, P.K. Panda, Electrospun polyacrylonitrile nanofiber membranes for air filtration application, Int. J. Environ. Sci. Technol. 19 (2022) 10233–10244, https://doi.org/10.1007/s13762-021-03705-4.

[180] H. Aamer, S. Heo, Y. Jo, Characterization of multifunctional PAN /ZnO nanofibrous composite filter for fine dust capture and photocatalytic activity, J. Appl. Polym. Sci. 138 (2021) 50607, https://doi.org/10.1002/app.50607.

[181] R. Orlando, Y. Gao, P. Fojan, J. Mo, A. Afshari, Filtration performance of ultrathin electrospun cellulose acetate filters doped with TiO_2 and activated charcoal, Buildings 11 (2021) 557, https://doi.org/10.3390/buildings11110557.

[182] J. Xiong, A. Li, Y. Liu, L. Wang, X. Qin, J. Yu, Multi-scale nanoarchitectured fibrous networks for high-performance, self-sterilization, and recyclable face masks, Small 18 (2022), 2105570, https://doi.org/10.1002/smll.202105570.

[183] V. Kadam, Y.B. Truong, J. Schutz, I.L. Kyratzis, R. Padhye, L. Wang, Gelatin/β–cyclodextrin bio–nanofibers as respiratory filter media for filtration of aerosols and volatile organic compounds at low air resistance, J. Hazard. Mater. 403 (2021), 123841, https://doi.org/10.1016/j.jhazmat.2020.123841.

[184] S. Ding, Y. Cao, F. Huang, Y. Wang, J. Li, S. Chen, Spontaneous polarization induced electrostatic charge in washable electret composite fabrics for reusable air-filtering application, Compos. Sci. Technol. 217 (2022), 109093, https://doi.org/10.1016/j.compscitech.2021.109093.

[185] J. Hu, Z. Xiong, Y. Liu, J. Lin, A biodegradable composite filter made from electrospun zein fibers underlaid on the cellulose paper towel, Int. J. Biol. Macromol. 204 (2022) 419–428, https://doi.org/10.1016/j.ijbiomac.2022.02.029.

[186] W. Han, D. Rao, H. Gao, X. Yang, H. Fan, C. Li, L. Dong, H. Meng, Green-solvent-processable biodegradable poly(lactic acid) nanofibrous membranes with bead-on-string structure for effective air filtration: kill two birds with one stone, Nano Energy 97 (2022), 107237, https://doi.org/10.1016/j.nanoen.2022.107237.

[187] J. Avossa, T. Batt, T. Pelet, S.P. Sidjanski, K. Schönenberger, R.M. Rossi, Polyamide nanofiber-based air filters for transparent face masks, ACS Appl. Nano Mater. 4 (2021) 12401–12406, https://doi.org/10.1021/acsanm.1c02843.

[188] H. Aamer, S.B. Kim, J.M. Oh, H. Park, Y.M. Jo, ZnO-impregnated polyacrylonitrile nanofiber filters against various phases of air pollutants, Nanomaterials 11 (2021) 2313, https://doi.org/10.3390/nano11092313.

[189] D.P.F. Bonfim, F.G.S. Cruz, R.E.S. Bretas, V.G. Guerra, M.L. Aguiar, A sustainable recycling alternative: electrospun PET-membranes for air nanofiltration, Polymers 13 (2021) 1166, https://doi.org/10.3390/polym13071166.

[190] Q. Su, Z. Wei, X. Wang, S. Long, W. Zeng, S. Wang, J. Yang, Electrospun composite membrane based on polyarylene sulfide sulfone/Ag/ZnO nanofibers for antibacterial effective $PM_{2.5}$ filtration, J. Appl. Polym. Sci. 139 (2022) 51693, https://doi.org/10.1002/app.51693.

[191] W. Du, F. Iacoviello, T. Fernandez, R. Loureiro, D.J.L. Brett, P.R. Shearing, Microstructure analysis and image-based modelling of face masks for COVID-19 virus protection, Commun. Mater. 2 (2021) 69, https://doi.org/10.1038/s43246-021-00160-z.

[192] C. Van Goethem, D. Op de Beeck, A. Ilyas, M. Thijs, G. Koeckelberghs, P.E. M. Aerts, I.F.J. Vankelecom, Ultra-thin and highly porous PVDF-filters prepared via phase inversion structure for potential medical (COVID-19) and industrial use, J. Memb. Sci. 639 (2021), 119710, https://doi.org/10.1016/j.memsci.2021.119710.

[193] W. Yim, D. Cheng, S.H. Patel, R. Kou, Y.S. Meng, J.V. Jokerst, KN95 and N95 respirators retain filtration efficiency despite a loss of dipole charge during decontamination, ACS Appl. Mater. Interfaces 12 (2020) 54473–54480, https://doi.org/10.1021/acsami.0c17333.

[194] M. Mirković, D.B. Stojanović, D. Mijailović, N. Barać, Đ. Janaćković, P. S. Uskoković, Electrospun polyacrylonitrile fibers incorporated with microporous carbon for improved airborne PM2.5 filtration, Mater. Chem. Phys. 285 (2022) 126103, https://doi.org/10.1016/j.matchemphys.2022.126103.

[195] P. Yadav, N. Ismail, M. Essalhi, M. Tysklind, D. Athanassiadis, N. Tavajohi, Assessment of the environmental impact of polymeric membrane production, J. Memb. Sci. 622 (2021) 118987, https://doi.org/10.1016/j.memsci.2020.118987.

[196] S. Saadat, D. Rawtani, C.M. Hussain, Environmental perspective of COVID-19, Sci. Total Environ. 728 (2020), 138870, https://doi.org/10.1016/j.scitotenv.2020.138870.

[197] S. Sangkham, Face mask and medical waste disposal during the novel COVID-19 pandemic in Asia, Case Stud. Chem. Environ. Eng. 2 (2020) 100052, https://doi.org/10.1016/j.cscee.2020.100052.

[198] T.A. Aragaw, Surgical face masks as a potential source for microplastic pollution in the COVID-19 scenario, Mar. Pollut. Bull. 159 (2020), 111517, https://doi.org/10.1016/j.marpolbul.2020.111517.

[199] H. Du, S. Huang, J. Wang, Environmental risks of polymer materials from disposable face masks linked to the COVID-19 pandemic, Sci. Total Environ. 815 (2022), 152980, https://doi.org/10.1016/j.scitotenv.2022.152980.

[200] A. Chamas, H. Moon, J. Zheng, Y. Qiu, T. Tabassum, J.H. Jang, M. Abu-Omar, S. L. Scott, S. Suh, Degradation rates of plastics in the environment, ACS Sustain. Chem. Eng. 8 (2020) 3494–3511, https://doi.org/10.1021/acssuschemeng.9b06635.

[201] H. Luo, C. Liu, D. He, J. Xu, J. Sun, J. Li, X. Pan, Environmental behaviors of microplastics in aquatic systems: a systematic review on degradation, adsorption, toxicity and biofilm under aging conditions, J. Hazard. Mater. 423 (2022), 126915, https://doi.org/10.1016/j.jhazmat.2021.126915.

[202] B. Mghili, M. Analla, M. Aksissou, Face masks related to COVID-19 in the beaches of the Moroccan Mediterranean: an emerging source of plastic pollution, Mar. Pollut. Bull. 174 (2022), 113181, https://doi.org/10.1016/j.marpolbul.2021.113181.

[203] Z. Pan, Q. Liu, Y. Sun, X. Sun, H. Lin, Environmental implications of microplastic pollution in the Northwestern Pacific Ocean, Mar. Pollut. Bull. 146 (2019) 215–224, https://doi.org/10.1016/j.marpolbul.2019.06.031.

[204] D.G. Oldal, F. Topuz, T. Holtzl, G. Szekely, Green electrospinning of biodegradable cellulose acetate nanofibrous membranes with tunable porosity, ACS Sustain. Chem. Eng. 11 (2023) 994–1005, https://doi.org/10.1021/acssuschemeng.2c05676.

[205] J. Hidalgo-Crespo, C.M. Moreira, F.X. Jervis, M. Soto, J.L. Amaya, L. Banguera, Circular economy of expanded polystyrene container production: environmental benefits of household waste recycling considering renewable energies, Energy Rep. 8 (2022) 306–311, https://doi.org/10.1016/j.egyr.2022.01.071.

[206] B. Sadeghi, Y. Marfavi, R. AliAkbari, E. Kowsari, F. Borbor Ajdari, S. Ramakrishna, Recent studies on recycled PET fibers: production and applications: a review, Mater. Circ. Econ. 3 (2021) 4, https://doi.org/10.1007/s42824-020-00014-y.

[207] FTIR-2020-PLA-COVID(aggiungere Review)(f).pdf, (2023).

[208] K. Li, C.M. Clarkson, L. Wang, Y. Liu, M. Lamm, Z. Pang, Y. Zhou, J. Qian, M. Tajvidi, D.J. Gardner, H. Tekinalp, L. Hu, T. Li, A.J. Ragauskas, J. P. Youngblood, S. Ozcan, Alignment of cellulose nanofibers: harnessing nanoscale properties to macroscale benefits, ACS Nano 15 (2021) 3646–3673, https://doi.org/10.1021/acsnano.0c07613.

[209] M.E. Lamm, K. Li, J. Qian, L. Wang, N. Lavoine, R. Newman, D.J. Gardner, T. Li, L. Hu, A.J. Ragauskas, H. Tekinalp, V. Kunc, S. Ozcan, Recent advances in functional materials through cellulose nanofiber templating, Adv. Mater. 33 (2021), 2005538, https://doi.org/10.1002/adma.202005538.

[210] K.J. Nagarajan, N.R. Ramanujam, M.R. Sanjay, S. Siengchin, B. Surya Rajan, K. Sathick Basha, P. Madhu, G.R. Raghav, A comprehensive review on cellulose nanocrystals and cellulose nanofibers: pretreatment, preparation, and characterization, Polym. Compos. 42 (2021) 1588–1630, https://doi.org/10.1002/pc.25929.

[211] D. Wong, S. Hartery, E. Keltie, R. Chang, J.S. Kim, S.S. Park, Electrospun polystyrene and acid-treated cellulose nanocrystals with intense pulsed light treatment for N95-equivalent filters, ACS Appl. Polym. Mater. 3 (2021) 4949–4958, https://doi.org/10.1021/acsapm.1c00722.

[212] C. Akduman, Cellulose acetate and polyvinylidene fluoride nanofiber mats for N95 respirators, J. Ind. Text. 50 (2021) 1239–1261, https://doi.org/10.1177/1528083719858760.

[213] D.S. de Almeida, L.D. Martins, E.C. Muniz, A.P. Rudke, R. Squizzato, A. Beal, P. R. de Souza, D.P.F. Bonfim, M.L. Aguiar, M.L. Gimenes, Biodegradable CA/CPB electrospun nanofibers for efficient retention of airborne nanoparticles, Process Saf. Environ. Prot. 144 (2020) 177–185, https://doi.org/10.1016/j.psep.2020.07.024.

[214] N. Yadav, M. Hakkarainen, Degradable or not? Cellulose acetate as a model for complicated interplay between structure, environment and degradation, Chemosphere 265 (2021), 128731, https://doi.org/10.1016/j.chemosphere.2020.128731.

[215] H. Samadian, S. Zamiri, A. Ehterami, S. Farzamfar, A. Vaez, H. Khastar, M. Alam, A. Ai, H. Derakhshankhah, Z. Allahyari, A. Goodarzi, M. Salehi, Electrospun cellulose acetate/gelatin nanofibrous wound dressing containing berberine for diabetic foot ulcer healing: *in vitro* and *in vivo* studies, Sci. Rep. 10 (2020) 8312, https://doi.org/10.1038/s41598-020-65268-7.

[216] X.H. Vu, T.T.T. Duong, T.T.H. Pham, D.K. Trinh, X.H. Nguyen, V.S. Dang, Synthesis and study of silver nanoparticles for antibacterial activity against *Escherichia coli* and *Staphylococcus aureus*, Adv. Nat. Sci. Nanosci. Nanotechnol. 9 (2018), 025019, https://doi.org/10.1088/2043-6254/aac58f.

[217] K.P. Priyanka, T.H. Sukirtha, K.M. Balakrishna, T. Varghese, Microbicidal activity of TiO_2 nanoparticles synthesised by sol–gel method, IET Nanobiotechnol. 10 (2016) 81–86, https://doi.org/10.1049/iet-nbt.2015.0038.

[218] M. Ahamed, H.A. Alhadlaq, M.A.M. Khan, P. Karuppiah, N.A. Al-Dhabi, Synthesis, characterization, and antimicrobial activity of copper oxide nanoparticles, J. Nanotechnol. 2014 (2014) 1–4, https://doi.org/10.1155/2014/637858.

[219] B. Lallo da Silva, B.L. Caetano, B.G. Chiari-Andréo, R.C.L.R. Pietro, L. A. Chiavacci, Increased antibacterial activity of ZnO nanoparticles: influence of size and surface modification, Colloids Surf. B 177 (2019) 440–447, https://doi.org/10.1016/j.colsurfb.2019.02.013.

[220] J. Maji, S. Pandey, S. Basu, Synthesis and evaluation of antibacterial properties of magnesium oxide nanoparticles, Bull. Mater. Sci. 43 (2020) 25, https://doi.org/10.1007/s12034-019-1963-5.

[221] N. Beyth, Y. Houri-Haddad, A. Domb, W. Khan, R. Hazan, Alternative antimicrobial approach: nano-antimicrobial materials, Evid. Based Complement. Altern. Med. 2015 (2015) 1–16, https://doi.org/10.1155/2015/246012.

[222] S. Karagoz, N.B. Kiremitler, G. Sarp, S. Pekdemir, S. Salem, A.G. Goksu, M. S. Onses, I. Sozdutmaz, E. Sahmetlioglu, E.S. Ozkara, A. Ceylan, E. Yilmaz, Antibacterial, antiviral, and self-cleaning mats with sensing capabilities based on electrospun nanofibers decorated with ZnO nanorods and Ag nanoparticles for protective clothing applications, ACS Appl. Mater. Interfaces 13 (2021) 5678–5690, https://doi.org/10.1021/acsami.0c15606.

[223] M.C. Sportelli, M. Izzi, D. Loconsole, A. Sallustio, R.A. Picca, R. Felici, M. Chironna, N. Cioffi, On the efficacy of ZnO nanostructures against SARS-CoV-2, IJMS 23 (2022) 3040, https://doi.org/10.3390/ijms23063040.

[224] Y. Li, Y. Liu, B. Yao, S. Narasimalu, Z. Dong, Rapid preparation and antimicrobial activity of polyurea coatings with RE-Doped nano-ZnO, Microb. Biotechnol. 15 (2022) 548–560, https://doi.org/10.1111/1751-7915.13891.

[225] S.V. Gudkov, D.E. Burmistrov, D.A. Serov, M.B. Rebezov, A.A. Semenova, A. B. Lisitsyn, A mini review of antibacterial properties of ZnO nanoparticles, Front. Phys. 9 (2021) 641481, https://doi.org/10.3389/fphy.2021.641481.

[226] A. Skalny, L. Rink, O. Ajsuvakova, A. Aschner, V. Gritsenko, S. Alekseenko, A. Svistunov, D. Petrakis, D. Spandidos, J. Aaseth, A. Tsatsakis, A. Tinkov, Zinc and respiratory tract infections: perspectives for COVID-19 (Review), Int. J. Mol. Med. (2020), https://doi.org/10.3892/ijmm.2020.4575.

[227] J. Alexander, A. Tinkov, T.A. Strand, U. Alehagen, A. Skalny, J. Aaseth, Early nutritional interventions with zinc, selenium and vitamin D for raising anti-viral resistance against progressive COVID-19, Nutrients 12 (2020) 2358, https://doi.org/10.3390/nu12082358.

[228] M. Maares, J. Hackler, A. Haupt, R.A. Heller, M. Bachmann, J. Diegmann, A. Moghaddam, L. Schomburg, H. Haase, Free zinc as a predictive marker for COVID-19 mortality risk, Nutrients 14 (2022) 1407, https://doi.org/10.3390/nu14071407.

[229] A.O. Dada, A.A. Inyinbor, O.S. Bello, B.E. Tokula, Novel plantain peel activated carbon–supported zinc oxide nanocomposites (PPAC-ZnO-NC) for adsorption of chloroquine synthetic pharmaceutical used for COVID-19 treatment, Biomass Convers. Biorefin. (2021), https://doi.org/10.1007/s13399-021-01828-9.

[230] D.A. Ghareeb, S.R. Saleh, M.G. Seadawy, M.S. Nofal, S.A. Abdulmalek, S. F. Hassan, S.M. Khedr, M.G. AbdElwahab, A.A. Sobhy, A. saber A. Abdel-Hamid, A.M. Yassin, A.A.A. Elmoneam, A.A. Masoud, M.M.Y. Kaddah, S.A. El-Zahaby, A. M. Al-mahallawi, A.M. El-Gharbawy, A. Zaki, I. k. Seif, M.Y. Kenawy, M. Amin, K. Amer, M.A. El Demellawy, Nanoparticles of ZnO/Berberine complex contract COVID-19 and respiratory co-bacterial infection in addition to elimination of hydroxychloroquine toxicity, J. Pharm. Investig. 51 (2021) 735–757, https://doi.org/10.1007/s40005-021-00544-w.

[231] K. Geetha, D. Sivasangari, H.S. Kim, G. Murugadoss, A. Kathalingam, Electrospun nanofibrous ZnO/PVA/PVP composite films for efficient antimicrobial face masks, Ceram. Int. 48 (2022) 29197–29204, https://doi.org/10.1016/j.ceramint.2022.05.164.

[232] D.A. Goncharova, E.N. Bolbasov, A.L. Nemoykina, A.A. Aljulaih, T. S. Tverdokhlebova, S.A. Kulinich, V.A. Svetlichnyi, Structure and properties of biodegradable PLLA/ZnO composite membrane produced via electrospinning, Materials 14 (2020) 2, https://doi.org/10.3390/ma14010002.

[233] H. Nageh, M.H. Emam, F. Ali, N.F. Abdel Fattah, M. Taha, R. Amin, E.A. Kamoun, S.A. Loutfy, A. Kasry, Zinc oxide nanoparticle-loaded electrospun polyvinylidene fluoride nanofibers as a potential face protector against respiratory viral infections, ACS Omega 7 (2022) 14887–14896, https://doi.org/10.1021/acsomega.2c00458.

[234] L.A. Alshabanah, N. Omran, B.H. Elwakil, M.T. Hamed, S.M. Abdallah, L.A. Al-Mutabagani, D. Wang, Q. Liu, N. Shehata, A.H. Hassanin, M. Hagar, Elastic nanofibrous membranes for medical and personal protection applications: manufacturing, anti-COVID-19, and anti-colistin resistant bacteria evaluation, Polymers 13 (2021) 3987, https://doi.org/10.3390/polym13223987.

[235] A. Salam, T. Hassan, T. Jabri, S. Riaz, A. Khan, K.M. Iqbal, S. ullah Khan, M. Wasim, M.R. Shah, M.Q. Khan, I.S. Kim, Electrospun nanofiber-based viroblock/ZnO/PAN hybrid antiviral nanocomposite for personal protective applications, Nanomaterials 11 (2021) 2208, https://doi.org/10.3390/nano11092208.

[236] M. Baselga, I. Uranga-Murillo, D. de Miguel, M. Arias, V. Sebastián, J. Pardo, M. Arruebo, Silver nanoparticles–polyethyleneimine-based coatings with antiviral activity against SARS-CoV-2: a new method to functionalize filtration media, Materials 15 (2022) 4742, https://doi.org/10.3390/ma15144742.

[237] I.M. El-Nahhal, J. Salem, F.S. Kodeh, A. Elmanama, R. Anbar, CuO–NPs, CuO–Ag nanocomposite and Cu(II)-curcumin complex coated cotton/starched cotton antimicrobial materials, Mater. Chem. Phys. 285 (2022), 126099, https://doi.org/10.1016/j.matchemphys.2022.126099.

[238] I. Foffa, P. Losi, P. Quaranta, A. Cara, T. Al Kayal, M. D'Acunto, G. Presciuttini, M. Pistello, G. Soldani, A Copper nanoparticles-based polymeric spray coating:

[239] nanoshield against Sars-Cov-2, J. Appl. Biomater. Funct. Mater. 20 (2022), 228080002210763, https://doi.org/10.1177/22808000221076326.

[239] S.M. Costa, D. Pacheco, W. Antunes, R. Vieira, N. Bem, P. Teixeira, R. Fangueiro, D.P. Ferreira, Antibacterial and biodegradable electrospun filtering membranes for facemasks: an attempt to reduce disposable masks use, Appl. Sci. 12 (2021) 67, https://doi.org/10.3390/app12010067.

[240] A.L. Kubo, K. Rausalu, N. Savest, E. Žusinaite, G. Vasiliev, M. Viirsalu, T. Plamus, A. Krumme, A. Merits, O. Bondarenko, Antibacterial and antiviral effects of Ag, Cu and Zn metals, respective nanoparticles and filter materials thereof against Coronavirus SARS-CoV-2 and Influenza A virus, Pharmaceutics 14 (2022) 2549, https://doi.org/10.3390/pharmaceutics14122549.

[241] S. Wang, X. Zhao, X. Yin, J. Yu, B. Ding, Electret polyvinylidene fluoride nanofibers hybridized by polytetrafluoroethylene nanoparticles for high-efficiency air filtration, ACS Appl. Mater. Interfaces 8 (2016) 23985–23994, https://doi.org/10.1021/acsami.6b08262.

[242] T.T. Bui, M.K. Shin, S.Y. Jee, D.X. Long, J. Hong, M.G. Kim, Ferroelectric PVDF nanofiber membrane for high-efficiency PM0.3 air filtration with low air flow resistance, Colloids Surf. A 640 (2022), 128418, https://doi.org/10.1016/j.colsurfa.2022.128418.

[243] C.X. Li, S.Y. Kuang, Y.H. Chen, Z.L. Wang, C. Li, G. Zhu, *In situ* active poling of nanofiber networks for gigantically enhanced particulate filtration, ACS Appl. Mater. Interfaces 10 (2018) 24332–24338, https://doi.org/10.1021/acsami.8b07203.

[244] W.W.F. Leung, Q. Sun, Electrostatic charged nanofiber filter for filtering airborne novel Coronavirus (COVID-19) and nano-aerosols, Sep. Purif. Technol. 250 (2020), 116886, https://doi.org/10.1016/j.seppur.2020.116886.

[245] J. Zhang, S. Gong, C. Wang, D. Jeong, Z.L. Wang, K. Ren, Biodegradable electrospun poly(lactic acid) nanofibers for effective PM 2.5 removal, Macromol. Mater. Eng. 304 (2019), 1900259, https://doi.org/10.1002/mame.201900259.

[246] Z. Shao, J. Jiang, X. Wang, W. Li, L. Fang, G. Zheng, Self-powered electrospun composite nanofiber membrane for highly efficient air filtration, Nanomaterials 10 (2020) 1706, https://doi.org/10.3390/nano10091706.

[247] C. Yongliang, W. Chunya, Z. Junwen, L. Shizhe, X. Yongjun, Z. Qize, J. Hulin, W. Nan, L. Wenbo, C. Shuwen, W. Bo, Z. Yingying, Z. Jun, Electrospun polyetherimide electret nonwoven for bi-functional smart face mask, Nano Energy 8 (2017), https://doi.org/10.1016/j.nanoen.2017.03.011.

[248] M. Mariello, A. Qualtieri, G. Mele, M. De Vittorio, Metal-free multilayer hybrid PENG based on soft electrospun/-sprayed membranes with cardanol additive for harvesting energy from surgical face masks, ACS Appl. Mater. Interfaces 13 (2021) 20606–20621, https://doi.org/10.1021/acsami.1c01740.

[249] M. Cho, V. Hiremath, J.G. Seo, Triboelectrification-based particulate matter capture utilizing electrospun ethyl cellulose and PTFE spheres, Atmos. Environ. X 12 (2021), 100138, https://doi.org/10.1016/j.aeaoa.2021.100138, 1-10.

[250] Y. Hu, Y. Wang, S. Tian, A. Yu, L. Wan, J. Zhai, Performance-enhanced and washable triboelectric air filter based on polyvinylidene fluoride/UiO-66 composite nanofiber membrane, Macro Mater. Eng. 306 (2021), 2100128, https://doi.org/10.1002/mame.202100128.

[251] Q. Fu, Y. Liu, T. Liu, J. Mo, W. Zhang, S. Zhang, B. Luo, J. Wang, Y. Qin, S. Wang, S. Nie, Air-permeable cellulosic triboelectric materials for self-powered healthcare products, Nano Energy 102 (2022), 107739, https://doi.org/10.1016/j.nanoen.2022.107739.

[252] G. Liu, J. Nie, C. Han, T. Jiang, Z. Yang, Y. Pang, L. Xu, T. Guo, T. Bu, C. Zhang, Z. L. Wang, Self-powered electrostatic adsorption face mask based on a triboelectric nanogenerator, ACS Appl. Mater. Interfaces 10 (2018) 7126–7133, https://doi.org/10.1021/acsami.7b18732.

[253] G.Q. Gu, C.B. Han, J.J. Tian, T. Jiang, C. He, C.X. Lu, Y. Bai, J.H. Nie, Z. Li, Z. L. Wang, Triboelectric nanogenerator enhanced multilayered antibacterial nanofiber air filters for efficient removal of ultrafine particulate matter, Nano Res. 11 (2018) 4090–4101, https://doi.org/10.1007/s12274-018-1992-1.

[254] R. Hao, S. Yang, K. Yang, Z. Zhang, T. Wang, S. Sang, H. Zhang, Self-powered air filter based on an electrospun respiratory triboelectric nanogenerator, ACS Appl. Energy Mater. 4 (2021) 14700–14708, https://doi.org/10.1021/acsaem.1c03328.

[255] W.G. Kim, D.W. Kim, I.W. Tcho, J.K. Kim, M.S. Kim, Y.K. Choi, Triboelectric nanogenerator: structure, mechanism, and applications, ACS Nano 15 (2021) 258–287, https://doi.org/10.1021/acsnano.0c09803.

[256] D.H. Kang, N.K. Kim, H.W. Kang, Electrostatic charge retention in PVDF nanofiber-nylon mesh multilayer structure for effective fine particulate matter filtration for face masks, Polymers 13 (2021) 3235, https://doi.org/10.3390/polym13193235.

[257] H. He, J. Guo, B. Illés, A. Géczy, B. Istók, V. Hliva, D. Török, J.G. Kovács, I. Harmati, K. Molnár, Monitoring multi-respiratory indices via a smart nanofibrous mask filter based on a triboelectric nanogenerator, Nano Energy 89 (2021), 106418, https://doi.org/10.1016/j.nanoen.2021.106418.

[258] S. Lin, S. Wang, W. Yang, S. Chen, Z. Xu, X. Mo, H. Zhou, J. Duan, B. Hu, L. Huang, Trap-induced dense monocharged perfluorinated electret nanofibers for recyclable multifunctional healthcare mask, ACS Nano 15 (2021) 5486–5494, https://doi.org/10.1021/acsnano.1c00238.

[259] T.T. Le, E.J. Curry, T. Vinikoor, R. Das, Y. Liu, D. Sheets, K.T.M. Tran, C. J. Hawxhurst, J.F. Stevens, J.N. Hancock, O.R. Bilal, L.M. Shor, T.D. Nguyen, Piezoelectric nanofiber membrane for reusable, stable, and highly functional face mask filter with long-term biodegradability, Adv. Funct. Mater. 32 (2022), 2113040, https://doi.org/10.1002/adfm.202113040.

[260] Y. Cho, Y. Son, J. Ahn, H. Lim, S. Ahn, J. Lee, P.K. Bae, I.D. Kim, Multifunctional filter membranes based on self-assembled core–shell biodegradable nanofibers for

persistent electrostatic filtration through the triboelectric effect, ACS Nano 16 (2022) 19451–19463, https://doi.org/10.1021/acsnano.2c09165.

[261] N. Wang, Y. Feng, Y. Zheng, L. Zhang, M. Feng, X. Li, F. Zhou, D. Wang, New hydrogen bonding enhanced polyvinyl alcohol based self-charged medical mask with superior charge retention and moisture resistance performances, Adv. Funct. Mater. 31 (2021), 2009172, https://doi.org/10.1002/adfm.202009172.

[262] Y. Mi, Y. Lu, Y. Shi, Z. Zhao, X. Wang, J. Meng, X. Cao, N. Wang, Biodegradable polymers in triboelectric nanogenerators, Polymers 15 (2022) 222, https://doi.org/10.3390/polym15010222.

[263] M. Rostami, N. Beheshtizadeh, F.E. Ranjbar, N. Najafi, A. Ahmadi, P. Ahmadi, H. Rostamabadi, Z. Pazhouhnia, E. Assadpour, M. Mirzanajafi-Zanjani, M. F. Kisomi, M.S. Kharazmi, S.M. Jafari, Recent advances in electrospun protein fibers/nanofibers for the food and biomedical applications, Adv. Colloid Interface Sci. 311 (2023), 102827, https://doi.org/10.1016/j.cis.2022.102827.

[264] L. De Sio, B. Ding, M. Focsan, K. Kogermann, P. Pascoal-Faria, F. Petronela, G. Mitchell, E. Zussman, F. Pierini, Personalized reusable face masks with smart nano-assisted destruction of pathogens for COVID-19: a visionary road, Chem. Eur. J. 27 (2021) 6112–6130, https://doi.org/10.1002/chem.202004875.

[265] D.T.S. Li, L.P. Samaranayake, Y.Y. Leung, P. Neelakantan, Facial protection in the era of COVID-19: a narrative review, Oral Dis. 27 (2021) 665–673, https://doi.org/10.1111/odi.13460.

[266] J.C. Rubio-Romero, M. del C. Pardo-Ferreira, J.A. Torrecilla-García, S. Calero-Castro, Disposable masks: disinfection and sterilization for reuse, and non-certified manufacturing, in the face of shortages during the COVID-19 pandemic, Saf. Sci. 129 (2020), 104830, https://doi.org/10.1016/j.ssci.2020.104830.

[267] J. Zhu, Q. Jiang, X. He, X. Li, L. Wang, L. Zheng, P. Jing, M. Chen, Filtration efficiency of N95 filtering facepiece respirators during multi-cycles of 8-hour simulated donning + disinfection, J. Hosp. Infect. 127 (2022) 91–100, https://doi.org/10.1016/j.jhin.2022.06.016.

[268] C. Liao, Y. Li, S.C. Tjong, Visible-light active titanium dioxide nanomaterials with bactericidal properties, Nanomaterials 10 (2020) 124, https://doi.org/10.3390/nano10010124.

[269] V.S. Mohite, M.M. Darade, R.K. Sharma, S.H. Pawar, Nanoparticle engineered photocatalytic paints: a roadmap to self-sterilizing against the spread of communicable diseases, Catalysts 12 (2022) 326, https://doi.org/10.3390/catal12030326.

[270] S. Kundu, N. Karak, Polymeric photocatalytic membrane: an emerging solution for environmental remediation, Chem. Eng. J. 438 (2022), 135575, https://doi.org/10.1016/j.cej.2022.135575.

[271] N. Kaushik, S. Mitra, E.J. Baek, L.N. Nguyen, P. Bhartiya, J.H. Kim, E.H. Choi, N. K. Kaushik, The inactivation and destruction of viruses by reactive oxygen species generated through physical and cold atmospheric plasma techniques: current status and perspectives, J. Adv. Res. 43 (2023) 59–71, https://doi.org/10.1016/j.jare.2022.03.002.

[272] Z. Tang, D. Ma, Q. Chen, Y. Wang, M. Sun, Q. Lian, J. Shang, P.K. Wong, C. He, D. Xia, T. Wang, Nanomaterial-enabled photothermal-based solar water disinfection processes: fundamentals, recent advances, and mechanisms, J. Hazard. Mater. 437 (2022), 129373, https://doi.org/10.1016/j.jhazmat.2022.129373.

[273] L. Wang, Y. Feng, K. Wang, G. Liu, Solar water sterilization enabled by photothermal nanomaterials, Nano Energy 87 (2021) 106158, https://doi.org/10.1016/j.nanoen.2021.106158.

[274] Z. Wu, H. Zheng, J. Gu, F. Li, R. Lv, Y. Deng, W. Xu, Y. Tong, Effects of different temperature and time durations of virus inactivation on results of real-time fluorescence PCR testing of COVID-19 viruses, Curr. Med. Sci. 40 (2020) 614–617, https://doi.org/10.1007/s11596-020-2224-y.

[275] H. Zhong, Z. Zhu, J. Lin, C.F. Cheung, V.L. Lu, F. Yan, C.Y. Chan, G. Li, Reusable and recyclable graphene masks with outstanding superhydrophobic and photothermal performances, ACS Nano 14 (2020) 6213–6221, https://doi.org/10.1021/acsnano.0c02250.

[276] P. Kumar, S. Roy, A. Sarkar, A. Jaiswal, Reusable MoS$_2$-modified antibacterial fabrics with photothermal disinfection properties for repurposing of personal protective masks, ACS Appl. Mater. Interfaces 13 (2021) 12912–12927, https://doi.org/10.1021/acsami.1c00083.

[277] R. Soni, S.R. Joshi, M. Karmacharya, H. Min, S.K. Kim, S. Kumar, G.H. Kim, Y. K. Cho, C.Y. Lee, Superhydrophobic and self-sterilizing surgical masks spray-coated with carbon nanotubes, ACS Appl. Nano Mater. 4 (2021) 8491–8499, https://doi.org/10.1021/acsanm.1c01082.

[278] S. Yan, C.A. Stackhouse, I. Waluyo, A. Hunt, K. Kisslinger, A.R. Head, D.C. Bock, E.S. Takeuchi, K.J. Takeuchi, L. Wang, A.C. Marschilok, Reusing face covering masks: probing the impact of heat treatment, ACS Sustain. Chem. Eng. 9 (2021) 13545–13558, https://doi.org/10.1021/acssuschemeng.1c04530.

[279] L. Liao, W. Xiao, M. Zhao, X. Yu, H. Wang, Q. Wang, S. Chu, Y. Cui, Can N95 respirators be reused after disinfection? How many times? ACS Nano 14 (2020) 6348–6356, https://doi.org/10.1021/acsnano.0c03597.

[280] W. He, Y. Guo, H. Gao, J. Liu, Y. Yue, J. Wang, Evaluation of regeneration processes for filtering facepiece respirators in terms of the bacteria inactivation efficiency and influences on filtration performance, ACS Nano 14 (2020) 13161–13171, https://doi.org/10.1021/acsnano.0c04782.

[281] D. Lv, M. Zhu, Z. Jiang, S. Jiang, Q. Zhang, R. Xiong, C. Huang, Green electrospun nanofibers and their application in air filtration, Macromol. Mater. Eng. 303 (2018) 1800336, https://doi.org/10.1002/mame.201800336.

[282] J. Avossa, G. Herwig, C. Toncelli, F. Itel, R.M. Rossi, Electrospinning based on benign solvents: current definitions, implications and strategies, Green Chem. 24 (2022) 2347–2375, https://doi.org/10.1039/D1GC04252A.

[283] D. Kim, S.P. Nunes, Green solvents for membrane manufacture: recent trends and perspectives, Curr. Opin. Green Sustain. Chem. 28 (2021), 100427, https://doi.org/10.1016/j.cogsc.2020.100427.

[284] W. Xie, T. Li, A. Tiraferri, E. Drioli, A. Figoli, J.C. Crittenden, B. Liu, Toward the next generation of sustainable membranes from green chemistry principles, ACS Sustain. Chem. Eng. 9 (2021) 50–75, https://doi.org/10.1021/acssuschemeng.0c07119.

[285] T. Zhong, W. Liu, H. Liu, Green electrospinning of chitin propionate to manufacture nanofiber mats, Carbohydr. Polym. 273 (2021), 118593, https://doi.org/10.1016/j.carbpol.2021.118593.

[286] C.Z. Mosher, P.A.P. Brudnicki, Z. Gong, H.R. Childs, S.W. Lee, R.M. Antrobus, E. C. Fang, T.N. Schiros, H.H. Lu, Green electrospinning for biomaterials and biofabrication, Biofabrication 13 (2021), 035049, https://doi.org/10.1088/1758-5090/ac0964.

[287] E. Lasseuguette, R. Malpass-Evans, S. Casalini, N.B. McKeown, M.C. Ferrari, Optimization of the fabrication of amidoxime modified PIM-1 electrospun fibres for use as breathable and reactive materials, Polymer 213 (2021), 123205, https://doi.org/10.1016/j.polymer.2020.123205.

[288] W. Zhou, X. Yu, L. Cao, M. Yang, Y. Li, Y. Si, J. Yu, B. Ding, Green and ethanol-resistant polyurethane nanofibrous membranes based on an ethanol solvent for waterproof and breathable textiles, Adv. Sustain. Syst. 4 (2020), 2000105, https://doi.org/10.1002/adsu.202000105.

[289] S. Jiang, H. Hou, S. Agarwal, A. Greiner, Polyimide nanofibers by "Green" electrospinning via aqueous solution for filtration applications, ACS Sustain. Chem. Eng. 4 (2016) 4797–4804, https://doi.org/10.1021/acssuschemeng.6b01031.

[290] M.K. Gaydhane, C.S. Sharma, S. Majumdar, Electrospun nanofibres in drug delivery: advances in controlled release strategies, RSC Adv. 13 (2023) 7312–7328, https://doi.org/10.1039/D2RA06023J.

[291] W.A. Abbas, B.S. Shaheen, L.G. Ghanem, I.M. Badawy, M.M. Abodouh, S. M. Abdou, S. Zada, N.K. Allam, Cost-effective face mask filter based on hybrid composite nanofibrous layers with high filtration efficiency, Langmuir 37 (2021) 7492–7502, https://doi.org/10.1021/acs.langmuir.1c00926.

[292] A.D. Doyle, S.S. Nazari, K.M. Yamada, Cell–extracellular matrix dynamics, Phys. Biol. 19 (2022), 021002, https://doi.org/10.1088/1478-3975/ac4390.

[293] G.Z. Tan, Y. Zhou, Electrospinning of biomimetic fibrous scaffolds for tissue engineering: a review, Int. J. Polym. Mater. Polym. Biomater. 69 (2020) 947–960, https://doi.org/10.1080/00914037.2019.1636248.

[294] H.A. Owida, J.I. Al-Nabulsi, F. Alnaimat, M. Al-Ayyad, N.M. Turab, A. Al Sharah, M. Shakur, Recent applications of electrospun nanofibrous scaffold in tissue engineering, Appl. Bionics Biomech. 2022 (2022) 1–15, https://doi.org/10.1155/2022/1953861.

[295] A.P. Rickel, X. Deng, D. Engebretson, Z. Hong, Electrospun nanofiber scaffold for vascular tissue engineering, Mater. Sci. Eng. C 129 (2021), 112373, https://doi.org/10.1016/j.msec.2021.112373.

[296] G. Jin, R. He, B. Sha, W. Li, H. Qing, R. Teng, F. Xu, Electrospun three-dimensional aligned nanofibrous scaffolds for tissue engineering, Mater. Sci. Eng. C 92 (2018) 995–1005, https://doi.org/10.1016/j.msec.2018.06.065.

[297] S. Wu, J. Liu, J. Cai, J. Zhao, S. Duan, S. Chen, Combining electrospinning with hot drawing process to fabricate high performance poly (L-lactic acid) nanofiber yarns for advanced nanostructured bio-textiles, Biofabrication 13 (2021), 045018, https://doi.org/10.1088/1758-5090/ac2209.

[298] J. Liu, T. Li, H. Zhang, W. Zhao, L. Qu, S. Chen, S. Wu, Electrospun strong, bioactive, and bioabsorbable silk fibroin/poly (L-lactic-acid) nanoyarns for constructing advanced nanotextile tissue scaffolds, Mater. Today Bio 14 (2022), 100243, https://doi.org/10.1016/j.mtbio.2022.100243.

[299] Y. Qi, C. Wang, Q. Wang, F. Zhou, T. Li, B. Wang, W. Su, D. Shang, S. Wu, A simple, quick, and cost-effective strategy to fabricate polycaprolactone/silk fibroin nanofiber yarns for biotextile-based tissue scaffold application, Eur. Polym. J. 186 (2023), 111863, https://doi.org/10.1016/j.eurpolymj.2023.111863.

[300] X. Zhang, M. Guo, Q. Guo, N. Liu, Y. Wang, T. Wu, Modulating axonal growth and neural stem cell migration with the use of uniaxially aligned nanofiber yarns welded with NGF-loaded microparticles, Mater. Today Adv. 17 (2023), 100343, https://doi.org/10.1016/j.mtadv.2023.100343.

[301] S. Wu, Y. Qi, W. Shi, M. Kuss, S. Chen, B. Duan, Electrospun conductive nanofiber yarns for accelerating mesenchymal stem cells differentiation and maturation into Schwann cell-like cells under a combination of electrical stimulation and chemical induction, Acta Biomater. 139 (2022) 91–104, https://doi.org/10.1016/j.actbio.2020.11.042.

[302] X. Wan, H. Cong, G. Jiang, X. Liang, L. Liu, H. He, A review on PVDF nanofibers in textiles for flexible piezoelectric sensors, ACS Appl. Nano Mater. 6 (2023) 1522–1540, https://doi.org/10.1021/acsanm.2c04916.

[303] W. Fan, Y. Zhang, Y. Sun, S. Wang, C. Zhang, Y. Wu, W. Wang, K. Dong, Durable antibacterial and temperature regulated core-spun yarns for textile health and comfort applications, Chem. Eng. J. 455 (2023), 140917, https://doi.org/10.1016/j.cej.2022.140917.

[304] W. Zhang, J. Miao, M. Tian, X. Zhang, T. Fan, L. Qu, Hierarchically interlocked helical conductive yarn enables ultra-stretchable electronics and smart fabrics, Chem. Eng. J. 462 (2023), 142279, https://doi.org/10.1016/j.cej.2023.142279.

[305] F. Fadil, N.D.N. Affandi, M.I. Misnon, N.N. Bonnia, A.M. Harun, M.K. Alam, Review on electrospun nanofiber-applied products, Polymers 13 (2021) 2087, https://doi.org/10.3390/polym13132087.

[306] L. Persano, A. Camposeo, C. Tekmen, D. Pisignano, Industrial upscaling of electrospinning and applications of polymer nanofibers: a review, Macromol. Mater. Eng. 298 (2013) 504–520, https://doi.org/10.1002/mame.201200290.

[307] F. Gomollón-Be, Nanofibers put a new spin on COVID-19 masks, Special to C&EN. 98, issue 45 (2020). https://cen.acs.org/materials/nanomaterials/Nanofibers-put-new-spin-COVID/98/i45.